2010

Computational intelligence and transient thermal analysis methods for exploratory analysis of source air quality

Gang Sun
Iowa State University

Computational intelligence and transient thermal analysis methods for exploratory analysis of source air quality

by

Gang Sun

A dissertation submitted to the graduate faculty

in partial fulfillment of the requirements for the degree of

DOCTOR OF PHILOSOPHY

Major: Agricultural Engineering

Program of Study Committee:
Steven J. Hoff, Major Professor
Dianne H. Cook
Jay D. Harmon
Ron M. Nelson
D. Raj Raman

Iowa State University

Ames, Iowa

2010

TABLE OF CONTENTS

CHAPTER 1. GENERAL INTRODUCTION

INTRODUCTION

Over the last decade, with the trend toward larger more intensive animal feeding operations (AFOs) in the United States, ammonia (NH_3), hydrogen sulfide (H_2S), carbon dioxide (CO_2) and particulate matter (PM_{10}) generated and emitted from livestock production facilities have become a growing environmental concern for animal producers and nearby residents. Poor air quality inside the buildings can affect the health and productivity of farm workers and animals; while emissions of gas and dust beyond AFOs can influence the wellness of the neighboring residences, thus increasing the number of disputes and lawsuits against livestock operations.

To assess health and ecological environmental impacts caused by livestock pollutants, there exists a rich body of previous work to conduct numerous air pollutants experiments for different livestock facilities (Aarnink et al., 1995; Groot Koerkamp et al., 1998; Zhu et al., 1999; Ni et al., 2002; Gay et al., 2003; Jacobson et al., 2005; Guo et al., 2006; Hoff et al., 2006; Sun et al., 2008a, 2010). However, direct and long-term measurements of gas and PM_{10} concentrations and emissions (GPCER) at all animal operations are not practical since every gas source is different and animal and weather conditions change constantly. In the absence of effective and efficient means to directly measure GPCER from each livestock production facility, development of source GPCER mathematical prediction models might be a good alternative to provide reasonably accurate estimates. Additionally, due to the absence of a nationwide monitoring network in the United States, state and federal regulatory agencies have identified a need for air quality predictive (AQP) models to quantify long-term

air emission inventories of livestock production facilities. State planners, environmental scientists, and livestock producers also need AQP models to determine science-based setback distances between animal feeding operations and neighboring residences, as well as to evaluate relevant emission abatement strategies, e.g., AQP models can be used by helping state planners and environment scientists to site new operations and to help livestock producers to understand the factors influencing air quality and odor and gas transmission so that they might make wise decisions regarding the selection and implementation of air quality mitigation techniques. In brief, air quality models could make an impact by helping to make government and livestock producers to be more profitable, sustainable and economically viable while protecting the environment and quality of life of all citizens. Up to now, three modeling approaches have been proposed for predicting source air quality: the emission factors method, the multiple regression analysis method, and the process-based modeling method.

Emission factors, expressed by the amount of each substance emitted per animal unit, are multiplied by the number of animal units to get average air emissions from animal operations. Arogo et al. (2003) attempted but could not assign empirical ammonia emission factors to estimate the average ammonia emission rates from various barns because of the many variables affecting air emissions. The under- or overestimated predictive results showed that using emission factors for all animals in all regions was not appropriate without direct and long-term measurements from a substantial number of representative animal feeding operations.

The regression analysis method uses standard least-squares multivariate regression equations to predict GPCER. The purpose of multiple regression analysis is to establish a

quantitative relationship between various predictor variables (e.g., weather and animal conditions, production systems, etc.) and air emissions. This relationship is used to understand which predictors have the greatest effect and to forecast future values of the equation response when only the predictors and the direction of their effects are known. Sun (2006) developed statistical multiple-linear regression models to predict diurnal and seasonal odor and gas concentrations and emissions from confined swine grower-finisher rooms. However, the main weakness of this method is that the complex and sometimes nonlinear relationships of multiple variables can make statistical models complicated and awkward (Comrie, 1997). Moreover, these models are highly site-specific, making it difficult to apply to the data from other experiments. The only way to establish a robust set of equations is to sample hundreds of animal feeding operations under different meteorological conditions in the U.S. The lack of sufficient data is the main cause of the uncertainty of the statistical regression models.

The process-based models (also called mechanical models) determine the movement of elements (e.g., nitrogen, carbon, and sulfur) into, through, and out of the livestock production system, investigate the underlying chemical and physical phenomenon, and identify the effects of changing one or more variables of the system. In many cases, this modeling method uses mass balance equations to describe the mechanisms of gaseous emissions and estimate their characteristic and amount at each transformation stage. Recently, Zhang et al. (2005) established a comprehensive and predictive ammonia emission model to estimate ammonia emission rates from animal feeding operations using a process-based modeling approach. The main processes treated in the model included nitrogen excretion from the animals, animal housing, manure storage, and land application of manure. The

results showed that the sensitivity analysis of various variables (e.g., manure production system, animal housing designs, and environmental conditions) needs to be quantified and that additional model validation is needed to improve model predictive accuracy. Other researchers also studied the process of mass (ammonia) transport and developed mechanical models for swine feeding operations (Aarnink and Elzing, 1998; Ni et al., 2000; Kai et al., 2006). Although there has been considerable value in the development and application of mechanistic modeling of ammonia volatilization from the main individual sources, some circumstances of gaseous emissions are not well understood and several parameters are difficult to determine experimentally. For example, adsorption, absorption, and desorption of ammonia from various materials in animal barns might be another emission source, but this mechanism is not easily acquired. Moreover, the gas release process is very complex due to abundant nonlinear relationships between gaseous emissions and the many variables that cause gas production. Therefore, a major effort would be required in future process-based model studies.

Due to the absence of adequate information available about the process of gas pollutant production, a black-box modeling approach using computational intelligence technology would be a powerful and promising tool for air quality prediction. Wikipedia (2010) defines computational intelligence (CI) as "CI is an offshoot of artificial intelligence. As an alternative to classical artificial intelligent, it rather relies on heuristic algorithms such as fuzzy systems, neural networks and evolutionary computation. Computational intelligence combines elements of learning, adaption, evolution, and fuzzy logic to create programs that are, in some sense, intelligent. Artificial neural network (ANN) is a branch of CI that is closely related to machine learning." It is noted that black-box models using CI technology

do not need detailed prior knowledge of the structure and different interactions that exist between important variables. Meanwhile, their learning abilities make the models adaptive to system changes. In recent years, there has been an increasing amount of applications of ANN models in the field of atmospheric pollution forecasting (Hooyberghs et al., 2005; Grivas et al., 2006; Sousa et al., 2007). The results show that ANN black-box models are able to learn nonlinear relationships with limited knowledge about the process structure, and the neural networks generally present better results than traditional statistical methods. Sun et al. (2008b) developed backpropagation and generalized regression neural network models to predict diurnal and seasonal gas and PM_{10} concentrations and emissions from swine deep-pit finishing buildings. It was found that the obtained forecasting results of the neural network models were in good agreement with actual field measurements, with coefficient of determination values between 81.2% and 99.5% and very low values of systemic performance indices. The promising results from this work indicated that artificial neural network technologies were capable of accurately modeling source air quality within and emissions from these livestock production facilities.

Although AQP models can be used as a useful tool to forecast air quality over a time period that are beyond an actual monitoring period, the main input variables for the model must be known which require field measurements. These variables include indoor environment (indoor, inlet and exhaust temperatures and relative humidity), outdoor climate conditions (outdoor temperature, relative humidity, wind speed, wind direction, solar energy and barometric pressure), pig size and density (animal units), building ventilation rate, animal activity, overall management practices, and properties of the stored manure, to name a few. Sun et al. (2008c) performed a multivariate statistical analysis and identified four

significant contributors to the AQP models: outdoor temperature, animal units, total building ventilation rate, and indoor temperature. The purpose of introducing fewer uncorrelated variables to the models is to reduce model structure complexity, eliminate model over-fitting problems, and minimize field monitoring costs without sacrificing model predictive accuracy. Conducting long-term field measurements of the identified four variables using current engineering approaches are still time consuming and expensive. Therefore, making use of simulation programs is a good alternative to obtain the required significant input variables for AQP models.

Basically, there are three steady-state models used to calculate indoor climate of livestock buildings which include those based on heat, moisture or carbon dioxide balances (Albright 1990). Pedersen et al. (1998) compared these three balance methods for estimating the ventilation rate in insulated animal buildings. They reported that the three methods could give good prediction results on a 24-hr basis when the differences between inside and outside temperature, absolute humidity and CO_2 concentrations were greater than 2 $°C$, 0.5×10^{-3} kg water per kg dry air and 200 ppm, respectively for the buildings tested in Northern Europe. A simple steady-state balance model (Schauberger et al., 1999) was developed for the sensible and latent heat fluxes and CO_2 mass flows resulting in the prediction of inside temperature and ventilation rate of mechanically ventilated livestock buildings. The obtained variables were further applied for diurnal and annual odor emission estimates. Due to the lack of field measurements, the accuracy of the predicted parameters could not be determined. Morsing et al. (2003) released a computer program entitled StaldVent^{TM} to help design and evaluate heating and ventilation systems in animal houses. They primarily used a steady-state energy

balance method to predict the required ventilation rate and heat capacity, room temperature, CO_2 concentration, and expected energy consumption throughout the year.

On the other hand, indoor climate can be predicted by studying thermal transients in buildings. Nannei and Schenone (1999) developed a simplified numerical model for building thermal transient simulation. The model can be applied to compute the room air temperature and the temperature of the inner surface of the walls. The good numerical results compared with the experimental data indicated that this model was useful for the study of unsteady thermal performance. Mendes et al. (2001) presented a dynamic multimodal capacitive nonlinear model to analyze transient indoor air temperature using Matlab/Simulink™ (Matlab 5.0, 1999). This thermal model was improved by introducing internal gains and the inter-surface long-wave radiation. The predicted results were not experimentally validated however. Morini and Piva (2007) investigated the dynamic thermal behavior of residential heating and cooling systems with control systems during a sinusoidal variation of the outside temperature. The core of their program employed mechanical and thermal energy conservation equations implemented in the Simulink™ environment. It was found that their transient model outperformed the standard steady-state approach.

OBJECTIVES

The over-arching goal of this study is to predict indoor climate and long-term air quality (NH_3, H_2S and CO_2 concentrations and emissions) for swine deep-pit finishing buildings using a transient building thermal analysis and air quality predictive (BTA-AQP) model and a typical meteorological year/specific weather year data base.

The specific objectives of this research were to:

1. Develop an artificial neural network based air quality predictive (AQP) model to forecast source air pollutants from swine deep-pit finishing buildings as affected by time of day, season, ventilation rate, animal growth cycles, in-house manure storage levels, and weather conditions.
2. Build a lumped capacitance model (BTA model) to predict the transient behavior of indoor environment (ventilation rate and indoor air temperature) according to the thermo-physical properties of a typical swine building, set-point temperature scheme, fan staging scheme, transient outside temperature, and the heat fluxes from pigs and supplemental heaters.
3. Evaluate the complete BTA-AQP model to estimate source air quality for a specific year and predict long-term air quality.
4. Apply the proposed BTA-AQP models to different husbandry management practices and geographical area scenarios in order to assess the potential simulated impacts of these scenarios on long-term air quality

DISSERTATION ORGANIZATION

This dissertation is organized in paper format and comprises five papers, corresponding to the four research objectives. The first paper entitled "Forecasting daily source air quality using multivariate statistical analysis and radial basis function networks" has been published in the Journal of the Air and Waste Management Association 58(12):1571-1578. The second paper entitled "Development and comparison of backpropagation and generalized regression neural network models to predict diurnal and seasonal gas and PM_{10} concentrations and emissions from swine buildings" has been

published in the Transactions of the ASABE 51(2): 685-694. The third paper entitled "Prediction of indoor climate and long-term air quality using the BTA-AQP model: Part I. BTA model development and evaluation" and the fourth paper entitled "Prediction of indoor climate and long-term air quality using the BTA-AQP model: Part II. Overall model evaluation and application" have been published in the Transactions of the ASABE 53 (3): 863-881. The fifth manuscript entitled "Simulated impacts of different husbandry management practices and geographical area on long-term air quality" will be submitted to the Transactions of the ASABE. The five papers are followed by an overall summary of the major conclusions of this research and recommendations for future research. Three appendixes, which present sensible heat production procedures, APECAB (Aerial Pollutant Emissions from Confined Animal Buildings) daily data, and TMY3 (Typical Meteorological Year) weather data, follow the overall summary chapter. The acknowledgements are included at the end of this dissertation.

REFERENCES

Aarnink, A. J. A., and A. Elzing. 1998. Dynamic model for ammonia volatilization in housing with partially slatted floors, for fattening pigs. *Livestock Prod. Sci.* 53(2): 153-169.

Albright, L. D. 1990. Chapter 5: Steady-state energy and mass balance. In *Environment Control for Animals and Plants*, 143-172. St. Joseph, Mich.: ASAE.

Arogo, J., P. W. Westerman, and A. J. Heber. 2003. A review of ammonia emissions from confined swine feeding operations. *Trans. ASAE* 46(3): 805-817.

Comrie, A.C. 1997. Comparing neural networks and regression models for ozone forecasting. *J. Air Waste Mgmt. Assoc.* 47: 653-663.

Gay, S.W.; Schmidt, D.R.; Clanton, C.J.; Janni, K.A.; Jacobson, L.D.; Weisberg, S. Odor, total reduced sulphur, and ammonia emissions from animal housing facilities and manure storage units in Minnesota. *Applied Eng. in Agric.* 2003, *19*, 347-360.

Groot Koerkamp, P.W.G.; Metz, J.H.M.; Uenk, G.H.; Phillips, V.R.; Holden, M.R.; Sneath, R.W.; Short, J.L.; White, R.P.; Hartung, J.; Seedorf, J.; Schroder, M.; Linkert, K.H.; Pedersen, S.; Takai, H.; Johnsen, J.O; Wathes, C.M. Concentrations and emissions of ammonia in livestock buildings in northern Europe; *J. Agric. Eng. Res.* 1998, *70*, 79-95.

Grivas, G., and A. Chaloulakou. 2006. Artificial neural network models for prediction of PM_{10} hourly concentrations, in the greater area of Athens, Greece. *Atmos. Environ.* 40(7): 1216-1229.

Guo, H.; Dehod, W.; Agnew, J.; Laguë, C.; Feddes, J. R.; Pang, S. Annual odor emission rate from different types of swine production buildings; *Trans. ASABE* 2006, *49*, 517-525.

Hoff, S. J., D. S. Bundy, M. A. Nelson, B. C. Zelle, L. D. Jacobson, A. J. Heber, J. Ni, Y. Zhang, J. A. Koziel, and D. B. Beasley. 2006. Emissions of ammonia, hydrogen sulfide, and odor before, during, and after slurry removal from a deep-pit swine finisher. *J. Air Waste Mgmt. Assoc.* 56(5): 581-590.

Hooyberghs, J., C. Mensink, G. Dumont, F. Fierens, and O. Brasseur. 2005. A neural network forecast for daily average PM_{10} concentrations in Belgium. *Atmos. Environ.* 39(18): 3279-3289.

Jacobson, L. D., H. Guo, D. R. Schmidt, R. E. Nicolai, J. Zhu, and K. A. Janni. 2005. Development of the OFFSET model for determination of odor-annoyance-free setback distances from animal production sites: Part I. Review and experiment. *Trans. ASABE* 48(6): 2259-2268.

Kai, P., B. Kaspers, and T. van Kempen. 2006. Modeling source of gaseous emissions in a pig house with recharge pit. *Trans. ASABE* 49(5): 1479-1485.

Mendes, N., G. H. C. Oliveira and H. X. de Araújo. 2001. Building thermal performance analysis by using Matlab/Simulink. In *Proc. 7th International IBPSA Conference on Building Simulation,* 473-480. Rio de Janeiro, Brazil.

Morini, G. L. and S. Piva. 2007. The simulation of transients in thermal plant. Part I: Mathematical model. *Applied Thermal Eng.* 27: 2138-2144.

Morsing, S., J. S. Strom, G. Q. Zhang and L. Jacobson. 2003. Prediction of Indoor Climate in Pig Houses. In *Proc. 2nd International Conference on Swine Housing II*, 41-47. Research Triangle Park, NC: ASAE.

Nannei E. and C. Schenone. 1999. Thermal transients in buildings: development and validation of a numerical model. *Energy and Buildings*. 29: 209-215.

Ni, J., J. Hendriks, C. Vinckier, and J. Coenegrachts. 2000. Development and validation of a dynamic mathematical model of ammonia release in pig house. *Environ. Intl*. 26(1-2): 97-104.

Ni, J.; Heber, A. J.; Lim, T. T.; Diehl, C. A.; Duggirala, R. K; Haymore, B. L. Hydrogen sulfide emission from two large pig-finishing buildings with long-term high-frequency measurements. *J. Agric. Sci*. 2002, *138*, 227-236.

Pedersen, S., H. Takai, J. O. Johnsen, J. H. M. Metz, P. W. G. Groot Koerkamp, G. H. Uenk, V. R. Phillips, M. R. Holden, R. W. Sneath, J. L. Short, R. P. White, J. Hartung, J. Seedorf, M. Schröder, K. H. Linkert and C. M. Wathes. 1998. A comparison of three balance methods for calculating ventilation rates in livestock buildings. *J. Agric. Eng. Res.* 70: 25-37.

Schauberger, G., M. Piringer and E. Petz. 1999. Diurnal and annual variation of odor emission from animal houses: a model calculation for fattening pigs. *J. Agric. Eng. Res.* 74: 251-259.

Sousa, S. I. V., F. G. Martins, M. C. M. Alvim-Ferraz, and M. C. Pereira. 2007. Multiple linear regression and artificial neural network based on principal components to predict ozone concentrations. *Environ. Modeling and Software* 22(1): 97-103.

Sun, G. 2006. Monitoring and modeling diurnal and seasonal odor and gas emission profiles for swine grower/finisher rooms. MS thesis. Saskatoon, Saskatchewan, Canada: University of Saskatchewan, Department of Agricultural and Bioresource Engineering.

Sun, G., H. Guo, J. Peterson, B. Predicala, and C. Laguë. 2008a. Diurnal odor , ammonia, hydrogen sulfide and carbon dioxide emission profiles of confined swine grower/finisher rooms. *Journal of the Air and Waste Management Association.* 58 (11):1434-1448.

Sun, G., S. J. Hoff, B. C. Zelle and M. A. Nelson. 2008b. Development and comparison of backpropagation and generalized regression neural network models to predict diurnal and seasonal gas and PM_{10} concentrations and emissions from swine buildings. *Trans. ASABE* 51(2):685-694.

Sun, G., S. J. Hoff, B. C. Zelle, and M. A. Smith. 2008c. Forecasting daily source air quality using multivariate statistical analysis and radial basis function networks. *J. Air Waste Mgmt. Assoc*. 58(12): 1571-1578.

Sun, G., H. Guo, and J. Peterson. 2010. Seasonal odor , ammonia, hydrogen sulfide and carbon dioxide concentrations and emissions from swine grower-finisher rooms. *Journal of the Air and Waste Management Association*. 60 (4): 471-480.

"Wikipedia". 2010. Wikimedia Foundation Inc.

Zhang, R. H., T. R. Rumsey, J. R. Fadel, J. Arogo, Z. Wang, G. E. Mansell, and H. Xin. 2005. A process-based ammonia emission model for confinement animal feeding operations: Model development. In *Proc. 14th Intl. Emission Inventory Conf.* Research Triangle Park, N.C.: U.S. EPA, Office of Air Quality Planning and Standards.

Zhu, J.; Jacobson, L.; Schmidt, S.; Nicolai, R. Daily variations in odor and gas emissions from animal facilities; *Applied Eng. in Agric.* 1999, *16*, 153-158.

CHAPTER 2. FORECASTING DAILY SOURCE AIR QUALITY USING MULTIVARIATE STATISTICAL ANALYSIS AND RADIAL BASIS FUNCTION NETWORKS

A paper published in the Journal of the Air and Waste Management Association[1]

Gang Sun, Steven J. Hoff, Brian C. Zelle, and Minda A. Nelson[2]

ABSTRACT

It is vital to forecast gas and particle matter concentrations and emission rates (GPCER) from livestock production facilities in order to assess the impact of airborne pollutants on human health, ecological environment and global warming. Modeling source air quality is a complex process due to abundant nonlinear interactions between GPCER and other factors. The objective of this study was to introduce statistical methods and Radial Basis Function (RBF) neural network to predict daily source air quality in Iowa swine deep-pit finishing buildings. The results show that four variables (outdoor and indoor temperature,

---

[1] Reprinted with permission of *J. Air & Waste Manage. Assoc.*, 2008, 58(12), 1571-1578.

[2] Gang Sun (Ph.D. candidate), Steven J. Hoff (professor), and Brian C. Zelle (research associate) are in the Department of Agricultural and Biosystems Engineering at Iowa State University. Minda A. Nelson, a former graduate research assistant at Iowa State University, is currently with Burns & McDonnell, Inc. (Kansas City, MO). Address Correspondence to: Dr. Steven J. Hoff, Agricultural and Biosystems Engineering Department, 212 Davidson Hall, Iowa State University, Ames, IA 50011; phone: +1-515-294-6180; fax: +1-515-294-2255; e-mail: hoffer@iastate.edu.

animal units, and ventilation rates) were identified as relative important model inputs using statistical methods. It can be further demonstrated that only two factors, the environment factor and the animal factor, were capable of explaining more than 94% of the total variability after performing principal component analysis (PCA). The introduction of fewer uncorrelated variables to the neural network would result in the reduction of the model structure complexity, minimize computation cost, and eliminate model over-fitting problems. The obtained results of RBF network prediction were in good agreement with the actual measurements, with values of the correlation coefficient between 0.741 and 0.995 and very low values of systemic performance indexes for all the models. The good results indicated the RBF network could be trained to model these highly nonlinear relationships. Thus, the RBF neural network technology combined with multivariate statistical methods is a promising tool for air pollutant emissions modeling.

IMPLICATION

State and federal regulatory agencies in the U.S. have a critical need to characterize annual or daily source air quality inventories of animal feeding operations in order to access health and environmental impacts caused by livestock pollutants. But it is almost impossible and impractical to measure air and dust emissions merely based on experiments because every air pollutant source is different, every surrounding area is different, and weather conditions change constantly. The RBF neural network technology combined with multivariate statistical methods described in this paper was demonstrated as a promising and useful tool for air pollutant emissions modeling.

INTRODUCTION

Over the last decade, with the trend toward larger, more intensive animal feeding operations (AFOs) in the United States, ammonia (NH_3), hydrogen sulfide (H_2S), carbon dioxide (CO_2) and particulate matter (PM_{10}) generated and emitted from livestock production facilities have become a growing environment concern for animal producers and nearby residents. Poor air quality inside the buildings can affect the health and productivity of farm workers and animals; while emissions of gas and dust beyond AFOs can influence the wellness of the neighboring residences, which leads to the increasing number of disputes and lawsuits against livestock operations. To understand health and environmental impacts caused by livestock and poultry pollutants, it is a critical need to characterize annual or daily air quality inventories as a basic database of U.S. animal facilities. State and federal regulatory agencies will enforce existing or enact new air quality standards based on this database.

Some research projects have been conducted to monitor the gaseous emissions from animal buildings.[1-3] However, direct and long-term measurements of air and dust emissions at all AFOs are not feasible or practical. Thus, the development of mathematical tools to forecast air quality of statistically representative AFOs is very important because it can reduce the number of monitoring sites and measurement costs, and provide reasonably accurate estimates of air concentrations and emissions at various times. Unfortunately, source air quality is very difficult to model due to the complex and nonlinear relationships between air concentrations and emissions and the many variables that determine air pollutant production. In recent years, neural network models have been successfully employed for the prediction of a wide range of pollutants at various time scales with very good results.[4-6]

The Artificial Neural Network (ANN) is an interconnected group of artificial neurons that uses a mathematical model or computational model for information processing based on a connectionist approach to computation. The findings of numerous air quality modeling projects [7,8] demonstrated that the performance of ANN was generally superior in comparison to traditional statistical methods and deterministic air modeling systems because of its computational efficiency, generalization ability, and its limited need of prior knowledge about the modeling process structure.

It is noted that nearly all the air quality models using ANN technologies are dealing with the prediction of atmosphere environment pollutants. Little information is available regarding source air concentrations and emissions, especially from animal buildings. Therefore, the aim of this work was to develop an artificial neural network model to forecast source air pollutants from swine deep-pit finishing buildings as affected by time of day, season, ventilation rate, animal growth cycles, in-house manure storage levels, and weather conditions.

MATERIALS AND METHODS

Description of Experiment

The air quality data were collected in 1000- head deep-pit swine finishing buildings in Iowa from January 2003 to April 2004. An instrument trailer (Mobile Emission Laboratory, MEL) was used to monitor gas and PM concentrations and emissions from the mechanically-ventilated, confined swine production buildings with one-year of manure storage. The MEL housed a gas sampling system (GSS), a computer, the data acquisition system, gas analyzers, environmental instrumentation, gas calibration cylinders, and other

supplies. Gas concentrations were measured with a chemiluminescence NH_3 analyzer (Model 17C, Thermal Environment Instruments, Franklin, MA), a pulsed fluorescence SO_2 detector (Model 45C, Thermal Environment Instruments, Franklin, MA), and two photoacoustic infrared CO_2 analyzers in the range from 0 to 2,000 and 10,000 ppm (Model 3600, Mine Safety Appliances CO., Pittsburg, PA). PM_{10} concentrations were measured continuously using two Tapered Element Oscillating Microbalance (TEOM) ambient PM_{10} monitors (Model 1400a, Rupprecht & Patashnick, Albany, NY). The environment parameters and total building ventilation rates were simultaneously monitored. Gas and PM_{10} emission rates were determined by multiplying the total airflow rate of the ventilation fans by the increase in gas and PM_{10} concentrations between the building ventilation inlet and outlet. The emission rates were expressed on an animal unit basis by dividing the total emissions by the total animal units (1AU=500kg). During the measurement period, approximately three complete production cycles of pigs raised from ~20 to 120 kg were monitored. Figure 1 shows the diurnal and seasonal NH_3 emission for one complete pig growth cycle with approximately 960 finishing pigs from December 21, 2003 to April 13, 2004.

Factors Affecting Source Air Quality

Daily amounts and temporal patterns of air concentrations and emissions from source swine buildings can be affected by various factors including: (1) physical characteristics of the site, indoor environment and outdoor weather conditions; (2) diurnal and seasonal effects; (3) swine growth cycle; (4) ventilation system and (5) barn management; and so forth.

Different regions in the U.S have different temperature, relative humidity, wind speed and direction, rainfall frequency and intensity, solar energy, and barometric pressure. Those

climate factors impact gas concentrations and emissions significantly if the rates of gaseous emissions were monitored in different areas of the country (e.g. northern, midwestern, and southern areas). Also, AFOs in different locations might have different swine breeding species and feed formulations, which influence source air quality as well.

Diurnal and seasonal variations of ambient and inside environment are important factors resulting in changes in gaseous emissions from swine buildings. The temperature between inside and outside and total building ventilation rates vary hourly, daily and seasonally under different weather conditions.

Swine size, density, and daily feed nutrient inputs during each growth cycle have a very strong impact on the gaseous concentrations and emissions. When pigs grow, the amount and composition of the feed intake change, as do the amount and composition of the manure. Thus, the daily amount of gas generation tends to increase. However, sharp decreases in the amount of daily nitrogen excreted were observed when the formulation changes due to the adjustment by the animal to the new feed composition.[9] This adjustment process alleviates the amount of nitrogen in the manure converted to ammonia and other gases. Additionally, for the individual animal, interruptions in its daily life rhythm resulting from illness, breakdown of barn equipment or disturbed by visitors may affect its appetite so that gas production might decrease slightly in response to changes of feed ingested and nutrients excreted.

Ventilation rates play a key role in indicating gaseous concentrations and emissions. The highest mean concentrations occur in the winter; while the lowest gas levels appear during the summer. The main reason is the large differences in the ventilation rate and ambient temperature during winter and summer. Low concentrations under warm weather

conditions are attributed to strong dilution effect and better indoor air mixing due to high ventilation rates; conversely, low ventilation rates during cold weather cause gas accumulation inside the swine barn.

Swine management is also a vital factor to determine air quality inside swine buildings and outside ecological systems. Good management practices can maintain proper environment needs for the animals and decrease daily air emissions. The under-floor deep pit designed to store manure for up to 1 year is also a concentrated source for gas emissions. This manure collection practice may smooth the variations in nitrogen emissions. Other event-processes such as flush cycles, manure scraping, and slurry removal are another source of variation in gas concentrations and emissions.

Accurate forecast of source air quality in swine buildings needs defined relationships between gaseous concentrations and emissions and various factors. However, assessing the overall impact of all the factors on estimates of daily air quality is currently impossible due to the absence of some measurement data about swine activity, management practices, and microbial cycles, etc. Without sufficient data support, it is difficult to know whether these variables would affect gaseous emissions significantly. Also, quantifying air emissions from animal agricultural sources is a complex process. There are definitely unknown factors that can determine air quality levels. Therefore, the choice of important variables used to make estimates of air quality is a challenge for model development.

In this study, the measurement variables included indoor environment (indoor, inlet and exhaust temperature and RH), outdoor climate conditions (outdoor temperature, relative humidity, wind speed, wind direction, solar energy and barometric pressure), time of a day, season (a total of 16 measurement months), pig size and density (animal units), and swine

building ventilation rates. Correlation coefficients between gas emissions and various variables were analyzed tentatively to evaluate the influence of each input variable on model outputs, that is, determining which variable had a significant effect on gas concentrations and emissions. These coefficients reflected the existence of co-linearity between the explanatory variables. Meanwhile, the correlation coefficients can be used as a tool to eventually discard input features that are highly correlated with others.

Data Processing Using Principal Component Analysis

The initial choice of input variables was guided based on the statistical method and some knowledge of air pollutant production. The characteristic of the initial set constituted by the selected features would be high correlations among the features and multi-dimensions due to many input variables. This large feature set would result in computation burden and make the problem unnecessarily complicated. Thus, it is necessary to perform some kind of dimensionality reduction by using an alternative and smaller set of features derived from the initial ones.

Principal components analysis (PCA)[10] is a method commonly used for data reduction purposes. It is based on the idea of performing an orthonormal transformation and retaining only significant eigenvectors. Each eigenvector is associated with a variance represented by the corresponding eigenvalue. Each eigenvector corresponding to an eigenvalue that represents a significant variance of the whole dataset is called a principal component of the data. Each principal component is a linear combination of the original variables. All the principal components are orthogonal to each other so that there is no redundant information.

The PCA method can reduce the number of input variables and obtain the new uncorrelated variables with sufficient contribution to the majority of the original variance. Therefore, the introduction of PCA to the neural network may simplify the structure of the prediction model, minimize computation cost, and eliminate network over-fitting problems.

Radial Basis Function Neural Network

Although the architecture of Radial Basis Function neural networks (RBF) is less widely used and well-known compared to Multilayer Perceptrons (MLP), the main important advantage of the RBF approach is that the RBF network can yield the minimum approximating error of any function.[11] This best approximation property does not apply to MLPs. Therefore, BRF networks are suitable for modeling complex input-output mappings.

Radial basis functions are embedded in a two-layer neural network topology (Figure 2), where each hidden unit implements a radial kernel function. The output units implement a weighted sum of hidden unit outputs. The input into an RBF network is nonlinear while the output is linear. The most common kernel function is the Gaussian function given by: $\varphi_i(x) = \exp\left(-\frac{\|x - x_i\|}{2\sigma^2}\right)$ where $\|x - x_i\|$ indicates the distance of a feature vector x to a prototype vector x_i and σ acts as smoothing parameter. The number of radial basis functions is typically much smaller than training patterns since they are chosen relative to some centroid patterns instead of relative to the training patterns. The centroid is adjusted as part of a training process in order to obtain good generalization. Each basis function has its own smoothing parameter σ which is determined during the network training. Bias parameters are included in the summation of the kernel values to compensate for the difference between the average value over the basis function and the average value of the targets.

The weights of the first layer of the RBF network are used to adjust the centroids and smoothing factors used by the kernel functions. The second layer weights are determined using pseudo-inverse techniques. These two layers' weights are independently trained so that RBF networks train much faster in general than equivalent MLP networks.

RESULTS AND DISCUSSION

Selection of Variables

The outdoor temperature and relative humidity, static pressure difference between the inside and outside of the swine building, barn inventory and average mass per pig, building fan RPM, indoor, inlet and exhaust temperatures, and inside relative humidity were considered as preliminary model input variables. These ten measured parameters could be reduced to seven variables instead, i.e. barn inventory and pig mass determine the animal unit variable and the building airflow rate variable can be obtained by measuring the fan speeds (*RPM*) and the static pressure. The incoming air temperature parameter was left out since this value was the same as the outdoor temperature.

Correlation coefficients analysis between pollutants and those seven variables were initially performed to evaluate the influence of each variable on air concentrations and emissions and the relationships between the input variables. Table 1 presents the correlation coefficients of the seven variables and gas and PM_{10} concentrations and emissions, and Figure 3 displays the pairwise scatterplot matrix. It was found that there were significant and negative correlations ($p<0.05$) between NH_3 concentrations and outdoor temperature (*Tout*), animal unit (*AU*), ventilation rates (*VR*), and indoor and exhaust temperatures (*Tin* and *Tex*). Outdoor and indoor relative humidity had no relationship associated with the NH_3

concentrations. Therefore, based on fundamental knowledge of livestock gas production, *Tout*, *AU*, *VR*, *Tin* and *Tex* variables were used as very important factors in a model to forecast source air quality in animal buildings. In addition, high correlation coefficients ($p<0.05$) were observed between some NH_3 concentration predictors, such as outdoor temperature and ventilation rates (0.8842), outdoor and indoor temperature (0.8600), and indoor temperature and ventilation rates (0.8678), demonstrating the existence of co-linearity between the explanatory variables.

It can be further seen in Figure 3 that the indoor and exhaust temperature variables were strongly linearly related with a very high correlation coefficient (0.9320). Discarding one of these two variables was reasonable due to the high correlation with each other [10]. It was decided to keep the indoor temperature variable as a model input.

Similar results about the relationships between the variables and NH_3 emissions, H_2S, CO_2 and PM_{10} concentrations and emissions were achieved regarding the correlation coefficient matrices (Table 1). It was also observed that different combinations of the parameters may affect significantly on gas and PM_{10} concentrations and emissions. However, the final selected variables as the model predictors were *Tout*, *AU*, *VR*, and *Tin*, because all the air quality neural network models using those four input variables can obtain better predictive performance in comparison to models using only the significant variables determined from the correlation coefficients (Table 1). Table 2 summarizes the means, standard deviations (S.D.) and range of the four input variables. There was substantially more variability in the ratings of the *AU* and *Tout* than in the rating of *VR* and *Tin*. It is not surprising since *VR* and *Tin* were the controlled parameters in the swine buildings.

Principal Component Analysis

Table 3 presents the principal component coefficient vectors, the variance of each principal component (PC) and the cumulative variances after computing PCA. As Table 3 shows, the third and fourth PCs were only responsible for about 2.99% and 2.79% of the total variance respectively, certainly the negligible factors; while the first two PCs were able to explain more than 94% of the total variability, which suggested that it would be adequate to use the corresponding first two PCs instead of the four original features. It can be further observed that the principal component coefficients presented the relative importance of each standardized predictor in the PC matrix. The largest coefficients in the first PC were the first, third and fourth elements, corresponding to the variables *Tout*, *VR* and *Tin*, which meant these three parameters revealed significant effects in the first PC; while only the *AU* variable had a large coefficient in the second PC.

The principal component coefficients for each variable and the principal component scores for each observation are illustrated in Figure 4. All the points in the plot were the scores of each observation for the two principal components, i.e. the original data set was mapped into a new coordinate system determined by the PCA. Each of the four variables was represented by a vector, and the direction and length of the vector indicated how each variable contributed to the two principal components in the plot. Note that the first principal component represented by the horizontal axis mainly consisted of the variables *Tout*, *VR* and *Tin*, which had positive coefficients. That corresponded to the vectors directed into the right half of the plot; while the significant contribution to the second principal component, represented by the vertical axis, was the *AU* variable. These two principal components were used as the final input variables and fed into the RBF neural network model. The first PC

reflected the impact of temperature and airflow rates on air quality, which may be called '*the Environment Factor*'. The second PC revealed the affect of swine growth cycle on air quality, which may be called '*the Animal Factor*'.

RBF Network Models

In the development of RBF neural network models, two variables (the environment and animal Factors) after performing the PCA were employed for the model input and gas and PM_{10} concentrations and emissions as the output. All the measured data were examined for missing values caused by measuring instrument failure. The variable mean was used to fill in the missing values. Fortunately, only a few missing values occurred in the data set so that this method nearly had no effect on the variance-covariance of the data. The input data of October 21 and 22, 2003 were removed from the model calculation due to the annual slurry removal events.

All the input data were then divided into training and test subsets, i.e. three-fourths of the data for the training set and one-fourth of the data for the test set. The training set was used for computing the gradient and updating the network weights and biases; while the test set was used for validating the network performance. The radial basis function was developed using the '*newrbe*' function in the Matlab Neural Network Toolbox. It can design a radial basis network with zero error on the design vectors very quickly. During the network training, different '*spread*' (spread of radial basis functions) values were adjusted until the best RBF models were obtained. A total of fifty training and testing times for each air quality model were conducted. In each training and testing process, the data set was randomized using the *'randperm'* function and the performance of the network was recorded.

Figure 5 depicts the predicted values of the best network models versus actual output. The solid line with the circle marks indicates the predicted values (P) and the dash line with the diamond marks indicates the actual output (O). The daily values shown were from randomly selected days which were not included in the training data set and were normalized using $(P - P_{min})/(P_{max} - P_{min})$ and $(O - O_{min})/(O_{max} - O_{min})$. It can been observed that the CO_2 concentration model had the highest correlation coefficient (0.995), followed by the CO_2 emission model (0.926), the H_2S emission model (0.925), the NH_3 concentration model (0.9119), and the NH_3 emission model, the PM_{10} emission models, and the H_2S concentration model (between 0.879 and 0.809). Also, Mean Absolute Error (*MAE*) and Root Mean Square Error (*RMSE*) results of these models were very low. The low systematic MAE and RMSE in particular were considered an indicator of a good model. Thus, it can be concluded that the selected independent variables (*Tin, AU, VR and Tin*) or the two new PCs and RBF neural network technology were able to yield very accurate predictive results. Meanwhile, the PM_{10} concentration model model did not achieve good results in comparison to the other models, the prediction outcome was still acceptable though. The explanation for the poorer performance of the model could be due to some factors missing in the model input, such as the activity of the pigs, the level of pen hygiene, management practices, the type of room flooring and microbial cycles etc. Although it is not easy to measure these parameters and evaluate how much they influence the air quality level, these variables should be investigated at some extent to improve predictive precision of the model.

CONCLUSIONS

The mechanisms involved in gas and particulate matter concentrations and emission rates (GPCER) from animal feeding operations are complex and time-dependent. Various factors affect the air quality level including physical characteristics of the site, indoor environment and outdoor weather conditions, diurnal and seasonal effects, swine growth cycle, ventilation system and barn management, etc. The relationships between GPCER and these factors are highly nonlinear and some factors are highly correlated with others. Also, it is currently impossible to assess the overall impact of all the factors on estimates of daily air quality due to the absence of measurement data and a clear knowledge of air pollutant production processes. Therefore, source air quality modeling is a challenge for environment engineers and researchers.

The statistical correlation coefficient analysis method was employed to evaluate the influence of relative important variables on source GPCER. The significant model input parameters were outdoor temperature, animal units, ventilation rates, and indoor temperature. The exhaust temperature variable was discarded because it was highly correlated with indoor temperature ($R^2=0.9320$). Other variables were not considered as model inputs due to their minimal contribution to the model output in the RBF network.

Principal component analysis was used to reduce dimensions of the input data and obtain the new uncorrelated variables that could account for the majority of the original variance. Fewer uncorrelated variables would simplify the structure of prediction model, minimize computation cost, and eliminate network over-fitting problems. It was found that only two principal components (PC) explaining more than 94% of the total variability can be used as the final model variables instead of the previous four predictors. The first PC

reflected the impact of temperature and airflow rates on the air quality, which may be called '*the Environment Factor*'. The second PC revealed the impact of swine size and density, which may be called '*the Animal Factor*'.

The RBF network presented here can yield the minimum approximating error of any function so that it is suitable for modeling complex and nonlinear input-output mappings. The '*newrbe*' function was used to develop the radial basis function in the Matlab Neural Network Toolbox. Different '*spread*' (spread of radial basis functions) values were adjusted until best performance indexes of RBF models were achieved. The results of RBF networks were rather satisfactory. Therefore, the RBF neural network technology combined with multivariate statistical methods is a promising tool for source air quality modeling.

REFERENCES

1. Ni, J.; Heber, A. J.; Lim, T. T.; Diehl, C. A.; Duggirala, R. K.; Haymore, B. L.; Sutton, A. L. Ammonia Emission From a Large Mechanically Ventilated Swine Building During Warm Weather; *J. Environ. Qual.* **2000**, *29*, 751-758.

2. Hoff , S.J.; Bundy, D. S.; Nelson, M. A.; Zelle, B. C.; Jacobson, L. D.; Heber, A. J.; Ni, J.; Zhang, Y.; Koziel, J. A.; Beasley, D. B. Emissions of Ammonia, Hydrogen Sulfide, and Odor Before, During, and After Slurry Removal From a Deep-pit Swine Finisher; *J. Air & Waste Manage. Assoc.* **2006**, *56*, 581-590.

3. Heber, A.J.; Ni, J.; Lim, T.T.; Schmidt, A.M.; Koziel, J.A.; Hoff, S.J.; Tao, P.; Nicolai, R.E.; Jacobson, L.D.; Beasley, D.B.; Zhang, Y. Quality Assured Measurements of Animal Building Emissions: Gas Concentrations; *J. Air & Waste Manage. Assoc.* **2006**, *56*, 1472-1483.

4. Abdul-Wahab, S. A.; Al-Alawi, S. M. Assessment and Prediction of Tropospheric Ozone Concentration Levels Using Artificial Neural Networks; *Environ. Modell. Softw.* **2002**, *17*, 219-228.

5. Hooyberghs, J.; Mensink, C.; Dumont, G.; Fierens, F.; Brasseur, O. A Neural Network Forecast for Daily Average PM_{10} Concentrations in Belgium; *Atmos. Environ*. **2005**, *39*, 3279-3289.

6. Sousa, S. I. V.; Martins, F. G.; Alvim-Ferraz, M. C. M.; Pereira, M.C. Multiple Linear Regression and Artificial Neural Network Based on Principle Components to Predict Ozone Concentrations; *Environ. Modell. Softw.* **2007**, *22*, 97-103.

7. Chaloulakou, A.; Grivas, G.; Spyrellis, N. Neural Network and Multiple Regression Models for PM_{10} Prediction in Athens: A Comparative Assessment; *J. Air & Waste Manage. Assoc.* **2003**, *53*, 1183-1190.

8. Agirre-Basurko, E.; Ibarra-Berastegi, G.; Madariaga, I. Regression and Multilayer Perceptron-based Models to Forecast Hourly O_3 and NO_2 Levels in the Bilbao Area. Environ; *Modell. Softw.* **2006**, *21*, 430-446.

9. U.S. NRC (National Research Council). *The scientific basis for estimating air emissions from animal feeding operation;* U.S. National Academy Press: Washington, DC, 2002.

10. Johnson, R.; Wichern, D.W. *Applied multivariate statistical analysis*; Pearson Education: London, UK, 2006.

11. Girosi, F.; Poggio, T. Networks and the Best Approximation Property; *Biol. Cybern.* **1990**, *63*, 169-176.

Table 1. Correlation coefficient matrix of the seven variables and gas and PM_{10} concentrations and emissions.

Variables	NH_3Con	NH_3ER	H_2SCon	H_2SER	CO_2Con	CO_2ER	PM_{10}Con	PM_{10}ER
Tout	-0.8077	0.1974	0.0291	0.7131	-0.9058	-0.2483	-0.3702	0.1733
RHout	-0.0755	-0.2689	0.0088	-0.1695	0.1324	-0.1198	-0.1259	-0.3802
AU	-0.2151	0.6137	-0.0976	0.3289	-0.5467	0.2136	0.1567	0.5996
VR	-0.7747	0.2168	0.0847	0.7992	-0.7781	-0.0316	-0.3620	0.2432
Tin	-0.6848	0.0988	0.2893	0.7885	-0.6698	-0.0630	-0.4112	0.0654
Tex	-0.6614	-0.0500	0.2461	0.7403	-0.5496	-0.1219	-0.5066	-0.0216
RHin	0.0043	-0.5466	0.2340	0.0117	0.3780	-0.0730	-0.2915	-0.5644

Note: RHout , outdoor RH; *RHin* , indoor RH; Con, concentration; ER, emission rate.

Table 2. The means, standard deviations (S.D.) and range of the four input variables.

Variables	Mean (S.D)	Min	Max
Tout (^oC)	6.7 (12.5)	-21.8	31.4
AU	128.8 (38.5)	50.0	196.0
VR ($m^3.sec^{-1}$)	7.0 (5.0)	1.5	21.2
Tin (^oC)	25.3 (2.2)	13.8	31.0

Table 3. PC coefficient vectors.

Variables	PC_1	PC_2	PC_3	PC_4
Tout	0.5740	-0.0258	-0.7872	0.2240
AU	0.1592	0.9733	0.1172	0.1164
VR	0.5756	-0.0226	0.1945	-0.7940
Tin	0.5603	-0.2268	0.5734	0.5531
Variance	2.7911	0.9776	0.1197	0.1116
Percent total variance	69.78	94.22	97.21	100

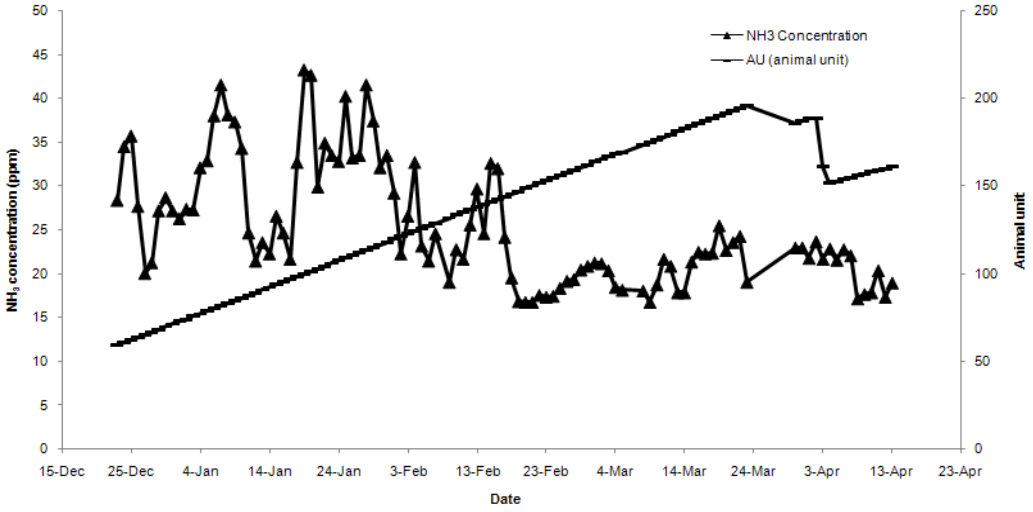

Figure 1. Diurnal and seasonal NH_3 emission for one complete pig growth cycle with approximately 960 pigs (December 21, 2003 to April 13, 2004).

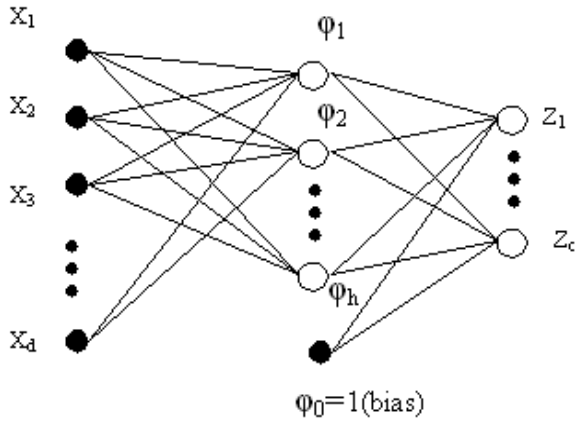

Figure 2. RBF network with kernel function φ_i .

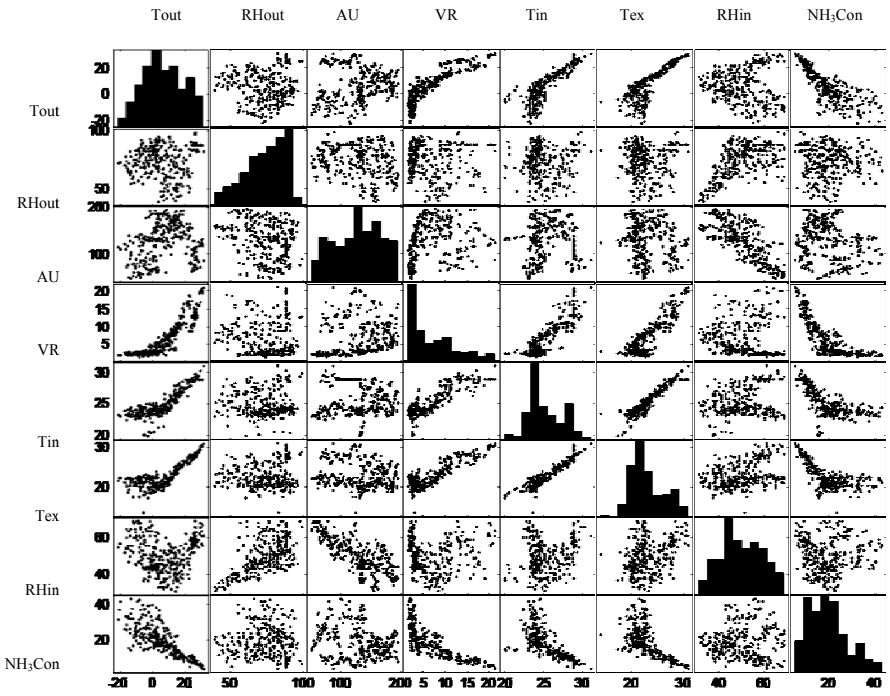

Figure 3. Scatter-plot matrix of the seven variables and NH_3 concentrations.

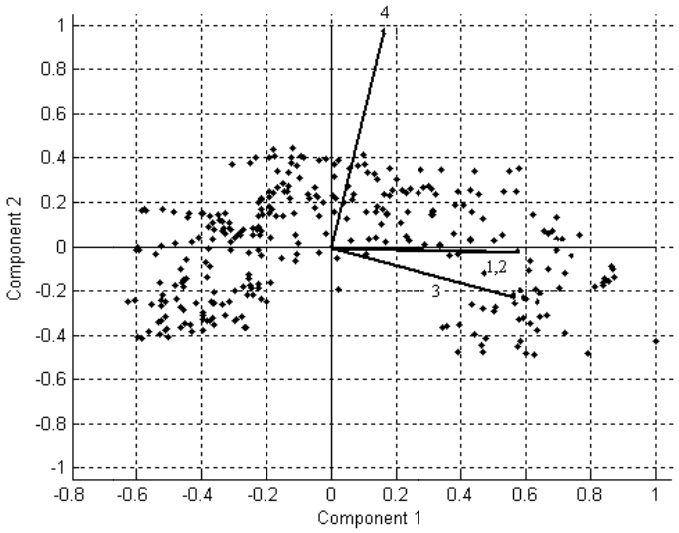

Figure 4. PC coefficients and scores (1=Tout; 2=VR; 3=Tin; 4=AU).

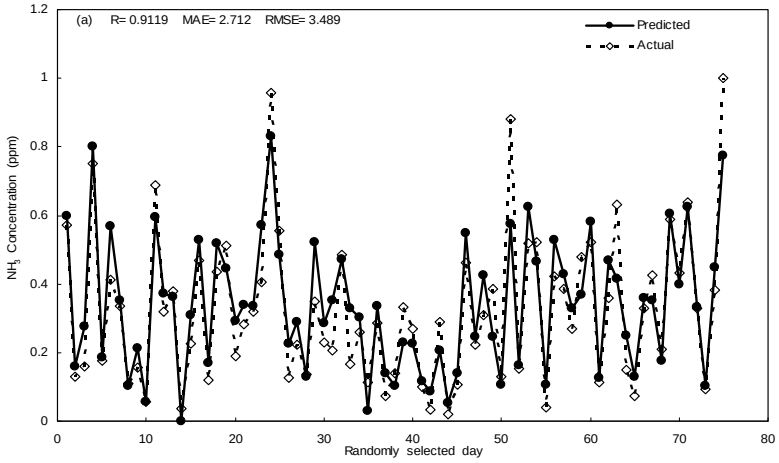
(a) R= 0.9119 MAE= 2.712 RMSE= 3.489
Predicted
Actual
NH3 Concentration (ppm)
Randomly selected day

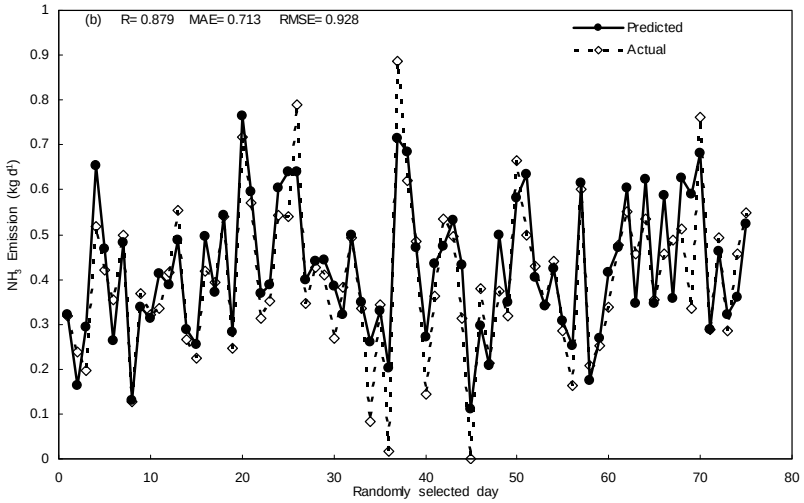
(b) R= 0.879 MAE= 0.713 RMSE= 0.928
Predicted
Actual
NH3 Emission (kg d-1)
Randomly selected day

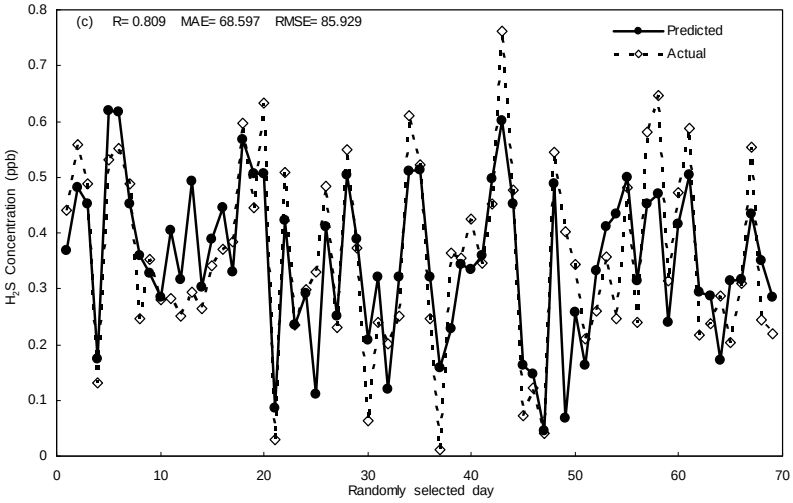
(c) R= 0.809 MAE= 68.597 RMSE= 85.929
Predicted
Actual
H2S Concentration (ppb)
Randomly selected day

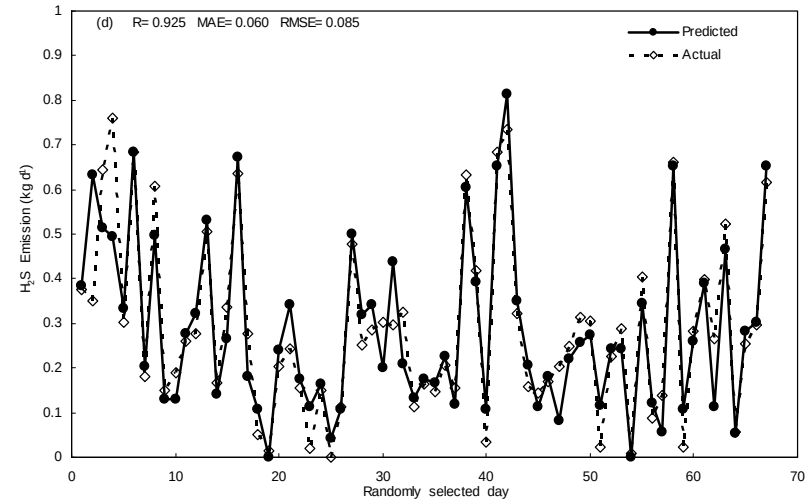
(d) R= 0.925 MAE= 0.060 RMSE= 0.085
Predicted
Actual
H2S Emission (kg d-1)
Randomly selected day

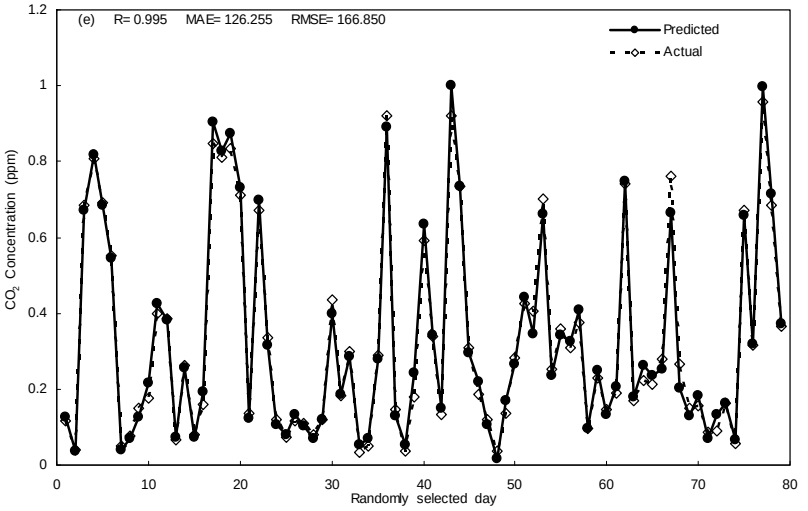
(e) R= 0.995 MAE= 126.255 RMSE= 166.850
Predicted
Actual
CO2 Concentration (ppm)
Randomly selected day

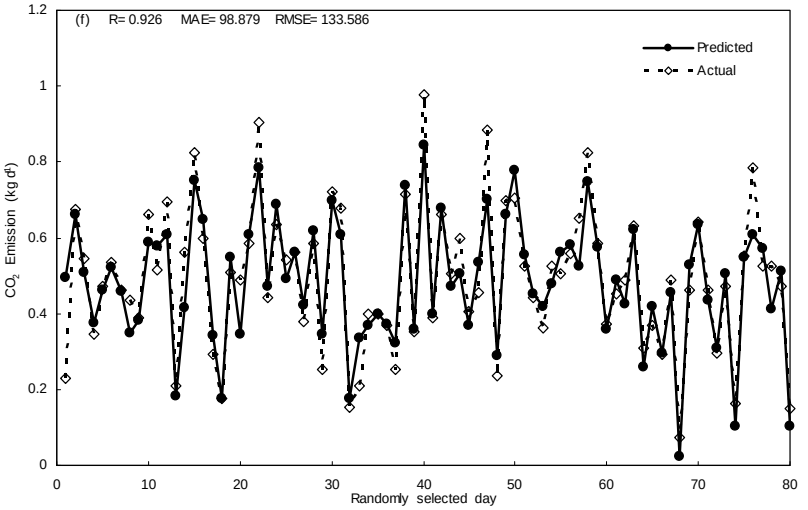
(f) R= 0.926 MAE= 98.879 RMSE= 133.586
Predicted
Actual
CO2 Emission (kg d-1)
Randomly selected day

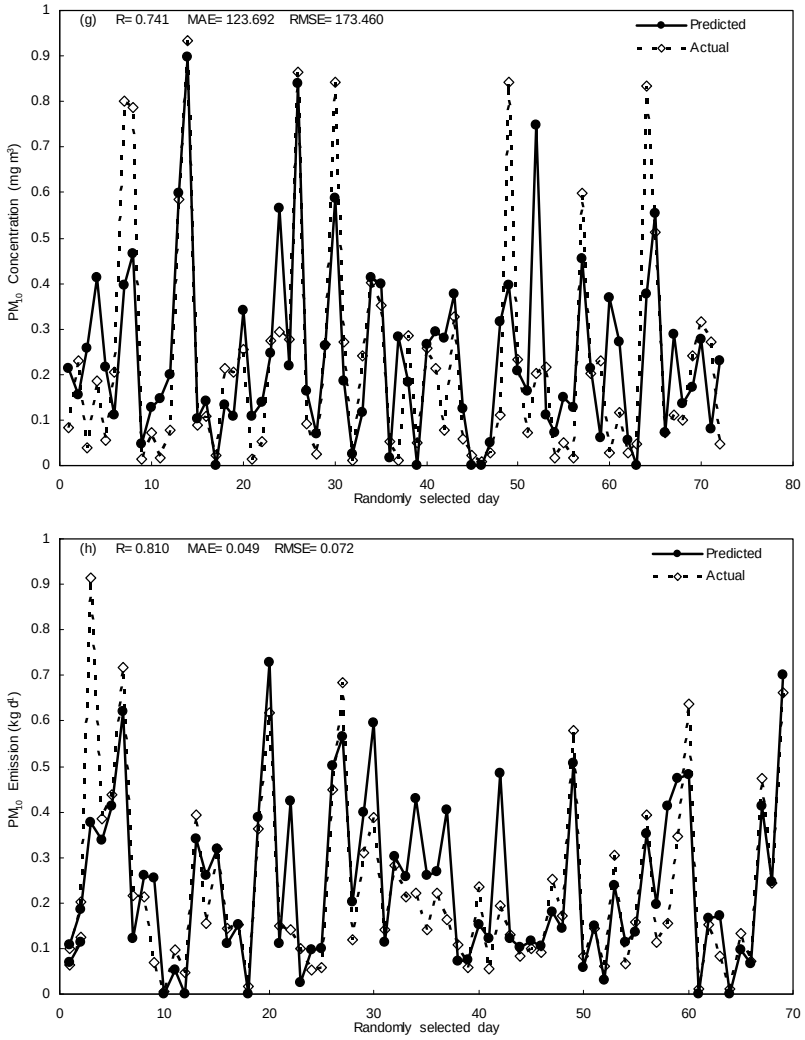

Figure 5. The predicted values of the best network models vs. actual output (a-h indicate NH_3, H_2S, CO_2 and PM_{10} concentration and emission, respectively).

CHAPTER 3. DEVELOPMENT AND COMPARISON OF BACKPROPAGATION AND GENERALIZED REGRESSION NETWORK MODELS TO PREDICT DIURNAL AND SEASONAL GAS AND PM_{10} CONCENTRATIONS AND EMISSIONS FROM SWINE BUILDINGS

A paper published in the Transaction of the American Society of Agricultural and Biological Engineers[1]

G. Sun, S. J. Hoff, B. C. Zelle, and M. A. Nelson[2]

ABSTRACT

The quantification of diurnal and seasonal gas (NH_3, H_2S, and CO_2) and PM_{10} concentrations and emission rates (GPCER) from livestock production facilities is indispensable for the development of science-based setback determination methods and evaluation of improved downwind community air quality resulting from the implementation of gas pollution control. The purpose of this study was to employ backpropagation neural network (BPNN) and generalized regression neural network (GRNN) techniques to model

---

[1] Reprinted with permission of *the Transactions of ASABE*, 2008, 51(2), 685-694.

[2] The authors are **Gang Sun, ASABE Student Member,** Graduate Student, **Steven J. Hoff, ASABE Member,** Professor, **Brian C. Zelle,** Research Associate, and **Minda A. Nelson,** Former Graduate Student, Department of Agricultural and Biosystems Engineering, Iowa State University, Ames, Iowa. **Corresponding author:** Steven J. Hoff, Department of Agricultural and Biosystems Engineering, 212 Davidson Hall, Iowa State University, Ames, IA 50011; phone: 515-294-6180; fax: 515-294-2255; e-mail: hoffer@iastate.edu.

GPCER generated and emitted from swine deep-pit finishing buildings as affected by time of day, season, ventilation rates, animal growth cycles, in-house manure storage levels, and weather conditions. The statistical results revealed that the BPNN and GRNN models were successfully developed to forecast hourly GPCER with very high coefficients of determination (R^2) from 81.15% to 99.46% and very low values of systemic performance indexes. These good results indicated that the artificial neural network (ANN) technologies were capable of accurately modeling source air quality within and from the animal operations. It was also found that the process of constructing, training, and simulating the BPNN models was very complex. Some trial-and-error methods combined with a thorough understanding of theoretical backpropagation were required in order to obtain satisfying predictive results. The GRNN, based on nonlinear regression theory, can approximate any arbitrary function between input and output vectors and has a fast training time, great stability, and relatively easy network parameter settings during the training stage in comparison to the BPNN method. Thus, the GRNN was characterized as a preferred solution for its use in air quality modeling.

Keywords. Backpropogation, Diurnal, Gas, Generalized regression neural network, PM_{10}, Seasonal, Swine buildings.

INTRODUCTION

To address gaseous pollutants generated by livestock and poultry industries, atmospheric dispersion models have been a useful tool for regulatory agencies and state planners to determine reasonable science-based setback distances between animal production facilities and neighboring residences. In addition, environmental researchers and livestock

producers can use models to evaluate downwind community air quality impacts resulting from the implementation of gas pollution control (Hoff et al., 2006). The accuracy of dispersion model predictions relies largely on the accuracy of source emission rates, which are highly variable because they depend on time of the day, seasons, building characteristics, ventilation rate, animal size and density, manure handling systems, and weather conditions (Jacobson et al., 2005). However, due to the lack of data, none of the existing models consider the diurnal, seasonal, and climate variations of odor and gas emission rates from animal buildings. Some researchers simply use randomly measured data or the mean or geometric mean of some data measured during the daytime at any time of the year as the emission rates for the model input (Jacobson et al., 2005), which may result in great uncertainties in predictions. Thus, there is a great need to obtain source gas and PM_{10} concentration and emission rate (GPCER) profiles for the time period of interest (e.g., an hour or a day) to ensure the accuracy of atmospheric dispersion models.

Several studies have investigated diurnal and seasonal odor and gas emission rates from different types of swine production buildings (Sun, 2005; Hoff et al., 2006; Guo et al., 2007). However, direct and long-term measurements of odor, gas, and PM_{10} concentrations and emissions at all animal operations are not practical since every gas source is different and animal and weather conditions change constantly. In the absence of effective and efficient means to directly measure GPCER from each livestock production facility, development of source GPCER mathematical prediction models might be a good alternative to provide reasonably accurate estimates. Three modeling approaches have been proposed for predicting source GPCER: the emission factors method, the multiple regression analysis method, and the process-based modeling method.

Emission factors, expressed by the amount of each substance emitted per animal, are multiplied by the number of animal units to get average air emissions from animal operations. Arogo et al. (2003) attempted but could not assign empirical ammonia emission factors to estimate the average ammonia emission rates from various barns because of the many variables affecting air emissions. The under- or overestimated predictive results showed that using emission factors for all animals in all regions was not appropriate if direct and long-term measurements from a substantial number of representative animal feeding operations have not been conducted.

The regression analysis method uses standard least-squares multivariate regression equations to predict GPCER. The purpose of multiple regression analysis is to establish a quantitative relationship between various predictor variables (e.g., weather and animal conditions, production systems, etc.) and air emissions. This relationship is used to understand which predictors have the greatest effect and to forecast future values of the equation response when only the predictors and the direction of their effects are known. Sun (2005) developed statistical multiple-linear regression models to predict diurnal and seasonal odor and gas concentrations and emissions from confined swine grower-finisher rooms. However, the main weakness of this method is that the complex and sometimes nonlinear relationships of multiple variables can make statistical models complicated and awkward (Comrie, 1997). Moreover, these models seem very dependent on the specifics of the experiment situation. Therefore, it is difficult to apply the developed model to the data from other experiments. The only way to establish a robust set of equations is to sample hundreds of animal feeding operations under different meteorological conditions. The lack of sufficient data is the main cause of the uncertainty of the statistical regression models.

The process-based models (also called mechanical models) determine the movement of elements (e.g., nitrogen, carbon, and sulfur) into, through, and out of the livestock production system, investigate the underlying chemical and physical phenomenon, and identify the effects of changing one or more variables of the system. In many cases, this modeling method uses mass balance equations to describe the mechanisms of gaseous emissions and estimate their characteristic and amount at each transformation stage. Recently, Zhang et al. (2005) established a comprehensive and predictive ammonia emission model to estimate ammonia emission rates from animal feeding operations using a process-based modeling approach. The main processes treated in the model included nitrogen excretion from the animals, animal housing, manure storage, and land application of manure. The results showed that the sensitivity analysis of various variables (e.g., manure production system, animal housing designs, and environmental conditions) needs to be quantified and that additional model validation is needed to improve model predictive accuracy. Other researchers also studied the process of mass (ammonia) transport and developed mechanical models for swine feeding operations (Aarnink and Elzing, 1998; Ni et al., 2000; Kai et al., 2006). Although there has been considerable value in the development and application of mechanistic modeling of ammonia volatilization from the main individual sources, some circumstances of gaseous emissions are not well understood and several parameters are difficult to determine experimentally. For example, adsorption, absorption, and desorption of ammonia from various materials in animal barns might be another emission source, but this mechanism is not easily acquired. Additionally, the gas release process is very complex due to abundant nonlinear relationships between gaseous emissions and the many variables that

cause gas production. Therefore, a major effort would be required in future process-based model studies.

Due to the absence of adequate information available about the process of gas pollutant production, a black-box modeling approach using artificial neural networks (ANN) would be a powerful and promising tool for air quality prediction. Black-box models do not need detailed prior knowledge of the structure and different interactions that exist between important variables. Meanwhile, their learning abilities make the models adaptive to system changes. In recent years, there has been an increasing amount of applications of ANN models in the field of atmospheric pollution forecasting (Hooyberghs et al., 2005; Grivas et al., 2006; Sousa et al., 2007). The results show that ANN black-box models are able to learn nonlinear relationships with limited knowledge about the process structure, and the neural networks generally present better results than traditional statistical methods.

In the literature, little attention has been paid to forecasting source air quality within and from animal buildings. The overarching goal of this project was to develop backpropagation and generalized regression neural network models (black-box models) to predict diurnal and seasonal concentrations and emissions of ammonia, hydrogen sulfide, carbon dioxide, and particulate matter less than or equal to 10 μm (PM_{10}) from swine finishing buildings.

MATERIALS AND METHODS

Experiment Data

The NH_3, H_2S, CO_2, and PM_{10} data were collected from two identical deep-pit swine finishing buildings in Iowa from January 2003 to April 2004. Each building had one room

and was designed to house 960 pigs ranging in weight between ~20 and 120 kg. Slurry was stored in a 2.4 m deep concrete holding pit below a fully slatted floor and was designed to store manure for one year.

An instrument trailer (Mobile Emission Laboratory, MEL) was used to monitor gas and particulate matter concentrations, environmental data, and barn airflow rates. A chemiluminescence NH_3 analyzer (model 17C, TEI, Franklin, Mass.), a pulsed fluorescence SO_2 detector (model 45C, TEI, Franklin, Mass.), and two photoacoustic infrared CO_2 analyzers (model 3600, MSA, Pittsburgh, Pa.) were used to measure gas concentrations at 12 locations within two buildings ("north barn" and "south barn"). A solenoid switching system enabled gas samples to be delivered to each analyzer simultaneously in 10 min switching increments, i.e., each location was monitored for 10 min every 120 min. PM_{10} concentrations were measured continuously using two tapered-element oscillating microbalance (TEOM) ambient PM_{10} monitors (model 1400a, Rupprecht & Patashnick, Albany, N.Y.). Environmental parameters (e.g., temperature, relative humidity, and static pressure) and total building ventilation rates were monitored simultaneously. The total ventilation rates were measured by recording the on/off status of four single-speed tunnel fans, and the on/off status and fan rpm levels of all variable-speed fans (two pit fans, one sidewall fan, and one tunnel fan). The ventilation rate of each fan was obtained *in situ* using a FANS unit, for which calibration equations were developed as a function of static pressure and fan rpm levels for the variable-speed fans (Heber et al., 2006). Gas and PM_{10} emission rates were determined by multiplying the total airflow rate of the exhaust fans by the increase in gas and PM_{10} concentrations between the building ventilation inlet and outlet. The total building emissions were calculated from three emission locations (the blended pit ventilation fans, the sidewall

fan, and the tunnel fans) and were expressed on an animal unit basis by dividing the total emissions by the total animal units (1 AU = 500 kg). During the whole measurement period, approximately three complete production cycles of pigs raised from ~20 to 120 kg were monitored.

The hourly average gas concentrations were determined based on the 10 min sampling data using interpolation, while the hourly gas emissions were obtained by multiplying real-time ventilation rates by the interpolated gas concentrations. Pig weight was measured twice for each group (entering and leaving), and linear interpolation was used to estimate intermediate weights.

The original data set of hourly average GPCER values from the north barn included 7366-9289 lines and four variables. The data set presented diurnal (hourly) and seasonal (16 continuous measurement months) variations of gas and PM_{10} concentrations and emission rates. A multivariate statistical analysis (Sun et al., 2008) was conducted, and from this analysis it was determined that four main variables were significant contributors to the GPCER models. These four input variables include: outdoor temperature (T_{out}), animal units (AU), total building ventilation rate (VR), and indoor temperature (T_{in}).

Backpropagation Neural Network

The multilayer perceptron (MLP) is the most common and successful neural network architecture with feed-forward network topologies in atmospheric science modeling applications; while the most common supervised learning technique used for training artificial neural networks is the multilayer backpropagation (BP) algorithm (Kecman, 2001). The term "backpropagation" refers to the process by which derivatives of network error, with respect to the networks, are fed back to the network and used to adjust the weights so that the

error decreases with each iteration and the neural model gets closer and closer to producing the desired outputs. In this way, BP offers a method of minimizing errors between obtained outputs and desired target values.

There are generally four steps to develop a BP neural network for modeling: (1) preprocess the data, (2) create the network object, (3) train the network, and (4) simulate the network response to new inputs. In this research, the first step (preprocess) was done to scale the inputs and targets to fall within a specified range (from 0 to 1) in case the higher values would drive the training process and mask the contribution of lower valued inputs, as well as to perform a principal component analysis to eliminate redundancy of the data set. In the second step (network construction), the data set was divided into training, validation, and test subsets: one-half for the training set, one-fourth of the data for the validation set, and one-fourth for the test set. The training set was used for computing the gradient and updating the network weights and biases. The validation set was used for improving generalization. The test set was used for validating the network performance. The data in each subset were selected randomly, and then a network was created. The third step (network training) initialized and trained the network. A total of five trainings were conducted. Finally, the trained network was employed to simulate the test data. The performances of the network in each training process and the best network with the highest prediction performances were recorded.

Generalized Regression Neural Network

The generalized regression neural network (GRNN) is a neural network architecture that can solve any function approximation problem if sufficient data are given. Figure 1 is a

schematic of the GRNN architecture with four layers: an input layer, a hidden layer (pattern layer), a summation layer, and an output layer.

The main function of a GRNN is to estimate a linear or nonlinear regression surface on independent variables, i.e., the network computes the most probable value of an output *y* given only training vectors *x* (Specht, 1991). Specifically, the network computes the joint probability density function (pdf) of *x* and *y*. The expected value of the output *y* given the input vector *x* is given by:

$$E\left[\frac{y}{x}\right] = \frac{\int_{-\infty}^{\infty} y f(x,y)\,dy}{\int_{-\infty}^{\infty} f(x,y)\,dy} \tag{1}$$

When the density $f(x, y)$ is not known, it must usually be estimated from a sample of observations of *x* and *y*. The probability estimator $\hat{f}(x,y)$ is based on sample values x^i and y^i of the random variables *x* and *y*:

$$\hat{f}(x,y) = \frac{1}{(2\pi)^{(p+1)/2}\sigma^{(p+1)}} \cdot \frac{1}{n}\sum_{i=1}^{n} \exp\left[-\frac{\left(x-x^i\right)^T\left(x-x^i\right)}{2\sigma^2}\right] \cdot \exp\left[-\frac{\left(y-y^i\right)^2}{2\sigma^2}\right] \tag{2}$$

where *n* is the number of sample observations, and *p* is the dimension of the vector variable *x*.

A physical interpretation of the probability estimate $\hat{f}(x,y)$ is that it assigns sample probability of width σ (smoothing factor or "spread") for each sample x^i and y^i, and the probability estimate is the sum of those sample probabilities.

The squared distance between the input vector x and the training vector x^j is defined as:

$$D_i^2 = \left(x - x^j\right)^T \left(x - x^j\right) \tag{3}$$

and the final output is determined by performing the integrations in equation 4. This result is directly applicable to problems involving numerical data.

$$\hat{f} = \frac{\sum_{i=1}^{n} y^i \exp\left(-\frac{D_i^2}{2\sigma^2}\right)}{\sum_{i=1}^{n} \exp\left(-\frac{D_i^2}{2\sigma^2}\right)} \tag{4}$$

The smoothing factor σ, considered as the size of the neuron's region, is a very important parameter of GRNN. When σ is large, the estimated density is forced to be smooth and in the limit becomes a multivariate Gaussian with covariance σ^2 I (I = unity matrix), whereas a smaller value of σ allows the estimated density to assume non-Gaussian shapes, but with the hazard that wild points may have a great effect on the estimate (Specht, 1991). Therefore, a range of smoothing factors and methods for selecting those factors should be tested empirically to determine the optimum smoothing factors for the GRNN models.

Performance Indicators and Software

The root mean square error (RMSE), mean absolute error (MAE), and coefficient of determination (R^2) between the modeled output and measures of the training and testing data set are the most common indicators to provide a numerical description of the goodness of the model estimates. They are calculated and defined according to equations 5, 6, and 7, respectively (Sousa et al., 2007):

$$\mathrm{RMSE} = \left(\frac{1}{N} \sum_{i=1}^{N} \left[A_i - T_i \right]^2 \right)^{1/2} \tag{5}$$

$$\mathrm{MAE} = \frac{1}{N} \sum_{i=1}^{N} \left| T_i - A_i \right| \tag{6}$$

$$\mathrm{R}^2 = \frac{\sum_{i=1}^{N} \left[A_i - \overline{T} \right]^2}{\sum_{i=1}^{N} \left[T_i - \overline{T} \right]^2} \tag{7}$$

where

N = number of observations

T_i = observed value

A_i = predicted value

$\overline{T}$ = average value of the explained variable on N observations.

RMSE and MAE indicate the residual errors, which give a global idea of the difference between the observed and predicted values. R^2 is the proportion of variability (sum of squares) in a data set that is accounted for by a model. When the RMSE and MAE are at the minimum and R^2 is high ($R^2 \geq 0.80$), a model can be judged as very good (Kasabov, 1998). Neural Network toolbox 5.1 and Statistics toolbox 6.1 in Matlab 7.4 (R2007a) were used in the present study to develop ANN models.

RESULTS AND DISCUSSION

Diurnal and Seasonal Data

Central Iowa climate information based on monthly measurement averages in 2003 could be separated into three typical weather conditions: warm weather (June, July, Aug.; 22.6°C to 27.9°C), mild weather (Apr., May, Sept., Oct.; 10.1°C to 16.4°C), and cold weather (Jan., Feb., Mar., Nov., Dec.; -7.4°C to 2°C). Figure 2 shows three different diurnal and seasonal variation patterns of NH_3 concentrations under different measurement months (Jan., Apr., and July). The mean NH_3 concentrations during the winter were much higher than the NH_3 levels in the summer, and large diurnal NH_3 variations between day and night were observed in April. Diurnal and seasonal fluctuations of other air pollutants also existed. These variations indicated that the gaseous concentrations and emissions during different periods of the day and different seasons must be obtained and considered in air dispersion models for setback distance determination in lieu of random data sampled from snapshot measurements.

BPNN Model Development

The development of a good BP neural network model depends on several important parameters determined using trial-and-error methods. The BP ANN model of NH_3 concentration is presented here as an example showing how to choose these parameters step by step. Other predictive models followed this modeling process and methods.

The initial problem faced in this study was deciding on the BP network architecture, i.e., the number of layers and neurons in the hidden layer as well as the type of activation functions for the layers. A three-layer BP network was constructed to determine if its

prediction performance was superior to a two-layer network. Unfortunately, the results were almost the same. It is worth noting that the bigger network architecture would need more computation and could cause overfitting of the data. In practical applications, one rarely encounters a structure more complex than a two-layer network. Thus, a two-layer BP network was employed, which could produce solutions arbitrarily close to the optimal solution.

Networks are sensitive to the number of neurons in their hidden layers. The optimum number of neurons required is problem dependent, being related to the complexity of the input and output mapping, the amount of noise in the data, and the amount of training data available. Too few neurons lead to underfitting, while too many neurons contribute to overfitting, in which all training points are well-fitted but the fitting curve oscillates widely between these points. Currently, there is no guiding rule to determine how many neurons to use in the hidden layer (Kecman, 2001). The only method available is to try different numbers of neurons to observe how the results look. Table 1 gives the predictive model results (e.g., R^2 between the predicted and actual values) using different numbers of neurons in the hidden layer. The initial number of neurons was 5, and the number was increased until a relatively stable and optimal value was achieved. It can be seen that 40 to 70 neurons in the hidden layer produced high R^2 results (around 0.90). The predictive performance improved slightly with increasing numbers of neurons (90 to 150), but the training time increased significantly. When the network had 5 or 10 neurons in the hidden layer, the R^2 decreased to 0.80. Thus, 40 or 50 were determined as the optimum number of neurons in the hidden layer to avoid low predictive results caused by too few neurons or the overfitting performance from too many neurons.

Note that networks with threshold units are hard to train because the threshold units are not continuous; a small change in the weights does not cause any change in the output. Sigmoid transfer functions are usually preferable to threshold activation functions. With sigmoid units, a small change in the weights produces a change in the output, which makes it possible to tell whether that change in the weights was good or bad. There are three sigmoid transfer functions often used for BP networks: *tansig* (hyperbolic tangent sigmoid) transfer function, *logsig* (log-sigmoid) transfer function, and *purelin* (linear) transfer function. The *tansig* transfer function, which can produce both positive and negative values, tended to yield faster training than the *logsig* transfer function, which can produce only positive values. Table 2 summarizes the BP network performance (e.g., R^2) using different transfer functions. In general, all of the transfer function combinations tested obtained nearly the same network performance expect for the combination of *logsig* and *purelin*. The *tansig* and *logsig* functions were employed in this research.

Once the BP network was constructed and the weights and biases were initialized, the network was ready for training. Neural Network toolbox 5.1 in Matlab offers several training algorithms, such as *traingd*, *traingdx*, *traingda*, *trainrp*, *trainlm*, *trainbfg*, *trainscg*, *trainoss*, *traincgf*, and *traincgp*, which are used for training BP networks. Their characteristics deduced from the experiments are shown in table 3. It was observed that the *traingd* (gradient descent BP) algorithm had the lowest training speed compared to all other algorithms, whereas *traingda* (gradient descent BP with adaptive learning rate) had the fastest training speed, followed by *trainscg* (scaled conjugate gradient BP) and *traingdx* (gradient descent BP with momentum and adaptive learning rate). The *trainoss* (one step secant BP), *trainrp* (resilient BP), *traincgp* (conjugate gradient BP with Polak-Ribiére updates), *trainbfg* (BFGS

quasi-Newton BP), and *traincgf* (conjugate gradient BP with Fletcher-Reeves updates) algorithms could obtain relatively fast training speeds, but their prediction performances were not as good as those made by the *trainlm* (Levenberg-Marquardt BP) algorithm, which was capable of achieving very satisfying statistical results with the highest R^2 and the smallest mean square error among the other algorithms.

Furthermore, although the *traingda* and *traingdx* algorithms trained the BP network much faster than the *trainlm* algorithm, the performances of the former algorithms were very sensitive to the proper setting of the learning rate and momentum. A large learning rate may lead to faster convergence, but it may also cause strong oscillations near the optimal solution or even diverge, while excessively small learning rates result in very long training times. The purpose of adding momentum was to allow the network to respond not only to the local gradient, but also to recent trends in the error surface and allow the network to ignore small features in the error surface. Without momentum, the network can get stuck in a shallow local minimum. Conversely, with momentum, the network can slide through such a minimum. The optimal learning rate and momentum can only be acquired experimentally using the trial-and-error method. Therefore, the *trainlm* algorithm was suitable for training the NH_3 concentration ANN model. However, it has a drawback in that it requires the storage of large matrices. If this is the case, the *trainrp* algorithm may be a good alternative due to its small memory requirement. The optimal parameters of the BP neural network model for the NH_3 concentrations are summarized in table 4.

GRNN Model Development

The only parameter particular to the GRNN is the use of the smoothing factor σ, which significantly affects network performance. Table 5 summarizes the results for the NH_3

concentration GRNN model using different smoothing factor values. The σ values 0.05 and 0.1 can fit data very closely, with higher R^2 values than when using the larger σ, but the larger smoothing factor can make the function approximation smoother.

Statistical Performance of Predictive Models

The statistical performance of the developed predictive models are given in table 6, and scatter plots of predicted values (output *A*) versus respective observed values (target *T*) for the GRNN and BPNN models are illustrated in figure 3. The data presented in figure 3 were normalized using $(A - A_{min})/(A_{max} - A_{min})$ and $(T - T_{min})/(T_{max} - T_{min})$. The intercept and slope of the least squares line between predictions and observations are also displayed. It is worth mentioning that a series of random tests was conducted to evaluate the effectiveness of the models. The results showed that all the models were quite stable. The value of each performance indicator (R^2, MAE, and RMSE) was within 2% change in every case. The results shown here were derived from the best network after the tests.

All the GRNN and BPNN predictive models, except for the PM_{10} concentration and emission BPNN models, had excellent predicting abilities with high R^2 values (81.15% to 99.46%) and low MAE and RMSE values, which implies that these models were well-developed (table 6). The high R^2 indicates that a majority of the variability in the air pollutant outputs could be explained by the four input variables (outdoor and indoor temperature, building ventilation rate, and animal units).

All the GRNN predictive models had higher R^2 values and lower MAE and RMSE values than the BPNN models. This demonstrates that the GRNN models outperformed the

BPNN models. Thus, the GRNNs were able to predict diurnal and seasonal gas and particulate matter concentrations and emissions more effectively.

SUMMARY AND CONCLUSIONS

Backpropagation and generalized regression neural network methods were employed to explore the complex and highly nonlinear relationships between air pollutants and four variables (outdoor temperature, animal units, ventilation rate, and indoor temperature) on the measurements of diurnal and seasonal NH_3, H_2S, CO_2, and PM_{10} levels and emissions from deep-pit swine buildings.

It was found that the obtained results of BPNN and GRNN predictions were in good agreement with the actual measurements, with coefficient of determination (R^2) values between 81.15% and 99.46% and very low values of systemic performance indexes. The good results indicated the ANN technologies were capable of accurately modeling source air quality within the livestock production facilities and emissions from these production facilities.

The process of constructing, training, and simulating the BP network models was very complicated. Likewise, determining the best values for several network parameters, such as the number of layers and neurons, type of activation functions and training algorithms, learning rates, and momentum, were difficult. The effective way of obtaining good BP modeling results was to use some trial-and-error methods and thoroughly understand the theory of backpropagation. Conversely, for the GRNN models, there was only one parameter (the smoothing factor) that needed to be adjusted experimentally. Moreover, the BP network performance was very sensitive to randomly assigned initial values. However,

this problem was not faced in GRNN simulations. The GRNN approach did not require an iterative training procedure as in the backpropagation method. The local minima problem was also not faced in the GRNN simulations. Other significant characteristics of the GRNN in comparison to the BPNN were the excellent approximation ability, fast training time, and exceptional stability during the prediction stage. Thus, the GRNN technology outperformed BP, which has been demonstrated in this study. It can be recommended that a generalized regression neural network be used instead of a backpropagation neural network in source air quality modeling.

REFERENCES

Aarnink, A. J. A., and A. Elzing. 1998. Dynamic model for ammonia volatilization in housing with partially slatted floors, for fattening pigs. *Livestock Prod. Sci.* 53(2): 153-169.

Arogo, J., P. W. Westerman, and A. J. Heber. 2003. A review of ammonia emissions from confined swine feeding operations. *Trans. ASAE* 46(3): 805-817.

Comrie, A.C. 1997. Comparing neural networks and regression models for ozone forecasting. *J. Air Waste Mgmt. Assoc.* 47: 653-663.

Kai, P., B. Kaspers, and T. van Kempen. 2006. Modeling source of gaseous emissions in a pig house with recharge pit. *Trans. ASABE* 49(5): 1479-1485.

Kasabov, N. K. 1998. *Foundations of Neural Networks, Fuzzy Systems and Knowledge Engineering*. Cambridge, Mass.: MIT Press.

Kecman, V. 2001. *Learning and Soft Computing*. Cambridge, Mass.: MIT Press.

Grivas, G., and A. Chaloulakou. 2006. Artificial neural network models for prediction of PM_{10} hourly concentrations, in the greater area of Athens, Greece. *Atmos. Environ.* 40(7): 1216-1229.

Guo, H., W. Dehod, J. Agnew, J. R. Feddes, C. Lague, and S. Pang. 2007. Daytime odor emission variations from various swine barns. *Trans. ASABE* 50(4): 1365-1372.

Heber, A. J., J. Ni, T. T. Lim, P. Tao, A. M. Schmidt, J. A. Koziel, D. B. Beasley, S. J. Hoff, R. E. Nicolai, L. D. Jacobson, and Y. Zhang. 2006. Quality assured measurements of animal building emissions: Gas concentrations. *J. Air and Waste Mgmt. Assoc.* 56(10): 1472-1483.

Hoff, S. J., D. S. Bundy, M. A. Nelson, B. C. Zelle, L. D. Jacobson, A. J. Heber, J. Ni, Y. Zhang, J. A. Koziel, and D. B. Beasley. 2006. Emissions of ammonia, hydrogen sulfide, and odor before, during, and after slurry removal from a deep-pit swine finisher. *J. Air Waste Mgmt. Assoc.* 56(5): 581-590.

Hooyberghs, J., C. Mensink, G. Dumont, F. Fierens, and O. Brasseur. 2005. A neural network forecast for daily average PM_{10} concentrations in Belgium. *Atmos. Environ.* 39(18): 3279-3289.

Jacobson, L. D., H. Guo, D. R. Schmidt, R. E. Nicolai, J. Zhu, and K. A. Janni. 2005. Development of the OFFSET model for determination of odor-annoyance-free setback distances from animal production sites: Part I. Review and experiment. *Trans. ASABE* 48(6): 2259-2268.

Lim, T.T., A. J. Heber, and J. Ni. 2000. Odor setback guideline for swine production systems. In *odors and VOC Emissions 2000*. Alexandria, Va.: Water Environment Federation.

Ni, J., J. Hendriks, C. Vinckier, and J. Coenegrachts. 2000. Development and validation of a dynamic mathematical model of ammonia release in pig house. *Environ. Intl*. 26(1-2): 97-104.

Sousa, S. I. V., F. G. Martins, M. C. M. Alvim-Ferraz, and M. C. Pereira. 2007. Multiple linear regression and artificial neural network based on principal components to predict ozone concentrations. *Environ. Modeling and Software* 22(1): 97-103.

Specht, D. F. 1991. A general regression neural network. *IEEE Trans on Neural Networks* 2(6): 568-576.

Sun, G. 2005. Monitoring and modeling diurnal and seasonal odor and gas emission profiles for swine grower/finisher rooms. MS thesis. Saskatoon, Saskatchewan, Canada: University of Saskatchewan, Department of Agricultural and Bioresource Engineering.

Sun, G., S. J. Hoff, B. C. Zelle, and M. A. Smith. 2008. Forecasting daily source air quality using multivariate statistical analysis and radial basis function networks. *J. Air Waste Mgmt. Assoc*. 58(12): 1571-1578.

Zhang, R. H., T. R. Rumsey, J. R. Fadel, J. Arogo, Z. Wang, G. E. Mansell, and H. Xin. 2005. A process-based ammonia emission model for confinement animal feeding operations: Model development. In *Proc. 14th Intl. Emission Inventory Conf.* Research Triangle Park, N.C.: U.S. EPA, Office of Air Quality Planning and Standards.

NOMENCLATURE

AU = animal units

BP = backpropagation

BPNN = backpropagation neural network

Con = concentration

ER = emission rate

GPCER = gas and PM_{10} concentration and emission rate

GRNN = generalized regression neural network

logsig = log sigmoid transfer function

MAE = mean absolute error

PCA = principal component analysis

purelin = linear transfer function

RMSE = root mean square error

R^2 = coefficient of determination

tansig = tangent sigmoid transfer function

T_{in} = indoor temperature (°C)

T_{out} = outdoor temperature (°C)

trainbfg = BFGS quasi-Newton BP training algorithm

traincgf = conjugate gradient BP with Fletcher-Reeves updates training algorithm

traincgp = conjugate gradient BP with Polak-Ribiére updates training algorithm

traingd = gradient descent BP training algorithm

traingda = gradient descent BP with adaptive learning rate training algorithm

traingdx = gradient descent BP with momentum and adaptive learning rate training algorithm

trainlm = Levenberg-Marquardt BP training algorithm

trainoss = one step secant BP training algorithm

trainrp = resilient BP training algorithm

trainscg = scaled conjugate gradient BP training algorithm

VR = ventilation rates ($m^3\ s^{-1}$)

Table 1. Results using different numbers of neurons in the hidden layer. [a]

No. of Neurons	R^2 of Predicted vs. Actual					Avg. R^2	Elapsed Time[b]
5	0.7926	0.7862	0.7898	0.8090	0.7906	0.7936	10.3905
10	0.8079	0.8283	0.7830	0.8207	0.8337	0.8147	11.1335
20	0.8697	0.8491	0.8610	0.8579	0.8596	0.8595	12.7646
40	0.8901	0.8796	0.8878	0.8951	0.8826	0.8870	33.8522
50	0.9281	0.9358	0.9194	0.9080	0.9263	0.9235	34.7166
70	0.9136	0.8786	0.8797	0.8968	0.9077	0.8953	52.8628
90	0.9556	0.9541	0.9313	0.9366	0.9622	0.9480	71.3110
120	0.9272	0.9646	0.9415	0.9305	0.9347	0.9397	99.6590
150	0.9400	0.9367	0.9448	0.9186	0.9359	0.9352	138.6449

[a] The testing network was a two-layer network with *tansig* and *logsig* transfer functions. Five training times were used for each training process. The training algorithm was *trainlm* .

[b] The elapsed time (s) indicates the time of one training. The computer had an Intel Pentium 3.0G processor and 3.0 Gb RAM.

Table 2. Results using different transfer functions.

Transfer Functions[a]	R^2 of Predicted vs. Actual					Avg. R^2	Max. R^2
tansig , *logsig*	0.9103	0.8985	0.9122	0.9284	0.9185	0.9136	0.9284
tansig , *tansig*	0.8883	0.8740	0.8478	0.8799	0.8880	0.8756	0.8883
logsig , *logsig*	0.8905	0.9067	0.9136	0.9067	0.8874	0.9010	0.9136
logsig , *tansig*	0.8845	0.8910	0.8908	0.8829	0.8556	0.8810	0.8910
tansig , *purelin*	0.8951	0.8759	0.8898	0.9023	0.8971	0.8920	0.9023
logsig , *purelin*	0.8571	0.8361	0.8331	0.8248	0.8337	0.8370	0.8571

[a] The first term indicates the transfer function for the hidden layer; the second term indicates the transfer function for the output layer. The testing network was a two-layer network with the *trainlm* algorithm and 50 neurons in the hidden layer. Five training times were used for each training process.

Table 3. Results using different training algorithms. [a]

Training Algorithm	R^2 of Predicted vs. Actual					Avg. R^2	Elapsed Time[b]
traingd	0.7447	0.8658	0.8127	0.9042	0.8541	0.8363	140.9733
traingdx	0.8447	0.7370	0.7583	0.7992	0.7872	0.7853	23.4912
traingda	0.7019	0.7385	0.7381	0.7120	0.7410	0.7263	18.3326
trainrp	0.8528	0.8356	0.8277	0.8146	0.8186	0.8299	30.6993
trainlm	0.9032	0.9222	0.9118	0.8705	0.8935	0.9002	34.0856
trainbfg	0.7913	0.7961	0.8101	0.8232	0.8206	0.8083	33.6143
trainscg	0.8119	0.8187	0.8090	0.8450	0.8097	0.8189	20.1881
trainoss	0.7935	0.7807	0.7722	0.7233	0.7728	0.7685	24.1788
traincgf	0.7932	0.7344	0.8269	0.8240	0.8230	0.8003	41.2675
traincgp	0.7236	0.8523	0.7988	0.8150	0.8085	0.7996	32.4685

[a] The testing network was a two-layer network with *tansig* and *logsig* transfer functions and 50 neurons in the hidden layer. Five training times were used for each training process.

[b] Elapsed time (s) indicates the time of one training. The computer had an Intel Pentium 3.0G processor and 3.0 Gb RAM.

Table 4. Optimal parameters of the BP ANN model.

Parameter	Value/Function/Method
Network architecture	2-layer network
Input features	T_{out}, AU, VR, and T_{in} [a]
Layer neurons	4-50-1 (input-hidden-output layer)
Missing data	Substituting the neighborhood mean
Data normalization	*mapstd* function
PCA[b]	*processpca* function
Transfer function	*tansig* (hidden layer); *logsig* (output layer)
Training algorithm	*trainlm*

[a] T_{out} = outdoor temperature (°C), AU = animal units, VR = ventilation rates (m^3 s^{-1}), T_{in} = indoor temperature (°C).

[b] PCA = principal component analysis.

Table 5. GRNN results using different smoothing factors. [a]

σ	R^2 of Predicted vs. Actual					Avg. R^2	Elapsed Time[b]
0.05	0.9702	0.9946	0.9536	0.9449	0.9471	0.9621	5.2021
0.1	0.9188	0.8965	0.9227	0.9194	0.9013	0.9117	5.6713
0.3	0.7546	0.7466	0.7375	0.7323	0.7116	0.7365	5.3201
0.5	0.6466	0.6988	0.6533	0.6635	0.6959	0.6716	5.4735
1	0.4840	0.5125	0.4922	0.5003	0.5006	0.4979	5.5726

[a] Five training times for each training process.

[b] The elapsed time (s) indicates the time of one training. The computer had an Intel Pentium 3.0G processor and 3.0 Gb RAM.

Table 6. Statistical performance of developed predictive models.

Model[a]	Number of Data Points[b]	GRNN			BPNN		
		R^2	MAE	RMSE	R^2	MAE	RMSE
NH_3Con (ppm)	8048	0.9946	1.92	3.12	0.9074	2.60	3.58
NH_3ER (kg d^{-1})	7973	0.9774	0.80	1.35	0.8825	1.38	2.12
H_2SCon (ppb)	7479	0.9167	102.54	181.37	0.8281	158.01	227.03
H_2SER (kg d^{-1})	7366	0.9258	0.08	0.14	0.8115	0.13	0.19
CO_2Con (ppm)	8500	0.9838	184.20	302.78	0.9785	242.93	376.19
CO_2ER (kg d^{-1})	8215	0.9410	144.02	217.29	0.8691	159.51	223.23
PM_{10}Con (μg m^{-3})	9187	0.8570	125.52	241.60	0.7726	180.86	290.40
PM_{10}ER (kg d^{-1})	9289	0.8719	0.07	0.14	0.6689	0.09	0.16

[a] Con and ER indicate the concentrations and emission rates, respectively.

[b] Indicates the number of total data points. The test data for the predictive models were 25% of the total data.

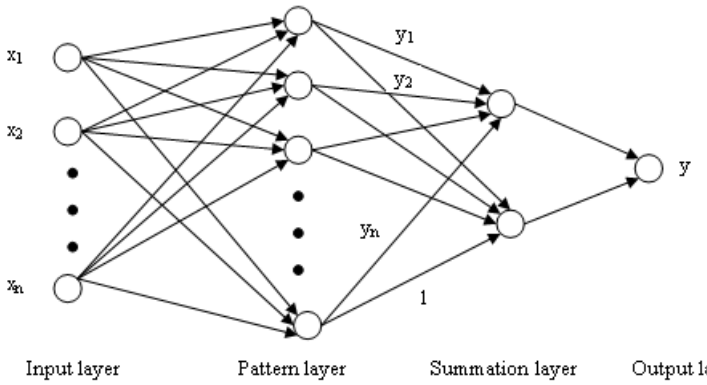

Figure 1. Generalized regression neural network architecture.

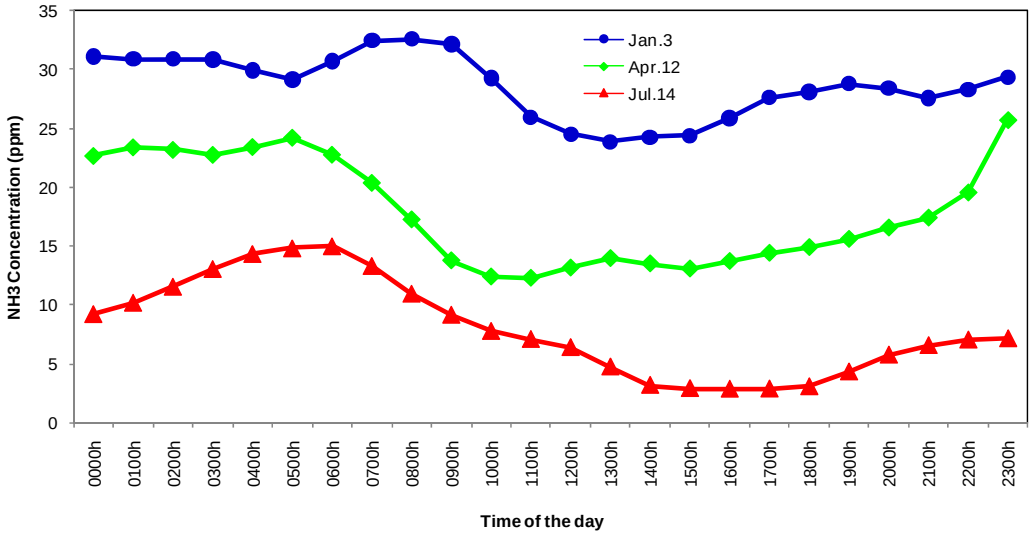

Figure 2. Different diurnal and seasonal variation patterns of NH_3 concentrations from the deep-pit swine finishing building (hourly averages presented for three selected days).

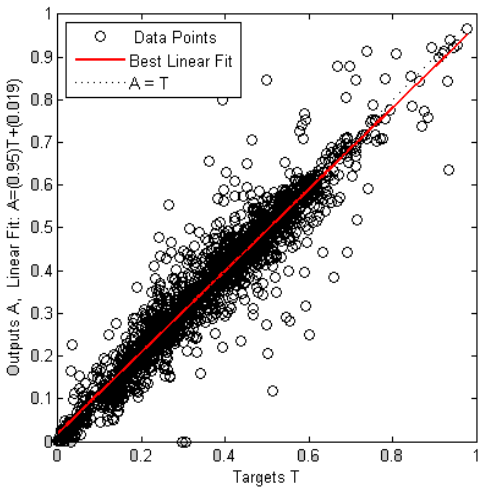

(a) NH_3Con- GRNN

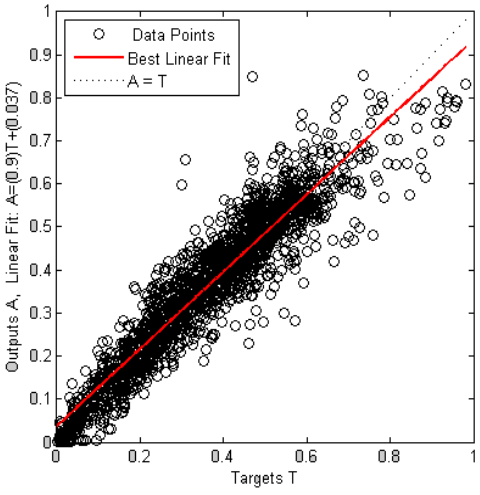

(b) NH_3Con- BPNN

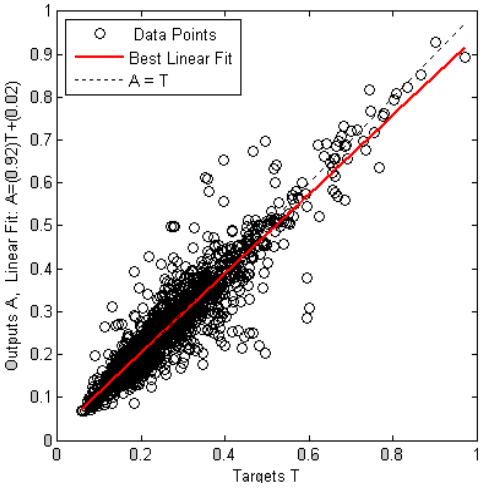

(c) NH_3ER- GRNN

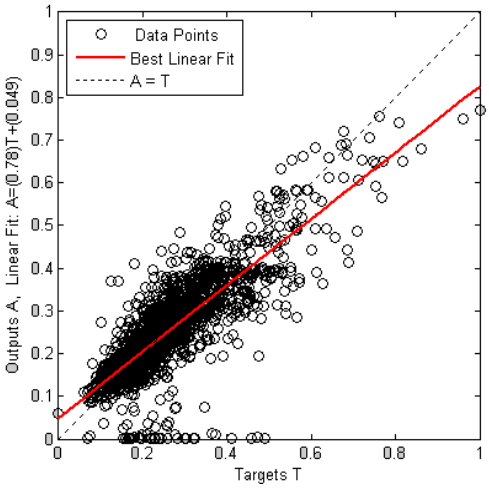

(d) NH_3ER- BPNN

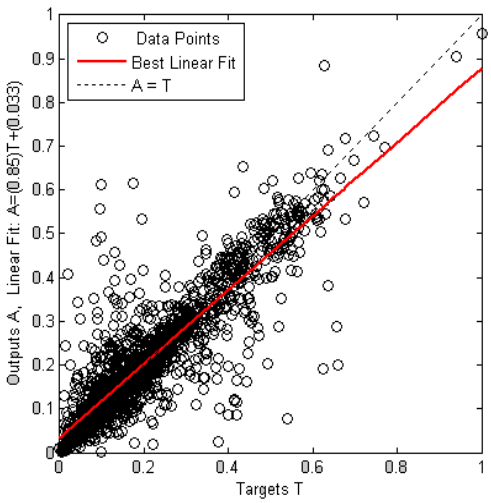

(e) H_2SCon- GRNN

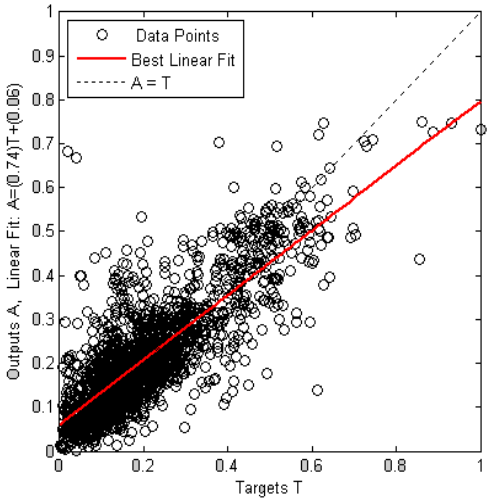

(f) H_2SCon- BPNN

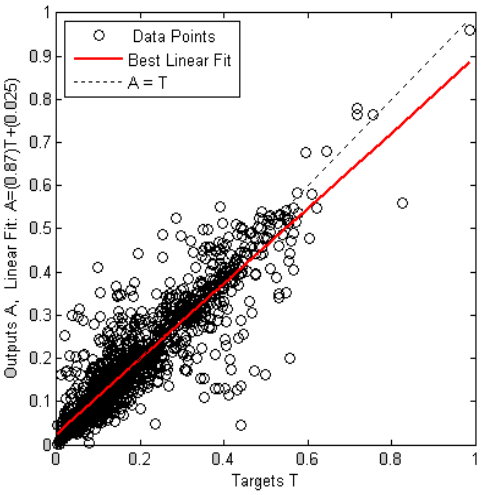

(g) H_2SER- GRNN

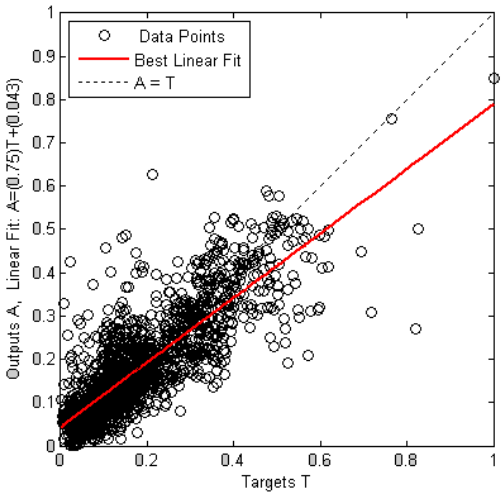

(h) H_2SER- BPNN

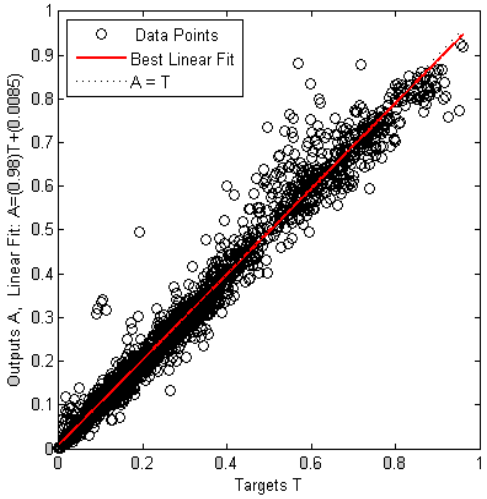

(i) CO_2Con- GRNN

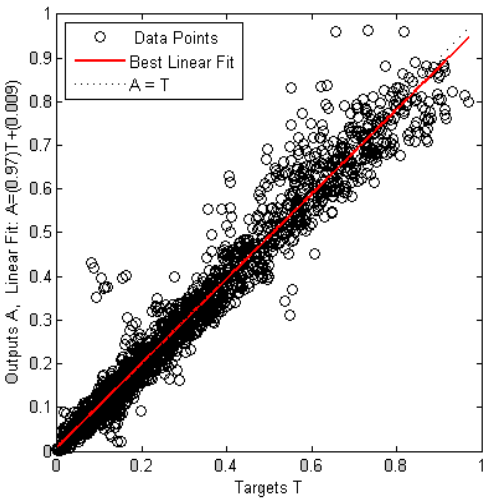

(j) CO_2Con- BPNN

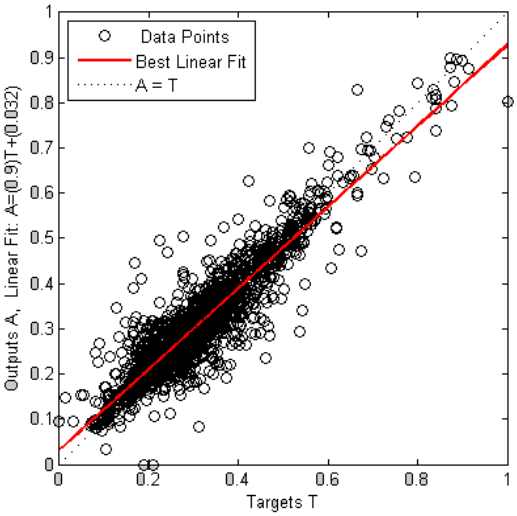

(k) CO_2ER- GRNN

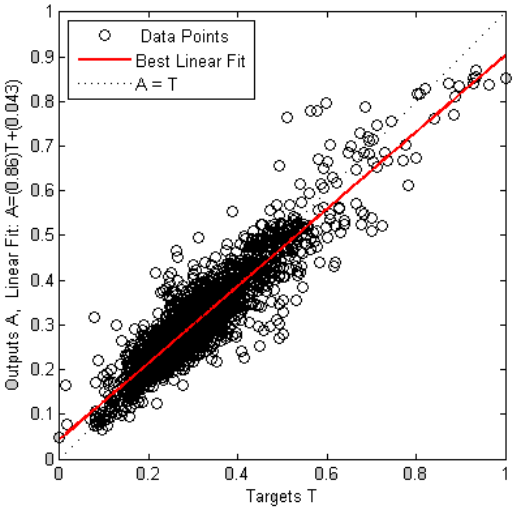

(l) CO_2ER- BPNN

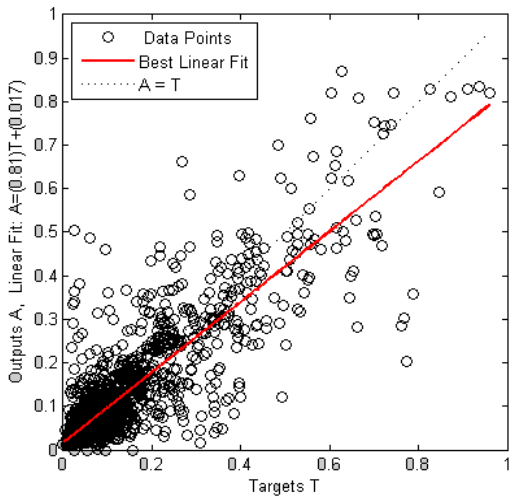

(m) PM10Con- GRNN

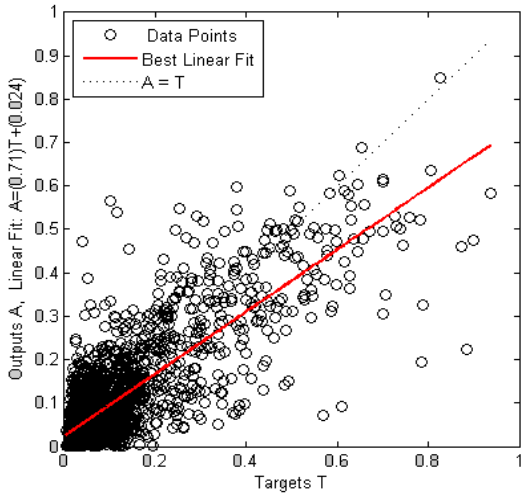

(n) PM10Con- BPNN

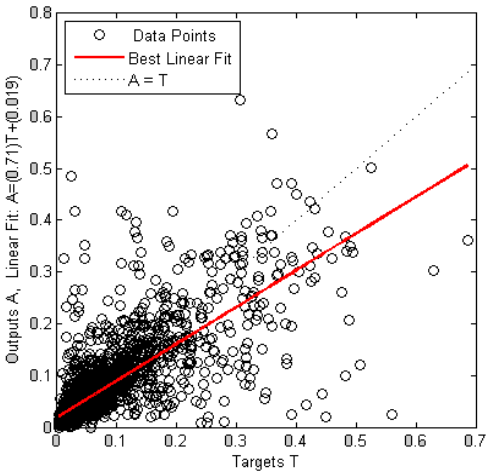

(o) PM10ER- GRNN

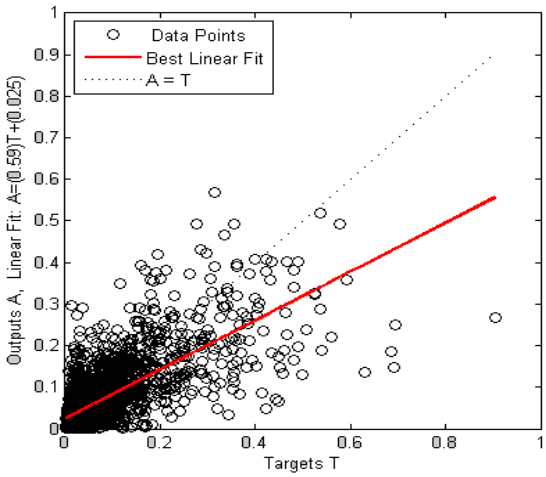

(p) PM10ER- BPNN

Figure 3. Scatter plots (a) to (p) of predicted values (output A) versus respective observed values (target T) for the GRNN and BPNN models (Con and ER indicate the concentrations and emission rates, respectively.

CHAPTER 4. PREDICTION OF INDOOR CLIMATE AND LONG-TERM AIR QUALITY USING THE BTA-AQP MODEL: PART I. BTA MODEL DEVELOPMENT AND EVALUATION

A paper published in the Transaction of the American Society of Agricultural and Biological Engineers[1]

G. Sun and S. J. Hoff [2]

ABSTRACT

The objective of this research was to develop a building thermal analysis and air quality predictive (BTA-AQP) model to predict ventilation rate, indoor temperature and long-term air quality (NH_3, H_2S and CO_2 concentrations and emissions) for swine deep-pit buildings. This paper, Part I of II, presents a lumped capacitance model (BTA model) to predict the transient behavior of ventilation rate and indoor air temperature according to the thermo-physical properties of a typical swine building, set-point temperature scheme, fan staging scheme, transient outside temperature, and the heat fluxes from pigs and supplemental heaters. The obtained ventilation rate and resulting indoor air temperature

---

[1] Reprinted with permission of *the Transactions of ASABE*, 2010, 53 (3), 863- 870.

[2] The authors are **Gang Sun, ASABE Member Engineer,** Graduate Student, **Steven J. Hoff, ASABE Member,** Professor, Department of Agricultural and Biosystems Engineering, Iowa State University, Ames, Iowa. **Corresponding author:** Steven J. Hoff, Department of Agricultural and Biosystems Engineering, 212 Davidson Hall, Iowa State University, Ames, IA 50011; phone: 515-294-6180; fax: 515-294-2255; e-mail: hoffer@iastate.edu.

combined with animal growth cycle, in-house manure storage level, and typical meteorological year (TMY3) data (NSRDB, 2008) were used as inputs to the air quality predictive model (Part II paper) based on the generalized regression neural network (GRNN-AQP model), which was presented in an earlier article. The statistical results indicated that the performance of the BTA model for predicting ventilation rate and indoor air temperature were very good in terms of low mean absolute error, a coefficient of mass residual values equal to 0, an index of agreement value close to 1, and Nash-Sutcliffe model efficiency values higher than 0.65. The graphical presentations of the predicted vs. actual ventilation rate and indoor temperature were also provided to demonstrate that the BTA model was able to accurately estimate indoor climate and therefore could be used as input variables for the GRNN-AQP model discussed in Part II of this research (Sun and Hoff, 2010).

Keywords. Building thermal analysis (BTA), Air quality, indoor climate, Nash-Sutcliffe model efficiency.

INTRODUCTION

Due to the absence of a nationwide monitoring network for quantifying long-term air emission inventories of livestock production facilities, state and federal regulatory agencies in the United States have identified a need for air quality predictive (AQP) models to assess the impact of annual airborne pollutants on human health, the ecological environment, and global warming. Moreover, with the increasing number of complaints and lawsuits against the livestock industry, state planners, environment scientists and livestock producers also need AQP models to determine science-based setback distances between animal feeding operations and neighboring residences as well as evaluate relevant emission abatement

strategies. Most of the AQP models proposed so far use mass balance equations to describe the mechanisms of gaseous emissions, estimate their characteristic and amount at each transformation stage, and forecast gas release from animal production sites (Aarnink et al., 1998; Ni et al., 2000; Kai et al., 2006). Source odor and gas concentrations and emission rates are very difficult to model because they are highly variable with time of day, season, weather conditions, building characteristics, ventilation rate, animal growth cycle, and manure handling method. Thus, the whole modeling process can be regarded as a complicated dynamic system with many nonlinear governing relationships. Also, there still exist some circumstances of gaseous emissions that cannot be explained with our current limited scientific understanding. On the contrary, neural network modeling techniques, unlike the traditional methods based on physical principles and detailed prior knowledge of the modeling structure, are able to capture the interactions of numerous multivariate parameters, learn the relationships between input and output variables, and give quite satisfying prediction results. Sun et al. (2008a) developed backpropagation and generalized regression neural network models to predict diurnal and seasonal gas and PM_{10} concentrations and emissions from swine deep-pit finishing buildings. It was found that the obtained forecasting results of the neural network models were in good agreement with actual field measurements, with coefficient of determination values between 81.2% and 99.5% and very low values of systemic performance indices. The promising results from this work indicated that artificial neural network technologies were capable of accurately modeling source air quality within and emissions from these livestock production facilities.

Although AQP models can be used as a useful tool to forecast air quality over a time period that are beyond an actual monitoring period, the main input variables for the model

must be known which require field measurements. These variables include indoor environment (indoor, inlet and exhaust temperature and relative humidity), outdoor climate conditions (outdoor temperature, relative humidity, wind speed, wind direction, solar energy and barometric pressure), pig size and density (animal units), building ventilation rate, animal activity, overall management practices, and properties of the stored manure, to name a few. Sun et al. (2008b) performed a multivariate statistical analysis and identified four significant contributors to the AQP models: outdoor temperature, animal units, total building ventilation rate, and indoor temperature. The purpose of introducing fewer uncorrelated variables to the models is to reduce model structure complexity, eliminate model over-fitting problems, and minimize field monitoring costs without sacrificing model predictive accuracy. Conducting long-term field measurements of the identified four variables using current engineering approaches are still time consuming and expensive. Therefore, making use of simulation programs is a good alternative to obtain the required significant input variables for AQP models.

Basically, there are three steady-state models used to calculate indoor climate of livestock buildings which include those based on heat, moisture or carbon dioxide balances (Albright 1990). Pedersen et al. (1998) compared these three balance methods for estimating the ventilation rate in insulated animal buildings. They reported that the three methods could give good prediction results on a 24-hr basis when the temperature differences between inside and outside, absolute humidity and CO_2 concentrations were greater than 2 $°C$, 0.5×10^{-3} kg water per kg dry air and 200 ppm, respectively for the buildings tested in Northern Europe. A simple steady-state balance model (Schauberger et al., 1999) was developed for the sensible and latent heat fluxes and CO_2 mass flows resulting in the

prediction of inside temperature and ventilation rate of mechanically ventilated livestock buildings. The obtained variables were further applied for diurnal and annual odor emission estimates. Due to the lack of field measurements, the accuracy of the predicted parameters could not be determined. Morsing et al. (2003) released a computer program entitled StaldVent™ to help design and evaluate heating and ventilation systems in animal houses. They primarily used a steady-state energy balance method to predict the required ventilation rate and heat capacity, room temperature, CO_2 concentration, and expected energy consumption throughout the year.

On the other hand, indoor climate can be predicted by studying thermal transients in buildings. Nannei and Schenone (1999) developed a simplified numerical model for building thermal transient simulation. The model can be applied to compute the room air temperature and the temperature of the inner surface of the walls. The good numerical results compared with the experimental data indicated that this model was useful for the study of unsteady thermal performance. Mendes et al. (2001) presented a dynamic multimodal capacitive nonlinear model to analyze transient indoor air temperature using Matlab/Simulink™ (Matlab 5.0, 1999). This thermal model was improved by introducing internal gains and the inter-surface long-wave radiation. The predicted results were not experimentally validated however. Morini and Piva (2007) investigated the dynamic thermal behavior of residential heating and cooling systems with control systems during a sinusoidal variation of the outside temperature. The core of their program employed mechanical and thermal energy conservation equations implemented in the Simulink™ environment. It was found that their transient model outperformed the standard steady-state approach.

The overall objective of this research is to predict indoor climate and long-term air quality (NH_3, H_2S and CO_2 concentrations and emissions) for swine deep-pit finishing buildings using a transient building thermal analysis and air quality predictive (BTA-AQP) model and a typical meteorological year data base. This paper acts as Part I and discusses the BTA model development and resulting indoor thermal climate predictions. A second paper acts as Part II (Sun and Hoff, 2010) where specific air quality predictive results are presented for the complete BTA-AQP model.

MATERIALS AND METHODS

Description of typical deep-pit swine building

A mechanically ventilated deep-pit (2.4 m) swine finishing building, located in central Iowa, was used for this research. As shown in figure 1, this swine building was 60 m long and 13 m wide, designed to house 960 finishing pigs from ~20 to 120kg. Gas concentrations inside the building, near wall and pit exhaust fans, and an outside location (background) were monitored *via* a mobile emission laboratory and accompanying air sampling lines. Also, pertinent environment parameters (temperature, relative humidity, and static pressure) and total building ventilation rate were simultaneously measured. During cold-to-mild seasons, pit fans 1 and 2, side wall fan 3, and tunnel fans 4 and 5 (figure 1) combined with a series of 10 rectangular center-ceiling inlets were used to distribute fresh air and remove moisture, odors and aerosols within the building; while all the fans (except side wall fan 3) and an adjustable curtain at the opposing end wall were used to maintain suitable indoor environment under warm and hot weather (i.e. tunnel ventilation). The total ventilation rate was obtained by recording the on/off status of four single-speed tunnel fans

(fans 5, 6, 7, and 8) and the on/off status along with fan rpm levels for all variable speed fans (fans 1,2,3, and 4). The ventilation rate of each fan was measured *in situ* using a FANS unit (Gates et al., 2004) where calibration equations were developed as a function of static pressure and fan rpm levels for variable speed fans. Gas emission rates were determined by multiplying fan airflow rate by representative gas concentration differences between inlet and outlet for all fans operating at any given time. Field monitoring was conducted for 15-months between January 2003 and March 2004, with the 1-year monitoring in 2003 used in this research for model prediction comparison. Details of the field monitoring and overall procedures used can be found in Heber et al. (2006).

Transient BTA model development

A generalized lumped capacitance model was used to predict inside barn temperature changes as a function of outdoor temperature, animal units, supplemental heat, the building envelope thermal characteristics, and the ventilation staging system for the monitored barn described above. In general, this model was developed from the following;

$$\frac{dU}{dt} = Energy_{in} - Energy_{out} \tag{1}$$

where

U = internal energy of the air mass inside the barn, J.

$= m\ C_{v,air}\ T_{in,i}$

m= mass of air inside barn, kg.

$= \rho_{air} V$

ρ_{air}= inside air density (an assumed constant of 1.20 kg/m^3).

V= volume of airspace in barn, m^3.

$C_{v,air}$= specific heat of air at constant volume (an assumed constant of 719 J/kg-^{o}C).

$T_{in,i}$= predicted inside barn temperature at current time i, ^{o}C.

t= time, s.

Assuming that the mass (m) and specific heat ($C_{v,air}$) are constant results in;

$$\frac{dT_{in,i}}{dt} = \frac{\{Energy_{in} - Energy_{out}\}}{\rho_{air} VC_{v\,air}} \tag{2}$$

The energy inputs ($Energy_{in}$) considered with this BTA model include sensible heat gained from the animals ($q_{animals}$) and any supplemental heat input (q_{heater}) required to maintain a desired set-point temperature inside the barn. The losses ($Energy_{out}$) considered with this BTA model include net envelope losses ($BHLF(T_{inside}-T_{out})$) and net enthalpy losses from the ventilation air ($VR\rho_{air}C_{p,air}(T_{inside}-T_{out})$. Integrating equation 2 results in the following generalized lumped-capacity BTA model used for this research;

$$T_{in,i} = T_{in,i-1} + \frac{\left\{q_{animals} + q_{heater} - \left[VR\rho_{air}C_{p\,air}(T_{in,i-1} - T_{out}) + BHLF\,(T_{in,i-1} - T_{out})\ \right]\right\} * \Delta t}{\rho_{air} VC_{v\,air}} \tag{3}$$

where;

$T_{in,i-1}$= predicted inside barn temperature at previous time i-1 (=t-Δt), ^{o}C.

$q_{animals}$= sensible heat produced by the pigs, J/s.

q_{heater}= sensible heat produced by supplemental heaters, J/s.

VR= current ventilation rate, m^3/s.

$C_{p,air}$= specific heat of air at constant pressure (an assumed constant of 1006 J/kg-^{o}C).

T_{out}= outside air temperature, ^{o}C.

$BHLF$= building heat loss factor, J/s-^{o}C.

Δt= time increment used in transient analysis, s, which was fixed at 36 s (0.01 hr).

The lumped capacitance BTA model was able to determine the time dependence of indoor temperature within a mechanically ventilated building and take into account the heat transfer through the components of the building structure and the ventilation system, set point temperature, transients of outdoor climate, the presence of different sensible heat sources inside the building, and the inertia of the transient system. To simplify the modeling process, the following assumptions were introduced:

- The thermal stratification of indoor air has been neglected, i.e., the indoor temperature is uniform at any location inside the building.
- Radiation exchange between the pigs and the surroundings is included within the overall pig sensible heat production available from published data.
- Constant thermal properties have been considered.
- The air is incompressible (i.e., constant air density).

Table 1 gives the approximate building heat loss factor (BHLF) for the deep-pit swine building used for the field measurements. Each end wall had one 0.9x2.1 m steel insulated door. The end wall containing fans (see figure 1) had a lower 0.9 m of 203 mm thick concrete with the balance 38x90 mm wood stud construction 0.4 m on-center, 19 mm thick plywood interior, steel outer siding and the cavity filled with fiberglass batt insulation. The inlet end wall had a lower 0.9 m of 203 mm thick concrete with a 1.2 m curtain and a top 0.30 m section of wood/insulation construction. The side wall containing the pit fans (see figure 1) had a 0.9 m lower portion of 203 mm concrete, a 1.22 m tall curtain used for emergency ventilation with the balance 0.3 m top section consisting of wood/insulation construction. The side wall containing the lone side wall fan (see figure 1) had a 0.9 m lower portion of 203 mm concrete, with the balance 1.5 m consisting of 38x90 mm stud

construction 406 mm on-center with the cavities filled with fiberglass batt insulation. The interior ceiling was flat consisting of a flexible woven material of inconsequential thickness, rafters spaced 1.22 m on-center, with the balance filled with 254 mm of blown-in cellulose insulation. The top chord of the rafters and gable ends were un-insulated and covered with conventional steel roofing/siding.

As shown in table 1, the total barn BHLF was 965 W/^{o}C. The ceiling/roof/gable system accounted for 18% of the total, the curtain containing side wall accounted for 31%, with the perimeter accounting for 23%. The remaining contributions are shown in table 1.

The ventilation system consisted of nine stages with eight fans having four different diameters (46, 61, 91, and 122 cm). These fans (table 2) were operated automatically to maintain an operator desired inside climate according to the difference between indoor air temperature and set point temperature (SPT). The airflow rates for each direct-drive fan used in the BTA model were downgraded to 85% of their published maximum free-air capacity to account for in-field fan performance negatively affected by a variety of factors including operating static pressure differences, dust accumulation on fan shutters and blades and changing power supply to the fans. The airflow rates for each belt-driven fan (i.e. the three 122 cm fans 6, 7, and 8) needed to be further corrected because of the influence of high operating static pressures when these belt-driven fans were used and belt-tightening effects. A value of 68% of the reported maximum free-air capacity (10.38 m^3/s downgraded to 7.06 m^3/s) for each of these belt-driven 122 cm fans were used in the BTA model. For example, fan number 7 shown in figure 1 had a maximum reported free-air capacity of 10.38 m^3/s. Actual in-field airflow testing using FANS (Heber et al., 2006) indicated an airflow delivery of 7.06 m^3/s at an operating static pressure difference of 20 Pa, or a factor of 0.68.

Therefore, correction factors of 0.85 for direct-drive fans and 0.68 for belt-driven fans had their basis from in-field FANS testing conducted at this research site (Hoff et al., 2009) and are not considered to be atypical. The rational for adjusting fan delivery rates was that in a generalized procedure, where in-field performance data on fans might not be available, a procedure is needed for modeling fan performance as might be expected in the field. Using published free-stream fan data would certainly over-estimate actual in-field fan delivery rates. Anticipating operating static pressures and using published fan delivery rates accordingly would not account for actual in-field performance as well. Therefore, the procedure used here was to model fan delivery based on published free-stream fan performance criteria, using adjustment factors that are based on in-field testing, to be then extrapolated to other fan-ventilated animal housing systems.

Table 3 outlines the fan staging scheme for the swine deep-pit building used for field monitoring. Fan stages 0 and 1 consisted of variable-speed fans 1 to 4 (two pit fans, one side wall fan, and one tunnel fan). These fans operated continuously at stages 0A-0B and 1A-1B when the temperature difference between indoor air temperature and the SPT fell into a range of -0.3 to 0.6 $^{\circ}C$ and 1.1 to 1.7 $^{\circ}C$, respectively; while higher stage fans (single-speed fans) were activated gradually with increased temperature differences until the maximum fan stage 9 was achieved, e.g., the pit fans 1 and 2 and tunnel fans 5 to 7 turned on when the temperature difference reached 6.1 $^{\circ}C$.

The SPT was set at 23.3 $^{\circ}C$ when pigs entered (~ 20 kg). This SPT was reduced manually by the producer about 0.2 $^{\circ}C$ every Monday until a lower limit of 20 $^{\circ}C$ was reached.

Typically, one complete growth production cycle (~20 to 120 kg) was 140 days or about 4.5 months. The sensible heat fluxes from the pigs were calculated by multiplying sensible heat production (SHP/kg) at a specific temperature by the total pig weight (Albright, 1990). Moreover, the swine buildings monitored were equipped with 148 kW of rated supplemental heating for cold weather make-up energy.

Model performance evalation measures

Statistical measures, such as mean absolute error (MAE), coefficient of mass residual (CMR), index of agreement (IoA), and Nash-Sutcliffe model efficiency (NSEF) can be used to quantify the differences between modeled output and actual measurements, and provide a numerical description of the goodness of the model estimates (Nash and Sutcliffe, 1970; Willmott, 1982; Sousa et al., 2007). The following statistical measures were employed to ensure the quality and reliability of the BTA model predictions.

$$\mathrm{MAE} = \frac{1}{N}\sum_{i=1}^{N}\left|P_i - O_i\right| \tag{4}$$

$$\mathrm{CMR} = \frac{\sum_{i=1}^{N} P_i - \sum_{i=1}^{N} O_i}{\sum_{i=1}^{N} O_i} \tag{5}$$

$$\mathrm{IoA} = 1 - \frac{\sum_{i=1}^{N}(P_i - O_i)^2}{\sum_{i=1}^{N}(\left|O_i - \overline{O}\right| + \left|P_i - \overline{O}\right|)^2} \tag{6}$$

$$\mathrm{NSEF} = \frac{\sum_{i=1}^{N}(O_i - \overline{O})^2 - \sum_{i=1}^{N}(P_i - O_i)^2}{\sum_{i=1}^{N}(O_i - \overline{O})^2} \quad (7)$$

Where N is the total number of observations, P_i is the predicted value of the *ith* observation, O_i is the observed value of the *ith* observation, and $\overline{O}$ is the mean of the observed values.

The MAE estimates the residual error, expressed in the same unit as the data, which gives a global idea of the difference between the observed and predicted values. The CMR measures the tendency of the model to overestimate or underestimate the measured values. The IoA compares the difference between the mean, the predicted and the observed values, indicating the degree of error for the predictions. The NSEF evaluates the relative magnitude of the residual variance in comparison with the measurement variance.

In addition to the statistical measures identified above, the predictive accuracy of model outputs were examined through graphical presentations of the predicted vs. observed ventilation rate and indoor air temperature.

RESULTS AND DISCUSSION

Model validation is possibly the most important step in any model development sequence. However, no standard model evaluation guidance has been established to judge model performance and further compare various models that were developed using different modeling approaches. The reason could be due to the fact that model validation guidelines are model and project specific. For this research, the BTA model was evaluated based on two main techniques: graphical presentation and statistical analysis. The graphical presentations

provide a visual comparison of the predicted vs. observed values and a first overview of model performance (ASCE, 1993); while the statistical analysis provide a numerical tool to quantify the goodness of model estimates.

Graphical presentation for model evaluation

Central Iowa climate based on the monthly averages from the measured 2003 data (calendar year) could be separated into three typical global categories that were defined as: warm weather (June, July, Aug.; 20.2°C to 23.5°C), mild weather (Apr., May, Sept., Oct.; 10.0°C to 16.4°C), and cold weather (Jan., Feb., Mar., Nov., Dec.; -7.6°C to 2.6°C). Figures 2 to 7 illustrate the different diurnal and seasonal patterns of the hourly predicted vs. actual ventilation rate and indoor air temperature during these three representative seasons (warm, mild, and cold weather).

Generally, the predicted values were visually in close agreement with actual measurements as shown in figures 2 to 7. Specifically, in August (warm weather), the mean and standard deviation for the actual and predicted ventilation rate and indoor air temperature were $12.03\pm5.91\ m^3/s$ vs. $13.82\pm7.50\,m^3/s$ and $27.8\pm2.3\ ^\circ C$ vs. $26.8\pm2.8\,^\circ C$, respectively. It is obvious to see in figures 2 and 3 that the diurnal patterns of ventilation rate and indoor temperature were very similar to those of outside temperature as expected. The predicted ventilation rate was overestimated by an average of 8% when the highest outside temperatures occurred for some days, whereas the predicted indoor temperature was underestimated by an average of 2% in comparison with the actual measurements.

In October (mild weather), the mean and standard deviation for the actual and predicted ventilation rate and indoor air temperature were $8.61\pm4.40\ m^3/s$ vs. 8.17 ± 6.14

m^3/s and 23.3±2.1 $°C$ vs. 22.5±2.2 $°C$, respectively. It can be seen in figures 4 and 5 that the ventilation rate and indoor air temperature seemed to show much less fluctuation compared with the August patterns except for a few days with high outside temperature. The ventilation rates were underestimated by the BTA model when the outside temperature dropped below 0 $°C$.

In February (cold weather), the mean and standard deviation for the actual and predicted ventilation rate and indoor air temperature were 1.95±0.39 m^3/s vs. 1.20±0.09 m^3/s and 23.4±0.9 $°C$ vs. 21.6±0.5 $°C$. It was observed in figures 6 and 7 that the ventilation rate and indoor air temperature were fairly constant since the minimum ventilation rate was being used in the building to maintain the room set point temperature during these cold periods. Almost all the predicted ventilation rate and indoor temperature were slightly lower than corresponding field measurements.

Statistical analysis for model evaluation

Table 4 summarizes the statistical performance of the BTA model to predict the hourly ventilation rate and indoor air temperature in calendar year 2003. The mean absolute error (MAE) tests the accuracy of the model, which is defined as the extent to which predicted values approach a corresponding set of measured values. The MAE values were 1.74 m^3/s and 1.2 $°C$ for the ventilation rate and indoor temperature, respectively. Singh et al. (2004) reported that MAE values less than half the standard deviation (MAE/SD<0.50) of the measured data can be considered low. In this research, MAE/SD<0.50 was used as a stringent criterion for evaluating the BTA model. The MAE/SD values for the ventilation rate and indoor air temperature were 0.32 and 0.41 respectively, which indicates that the BTA

model performance for the residual variations were very good. The coefficient of mass residual (CMR) expresses the relative size and nature of the error. The closer CMR is to 0 the better the model simulation. A negative value of CMR shows model underestimation tendency, and positive values indicate overestimation tendency. The CMR for the ventilation rate and indoor temperature were equal to -0.03 and -0.04 respectively, which means that there was no systematic under- or over- prediction of the ventilation rate and indoor temperature by the BTA model. The index of agreement (IoA) measures the agreement between predicted and measured data and ranges from 0 (no agreement) to 1 (perfect agreement) (Willmott, 1981). The IoA values for the ventilation rate and indoor air temperature were 0.96 and 0.92 respectively, which indicates that the predicted values had a very good agreement with the field measurements. Nash-Sutcliffe model efficiency (NSEF) evaluates the error relative to the natural variation of the actual measurements and varies from -∞ to 1. $NSEF = 1$ means a perfect match of predicted data to the observed data. $NSEF = 0$ indicates that the model predictions are as accurate as the mean of the observed data, whereas the NSEF value less than 0 suggests that using the observed mean would be better than the predictions by the model. Values between $0.5 \le NSEF \le 1.0$ are considered good (Helweig et al., 2002). The NSEF values for the ventilation rate and indoor air temperature were 0.79 and 0.68 respectively, which fell within the good range.

The graphical data along with the statistical parameters suggest that the performance of the BTA model for predicting ventilation rate and indoor air temperature were very good and could be used to provide predicted climate parameters for the ultimate goal of predicting inside barn concentrations and emissions as presented in Part II of this research (Sun and Hoff, 2010).

SUMMARY AND CONCLUSIONS

Due to the absence of a nationwide monitoring network for quantifying long-term air emission inventories of livestock production facilities, a building thermal analysis and air quality predictive (BTA-AQP) model was developed to forecast indoor climate and long-term air quality (NH_3, H_2S and CO_2 concentrations and emissions) for swine deep-pit finishing buildings.

In this paper, comprising Part I of II, a lumped capacitance model (BTA model) was developed to study the transient behavior of indoor air temperature and ventilation rate according to the thermo-physical properties of a typical swine building, the set-point temperature scheme, fan staging scheme, transient outside temperature, and the heat fluxes from pigs and supplemental heaters. The obtained indoor air temperature and ventilation rate developed from the BTA model could then be combined with animal growth cycle, in-house manure storage level, and typical meteorological year (TMY3) data to predict indoor air quality and emissions based on the generalized regression neural network (GRNN-AQP model; Sun and Hoff, 2010). The overall purpose of this paper was to acquire accurate estimates of significant input parameters required for the GRNN-AQP model without relying on expensive field measurements.

The performance of the BTA model for predicting ventilation rate and indoor air temperature was very good in terms of the statistical analysis and graphical presentations. The statistical results showed that:

(1) The mean absolute error values of the VR and Tin were less than half the standard deviation of the measured data;

(2) The coefficient of mass residual values for the VR and Tin were equal to -0.03 and -0.04, respectively;

(3) The index of agreement values were 0.96 and 0.92 for the VR and Tin, respectively; and

(4) The Nash-Sutcliffe model efficiency values were all higher than 0.65.

These good results indicated that this BTA model was capable of accurately predicting ventilation rate and indoor air temperature in swine deep-pit buildings.

ACKNOWLEDGEMENTS

The authors wish to acknowledge the USDA-IFAFS funding program for providing the funds required to collect the field data used in this research project and the USDA-Special Grants funding program for providing the funds for this specific research project. Their support is very much appreciated.

REFERENCES

Aarnink, A.J.A. and A. Elzing. 1998. Dynamic model for ammonia volatilization in housing with partially slatted floors, for fattening pigs. *Livestock Prod. Science* 53(2): 153-169.

ASCE. 1993. Criteria for evaluation of watershed models. *J. Irrigation Drainage Eng.* 119(3): 429-442.

Albright, L. D. 1990. Chapter 5: Steady-state energy and mass balance. In *Environment Control for Animals and Plants*, 143-172. St. Joseph, Mich.: ASAE.

Gates, R. S., K. D. Casey, H. Xin, E. F. Wheeler, and J. D. Simmons. 2004. Fan assessment numeration system (FANS) design and calibration specifications. *Trans. ASAE* 47(5): 1709-1715.

Heber, A.J., J. Ni, T.T. Lim, P. Tao, A.M. Schmidt, J.A. Koziel, D.B. Beasley, S.J. Hoff, R.E. Nicolai, L.D. Jacobson and Y. Zhang. 2006. Quality assured measurements of animal building emissions: Gas concentrations. *J. Air and Waste Mgmt. Assoc.* 56(10): 1472-1483.

Helweig, T. G., C. A. Madramootoo and G. T. Dodds. 2002. Modeling nitrate losses in drainage water using DRAINMOD 5.0. Agric. Water Management 56 (2): 153-168.

Hoff, S.J., D.S. Bundy, M.A. Nelson, B.C. Zelle, L.D. Jacobson, A.J. Heber, J. Ni, Y. Zhang, J.A. Koziel, D.B. Beasley. 2009. Real-time airflow rate measurements from mechanically ventilated animal buildings. *J. Air and Waste Mgmt. Assoc.* 59: 683-694.

Nash, J. E. and J. V. Sutcliffe. 1970. River flow forecasting through conceptual models: Part 1. A discussion of principles. *J. Hydrology* 10(3): 282-290.

Ni, J., J. Hendriks, C. Vinckier and J. Coenegrachts. 2000. Development and validation of a dynamic mathematical model of ammonia release in pig houses. *Environ. Intl.* 26(1-2): 97-104.

Kai, P., B. Kaspers and T. van Kempen. 2006. Modeling source gaseous emissions in a pig house with recharge pit. *Trans. ASABE* 49(5): 1479-1485.

Matlab. 1999. User's dynamic system simulation software. Ver.5.0. Natick, MA: The Math Works, Inc.

Mendes, N., G. H. C. Oliveira and H. X. de Araújo. 2001. Building thermal performance analysis by using Matlab/Simulink. In *Proc. 7th International IBPSA Conference on Building Simulation,* 473-480. Rio de Janeiro, Brazil.

Morini, G. L. and S. Piva. 2007. The simulation of transients in thermal plant. Part I: Mathematical model. *Applied Thermal Eng.* 27: 2138-2144.

Morsing, S., J. S. Strom, G. Q. Zhang and L. Jacobson. 2003. Prediction of Indoor Climate in Pig Houses. In *Proc. 2nd International Conference on Swine Housing II*, 41-47. Research Triangle Park, NC: ASAE.

Nannei E. and C. Schenone. 1999. Thermal transients in buildings: development and validation of a numerical model. *Energy and Buildings*. 29: 209-215.

NSRDB. 2008. Users manual for TMY3 data sets. Golden, Co: USDE National Renewable Energy Laboratory.

Pedersen, S., H. Takai, J. O. Johnsen, J. H. M. Metz, P. W. G. Groot Koerkamp, G. H. Uenk, V. R. Phillips, M. R. Holden, R. W. Sneath, J. L. Short, R. P. White, J. Hartung, J. Seedorf, M. Schröder, K. H. Linkert and C. M. Wathes. 1998. A comparison of three balance methods for calculating ventilation rates in livestock buildings. *J. Agric. Eng. Res.* 70: 25-37.

Schauberger, G., M. Piringer and E. Petz. 1999. Diurnal and annual variation of odor emission from animal houses: a model calculation for fattening pigs. *J. Agric. Eng. Res.* 74: 251-259.

Singh, J., H. V. Knapp and M. Demissie. 2004. Hydrologic modeling of the Iroquois River watershed using HSPF and SWAT. ISWS CR 2004-08. Champaign, Ill.: Illinois State Water Survey. Available at: www.sws.uiuc.edu/pubdoc/CR/ISWSCR2004-08.pdf. Accessed 12 March 2009.

Sousa, S.I.V., F.G. Martins, M.C.M. Alvim-Ferraz and M.C. Pereira. 2007. Multiple linear regression and artificial neural network based on principal components to predict ozone concentrations. *Environ. Modeling and Software* 22(1): 97-103.

Sun, G. and S. J. Hoff. 2010. Prediction of indoor climate and long-term air quality using the BTA-AQP model: Part II. Overall model evaluation and application. *Trans. ASABE* 53(3): 871-881.

Sun, G., S. J. Hoff, B. C. Zelle and M. A. Nelson. 2008a. Development and comparison of backpropagation and generalized regression neural network models to predict diurnal and seasonal gas and PM_{10} concentrations and emissions from swine buildings. *Trans. ASABE* 51(2):685-694.

Sun, G., S. J. Hoff, B. C. Zelle and M. A. Nelson. 2008b. Forecasting daily source air quality using multivariate statistical analysis and radial basis function networks. *J. Air & Waste Manage. Assoc.* 58 (12): 1571-1578.

Willmott, C. J. 1982. Some comments on the evaluation of model performance. *Bull. Am. Meteorol. Soc*. 63: 1309-1313.

Table 1. Building heat loss factor for the modeled deep-pit swine building.

Component	L (m)	H or W (m)	Area (m^2)	R-Values (^oC-m^2/W)	BHLF (W/ ^oC)	Component (%)
Ceiling/Roof/Gable	59.7	12.8	765	4.5	170	17.6
SW1 lower	59.7	0.9	55	0.4	152	15.8
SW1 upper (solid)	59.7	1.5	91.0	3.4	27	2.8
SW2 lower	59.7	0.9	55	0.4	152	15.8
SW2 upper (w/curtain)	59.7	1.5	91.0	0.6	148	15.3
EW1 (fan end)	12.8	2.4	29.3	0.8	36	3.7
EW1 door	0.9	2.1	2	2.0	1	0.1
EW2 (w/curtain)	12.8	2.4	29.3	0.5	60	6.2
EW2 door	0.9	2.1	2	2.0	1	0.1
Perimeter	145			1.50 [a]	218	22.6
Total Barn BHLF					965	100%

[a] The perimeter heat loss factor is expressed in W/m-C estimated using the suggested uninsulated perimeter heat loss factor value from Albright (1990).

Table 2. Fan type and airflow rate used for the swine deep-pit building.[a]

Fan	Fan Diameter (cm)	Rate (m^3/s)	Modeled Rate (m^3/s)
PF (1,2) [b]	46	1.06	0.90[c]
SF (3), TF (4)	61	2.83	2.41[c]
TF (5)	91	4.96	4.21[c]
TF (6, 7, 8)	122	10.38	7.06[d]

[a] PF: Pit Fan; SF: Side Wall Fan; TF: Tunnel Fan.

[b] Number in parenthesis indicates the fan ID number as shown in figure 1.

[c] Modeled rate at 85% of published free-stream value.

[d] Modeled rate at 68% of published free-stream value.

Table 3. Fan staging scheme for the swine deep-pit building.[a]

Stage	Fan ON	Rate (m^3/s)	Activation Delta T (°C)
0A	PFs-1,2 at 65% VFC	1.17	-0.3
0B	PFs-1,2 at 100% VFC	1.81	0.6
1A	PFs-1,2; SF-3, TF-4 at 70% VFC	5.17	1.1
1B	PFs-1,2; SF-3, TF-4 at 100% VFC	6.62	1.7
2	PFs-1,2; TF-3,5	8.42	2.2
3	PFs-1,2; SF-3; TF-4, 5	10.83	3.3
4	PFs-1,2; TF-5,6	13.08	4.4
5	PFs-1,2; TF-5, 6, 7	20.14	6.1
6	PFs-1,2; TF-4,5,6,7,8	29.60	7.8

[a] Delta T is equal to Tin-SPT. Tin: indoor temperature. VFC: ventilation full capacity.

Table 4.The statistical performance of the BTA model.[a]

Variable	A-Mean (S.D.)	P-Mean (S.D.)	MAE	CMR	IoA	NSEF
Ventilation rate	7.03±5.43 (m^3/s)	6.83±6.66 (m^3/s)	1.74 (m^3/s)	-0.03	0.96	0.79
Indoor air temperature	23.8±2.8 (^oC)	22.8±2.7 (^oC)	1.2 (^oC)	-0.04	0.92	0.68

[a] A: actual data; P: Predicted data.

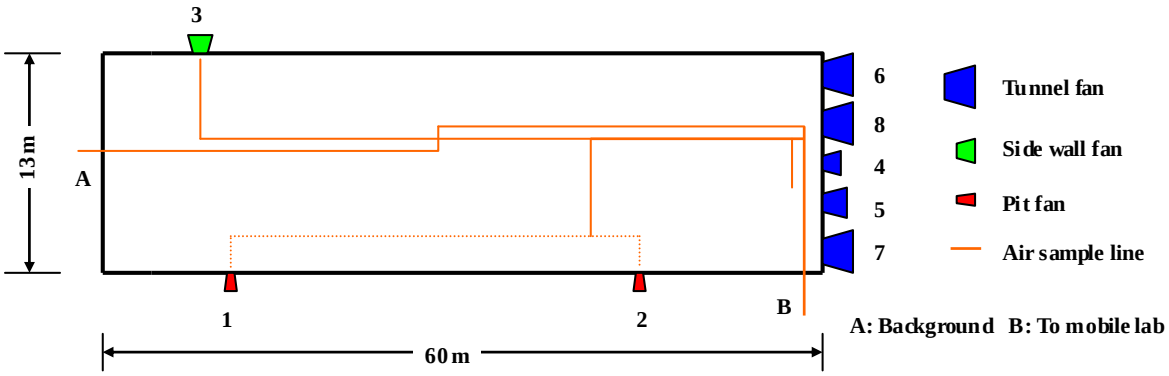

Figure1. Layout of deep-pit swine finishing building.

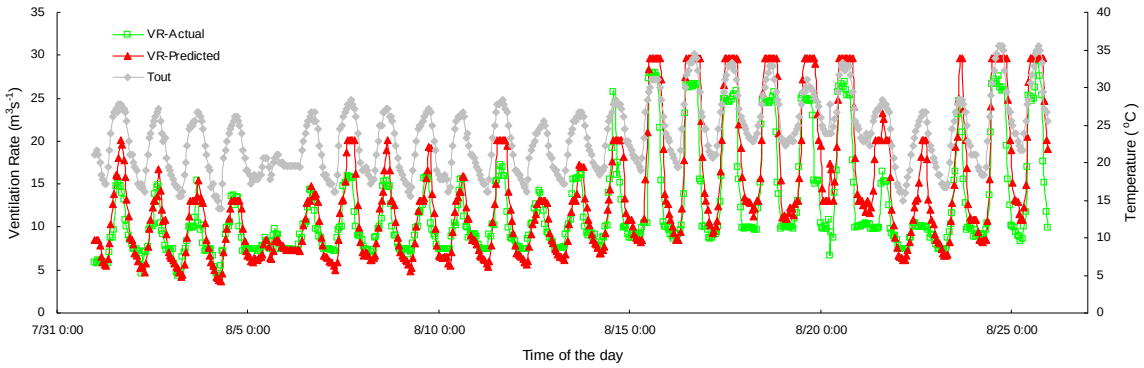

Figure 2. The predicted vs. actual ventilation rate (VR) with outside temperature (Tout) in August, 2003.

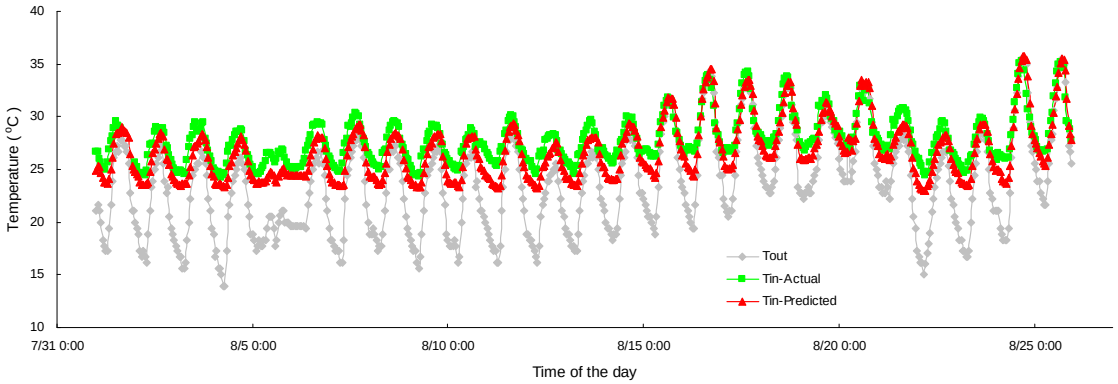

Figure 3. The predicted vs. actual indoor air temperature (Tin) with outside temperature in August, 2003.

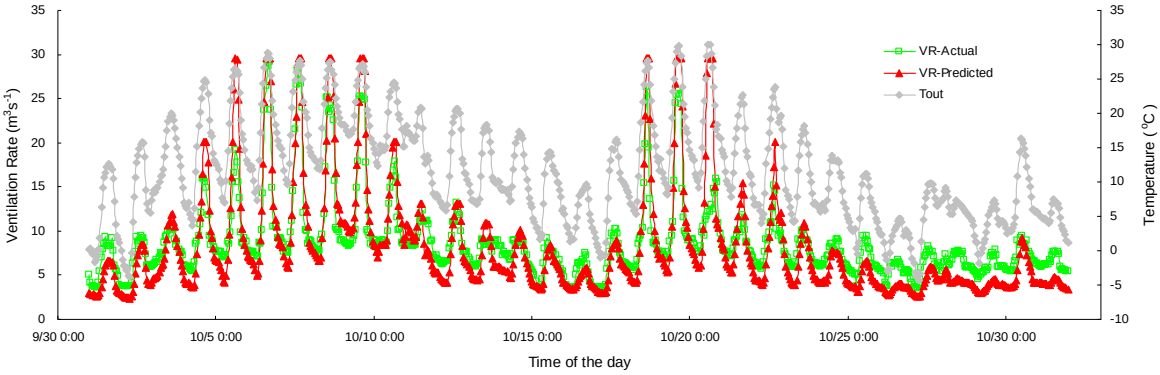

Figure 4. The predicted vs. actual ventilation rate (VR) with outside temperature in October, 2003.

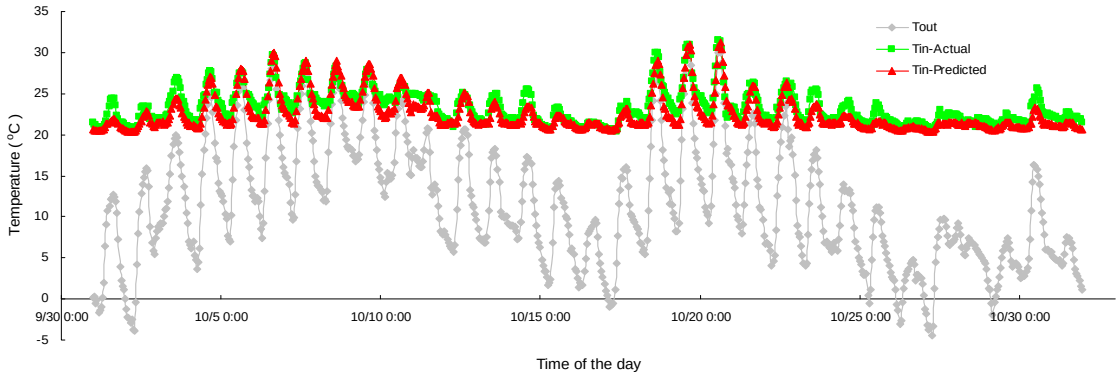

Figure 5. The predicted vs. actual indoor air temperature (Tin) with outside temperature in October, 2003.

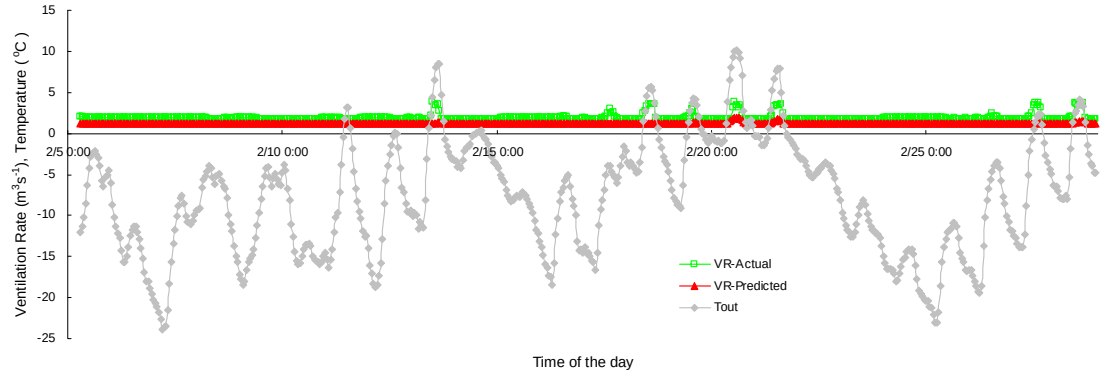

Figure 6. The predicted vs. actual ventilation rate (VR) with outside temperature in February, 2003.

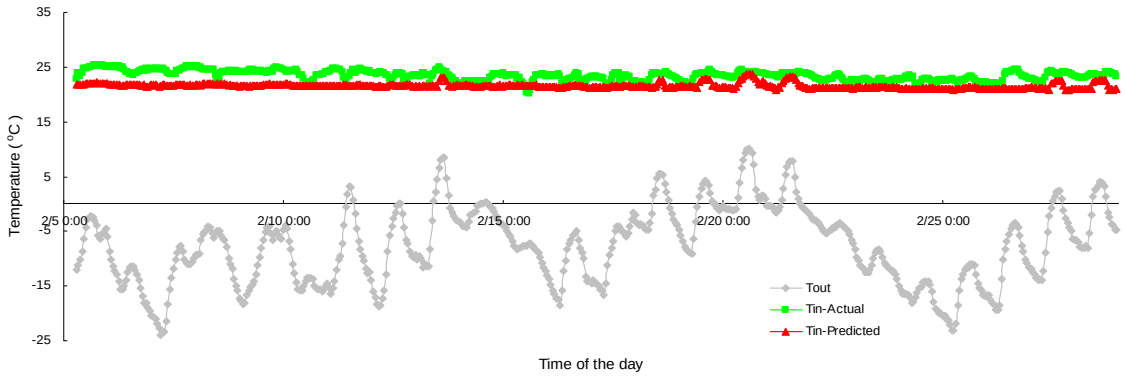

Figure 7. The predicted vs. actual indoor air temperature (Tin) with outside temperature in February, 2003.

CHAPTER 5. PREDICTION OF INDOOR CLIMATE AND LONG-TERM AIR QUALITY USING THE BTA-AQP MODEL: PART II. OVERALL MODEL EVALUATION AND APPLICATION

A paper published in the Transaction of the American Society of Agricultural and Biological Engineers[1]

G. Sun and S. J. Hoff [2]

ABSTRACT

The objective of this research was to develop a building thermal analysis and air quality predictive (BTA-AQP) model to predict indoor climate and long-term air quality (NH_3, H_2S and CO_2 concentrations and emissions) for swine deep-pit buildings. This paper presents Part II of this research where the performance of the BTA-AQP model is evaluated using typical meteorological year (TMY3) data in predicting long-term air quality trends. The good model performance ratings (MAE/SD<0.5, CRM≈0; IoA≈1; and NSEF > 0.5 for all the predicted parameters) and the graphical presentations reveal that the BTA-AQP model was able to accurately forecast indoor climate and gas concentrations and emissions for

---

[1] Reprinted with permission of *the Transactions of ASABE*, 2010, 53 (3), 871-881.

[2] The authors are **Gang Sun, ASABE Member Engineer,** Graduate Student, **Steven J. Hoff, ASABE Member,** Professor, Department of Agricultural and Biosystems Engineering, Iowa State University, Ames, Iowa. **Corresponding author:** Steven J. Hoff, Department of Agricultural and Biosystems Engineering, 212 Davidson Hall, Iowa State University, Ames, IA 50011; phone: 515-294-6180; fax: 515-294-2255; e-mail: hoffer@iastate.edu.

swine deep-pit buildings. By comparing the air quality results simulated by the BTA-AQP model using the TMY3 data set with those from a five-year local weather data set, it was found that the TMY3-based predictions followed the long-term mean patterns well, which indicates that the TMY3 data could be used to represent the long-term expectations of source air quality. Future work is needed to improve the accuracy of the BTA-AQP model in terms of four main sources of error: (1) Uncertainties in air quality data; (2) Prediction errors of the BTA model; (3) Prediction errors of the AQP model, and (4) Bias errors of the TMY3 and its limited application.

Keywords. Air quality predictive model, Typical meteorological year, Modeling, Long-term mean.

INTRODUCTION

The overall goal of this research was to develop a building thermal analysis and air quality predictive (BTA-AQP) model to quantify long-term indoor climate and air quality (ammonia, hydrogen sulfide and carbon dioxide concentrations and emissions) for swine deep-pit buildings. In the companion paper forming Part I of this study (Sun and Hoff, 2010), it has been demonstrated, based on statistical evaluation measures and graphical presentations, that the developed BTA model was capable of predicting indoor climate and building ventilation rate in swine deep-pit buildings and could be used as accurate estimates of significant input variables for the AQP model.

Part II of this study, detailed in this paper, deals with the development and evaluation of the BTA-AQP model under typical weather conditions (TMY3). The proposed modeling technology was intended to perform long-term simulation of source air quality in a rapid,

economical, reliable, and accurate way in order to significantly reduce expensive and time-consuming field measurements. Therefore, this BTA-AQP model can be used for livestock producers to extrapolate annual air emission inventories, for the research scientists to obtain a diurnal and seasonal air quality database for science-based setback distance determination, and for state and federal regulatory agencies to make relevant environment policy decisions.

MATERIALS AND METHODS

Long-term Air Quality Prediction Method

Long-term air quality predictions can be separated into three components as shown in figure 1: the building thermal analysis (BTA) model, the air quality predictive (AQP) model, and a typical meteorological year (TMY3) database (NSRDB, 2008). Specifically, a lumped capacitance model (BTA model) was developed to study the transient behavior of indoor air temperature and ventilation rate according to the thermo-physical properties of a typical Iowa swine building, a typical set-point temperature scheme, a typical fan staging scheme, transient outside temperature, and the heat fluxes from pigs and supplemental heaters. The obtained indoor room temperature and ventilation rate combined with animal growth cycle, in-house manure storage level, and typical meteorological year (TMY3) data were fed into the generalized regression neural network (GRNN) air quality predictive model to calculate hourly ammonia, hydrogen sulfide and carbon dioxide concentrations and emission rates. The corresponding monthly and average annual air quality values were then obtained based on the hourly predictions. The TMY3 data used for this research project consists of representative hourly solar radiation and meteorological values for a 1-year period in Des Moines, Iowa, about 100 kilometers away from the swine deep-pit finishing facility where

field data was collected (calendar year 2003 data collection). Animal growth cycle includes pig number and average pig weight in the room, which were used to estimate total animal units (AU). The total AU was obtained by dividing the total pig weight by 500 kg animal live weight. In-house manure storage level was considered as an additional input variable representing a deep-pit system for the AQP model.

Description of field gas measurements

Field monitoring was conducted for 15-months between January 2003 and March 2004, with the 1-year monitoring in 2003 used in this research for model prediction comparison. Details of the field monitoring and overall procedures used can be found in Heber et al. (2006). Two identical deep-pit swine finishing buildings located in central Iowa were monitored. Each building was 60 m long and 13 m wide, which can house 960 finishing pigs from ~20 to 120kg. Slurry was collected in a 2.4-m-deep pit below a fully slatted floor and was stored for one year. Once a year in the fall, the under-floor deep pit was emptied and the slurry was injected to nearby cropland as a fertilizer source.

The real-time gas concentrations and emission rates, environmental data, and building ventilation rate were measured by a mobile emission laboratory (MEL) that included a gas sampling system (GSS), a computer-based data acquisition system, gas analyzers, environmental instrumentation, standard gas calibration cylinders, and other supplies. Gas concentrations from multiple sampling locations within the swine building were quantified with a chemiluminescence NH_3 analyzer (Model 17C, Thermal Environment Instruments, Franklin, MA), a pulsed fluorescence SO_2 detector (Model 45C, Thermal Environment Instruments, Franklin, MA), and two photoacoustic infrared CO_2 analyzers in the range from

0 to 2,000 and 10,000 ppm (Model 3600, Mine Safety Appliances CO., Pittsburg, PA). A three-way solenoid system was used to automatically switch between 12 measuring locations with 10-min sampling intervals and sequentially delivered gas from each location to the gas analyzers. Therefore, gas samples were taken during twelve, 120-min measurement cycles per day. Details of the monitoring method and QA/QC can be found in Heber et al. (2006). Climate parameters (temperature, relative humidity, and static pressure) and total building ventilation rate were also simultaneously monitored. Gas emission rates were determined by multiplying fan airflow rate by representative gas concentration differences between inlet and outlet for all fans operating at any given time. The maximum estimated uncertainty in ventilation rate and gas concentrations were ± 7.2 % (Hoff et al., 2009) and ± 5.0 %, respectively. These individual uncertainties resulted in an average uncertainty in emission rate of about ± 9.0 %.

Air quality database and initial data analysis

The BTA-AQP model development was based on source air quality measurements which included real-time gas concentrations and emission rates, indoor and outdoor environmental data (indoor, inlet and exhaust temperature and relative humidity, outdoor temperature, relative humidity, wind speed, wind direction, solar energy and barometric pressure), pig size and density (animal units), and building ventilation rate. These measured data can be used as a fundamental database to help develop air quality predictive models and evaluate model forecasting performance. Thus, data quality is of paramount importance. Heber et al. (2006) pointed out that more efforts should be made to maximize confidence, credibility, and consistency of measured data for obtaining a high quality database. In this

study, the established principles of quality assurance and quality control were applied throughout the gas sample collection and great emphasis was placed on data quality. However, the final data set still presented three main types of problems: general errors, outliers, and missing observations. The general errors are wrongly recorded observations, probably due to calibration and other reasons, which could result in biased measurements. A 70% valid data policy (Heber et al., 2006) was used to calculate hourly, daily, and monthly averages to avoid those errors. The outliers are extreme observations which do not appear to be consistent with the rest of the data. Outliers arise for several reasons and can cause severe problems. Hoff et al. (2006) reported that the H_2S emissions measured during the independent slurry removal event would increase by an average of 62 times relative to the H_2S emission levels before the removal. Thus, air quality data during the slurry agitation process should be considered as outliers and removed from the database. The missing observations are due to a variety of reasons, such as lost samples, malfunctioning instruments and sensors, and challenging weather (lightning), to name a few. A majority of air quality missing data in this research belonged to Missing Not at Random (MNAR). The best way to handle MNAR data is to develop a regression model to estimate missing values (Dunning and Freedman, 2008). In a word, initial data analysis must be applied to ensure database quality.

Another important issue for an air quality database is the sample representativeness and completeness. Representative and complete sample measurements should fully characterize long-term (at least one year) air emission profiles and corresponding emission factors since gas concentrations and emissions vary with time of day, season, building

characteristics, ventilation rate, animal size and density, manure handling system, and weather conditions (Jacobson et al., 2005).

Typical meteorological year

Selecting appropriate representative meteorological data is vitally important to accurately predict indoor climate and long-term air quality levels. Normally, a representative meteorological data consists of a multi-year and long-term average measured data series which would represent a year of prevailing weather conditions for a specific location. It is noted that the use of typical climatic parameters instead of multiple-year data can reduce a great deal of time and computation in computer simulation and facilitate performance comparisons of different system types, configurations, and locations. Therefore, typical weather data has been extensively used for building energy simulation and solar energy analysis to assess the expected heating and cooling costs for the design of industrial and residential buildings. Currently, the most prevalent weather representations are test reference year (TRY), typical meteorological year (TMY3), and weather year for energy calculations (WYEC2). These data sets are used for different simulation purposes (Pedersen, 2007): TRY is suited to short-term energy predictions due to the representation of weather characteristics; while TMY3 and WYEC2 are most suitable for long-term energy estimations because the data represents long-term weather features. Yang et al. (2008) investigated the energy simulation results for office buildings in the five main climate zones of China and compared the results using TMY2 with those using multi-year data (1971-2000). It was found that the TMY2 was able to predict monthly load and energy use within 5.4% of the long-term mean. Based on these results, it was concluded that the TMY3 data was an acceptable meteorological data set to be used for this current study.

TMY3 is composed of typical hourly meteorological values at a specific location over a long period of time (30 years). For each TMY3 dataset, 12 typical months are selected using statistics (Sandia method; NSRDB, 2008) determined by five important parameters: global radiation on a horizontal surface, direct normal radiation, dry bulb and dew point temperatures, and wind speed (NSRDB, 2008). These important parameters were chosen because solar radiation determines the heat gain; dry bulb temperature and wind speed determine heat loss by convection; and dew point temperature is an absolute measure of humidity, which determines latent energy. The 12 judged most typical months were picked by the Sandia approach to form a complete year. Due to adjacent TMY3 months from different years, linear interpolation was performed to smooth the gap for 6 hours on each side of adjacent months. In each TMY3 month, mean values of the TMY3 elements are the closest to the averages of the elements for multiple years. Thus, the TMY3 can represent long-term average climatic conditions.

Air quality model

Modeling source air quality in a swine deep-pit building is a complicated dynamic system with many nonlinear governing relationships. Moreover, there still exist some circumstances of gaseous emissions that can not be explained with our current limited scientific understanding (Sun et al., 2008). Therefore, a black-box modeling approach using artificial neural networks (ANN) would be a potential method for handling air quality predictions. Black-box models do not need detailed prior knowledge of the structure and different interactions that exist between important variables. Meanwhile, their learning abilities make the models adaptive to system changes. Recently, there has been an increasing amount of applications of ANN models in the field of atmospheric pollution forecasting

(Hooyberghs et al., 2005; Grivas et al., 2006; Sousa et al., 2007; Sun et al., 2008). The results show that ANN black-box models are able to learn nonlinear relationships with limited knowledge about the process structure.

Sun et al. (2008) employed backpropagation neural network (BPNN) and generalized regression neural network (GRNN) techniques to model gas and PM_{10} concentrations and emissions generated and emitted from a swine deep-pit finishing building. Note that GRNN is a term to represent the Nadaraya-Watson kernel regression used in artificial neural networks (ANN). The obtained BPNN and GRNN predictions were in good agreement with field measurements, with coefficient of determination (R^2) values between 81.2% and 99.5% and very low values of systemic performance indexes. The good results indicated that ANN technologies were capable of accurately modeling source air quality within and from these livestock production facilities. Furthermore, it was found that the process of constructing, training, and simulating the BP network models was very complicated. The effective way of obtaining good BP modeling results was to use some trial-and-error methods and thoroughly understand the theory of backpropagation. Conversely, for the GRNN models, there was only one parameter (the smoothing factor) that needed to be adjusted experimentally. Additionally, the GRNN performance was not sensitive to randomly assigned initial values and the GRNN approach did not require an iterative training procedure as in the backpropagation method. Other significant characteristics of the GRNN in comparison to the BPNN were the excellent approximation ability, fast training time, and exceptional stability during the prediction stage. Thus, it was recommended in Sun et al. (2008) that a GRNN be used for source air quality modeling.

In this current research, a GRNN model was developed to explore the complex and highly nonlinear relationships between air pollutants and many input variables on the diurnal and seasonal NH_3, H_2S, and CO_2 levels and emissions. This developed air quality model was then used to forecast long-term gas concentrations and emissions from a typical swine deep-pit building associated with five significant input elements: outdoor temperature obtained from a specific year or the TMY3 data; a typical swine growth cycle; and ventilation rate and indoor air temperature predicted by the transient BTA model (Sun and Hoff, 2010). It is noted that in the midwestern United States, it is common practice to store manure in deep holding concrete pits for one calendar year. This year-long slurry storage system is also a concentrated source for gas concentrations and emissions (Hoff et al., 2006). Therefore, in-house manure storage level was considered as an additional factor representing the deep-pit system for the AQP model. The manure depth changes with swine production time, from 0.3 m (empty pit) to 2.1 m (full pit) throughout the year. The full and empty events generally occur before and after slurry removal which is typically conducted once per year in the fall after harvest (i.e. October).

RESULTS AND DISCUSSION

In this section, a comparison was made between the predicted and actual gas concentrations and emissions in 2003 to evaluate the accuracy of the BTA-AQP model estimates. In addition, the simulated results using the TMY3 data set and a five-year mean weather data set were compared to validate the assumption that the TMY3 could accurately represent long-term source air quality levels. Finally, overall prediction errors of the BTA-AQP model were analyzed and future work is identified for improving the model.

BAT-AQP Model Evaluation using 2003 weather data

Boxplots were used to provide graphical information on the median, the spread, the skewness, and potential outliers of actual vs. predicted data sets. The primary purpose was to evaluate early the data before conducting in-depth statistical analysis. The comparative boxplots of hourly actual vs. predicted NH_3, H_2S, and CO_2 concentrations for each month in 2003, are shown in figure 2. It was observed that the field collected and predicted gas concentrations during the majority of the time had similar median, spread, and skewness, which indicated that those comparative data sets were generally distributed in a similar way; an indication of good model performance. However, significant differences between the two data sets in some months can be seen, e.g., gas (NH_3, H_2S and CO_2) concentration predictions in December, NH_3 concentration predictions in April, H_2S concentration predictions in July, and CO_2 concentration predictions in February. The poor gas concentration predictions in December were probably due to two growth cycles appearing in the same month, i.e., mature pigs (120 kg) were gradually shipped to market in early December and smaller pigs (~20kg) entered at the end of December. During these times, air quality levels and indoor climate were highly influenced by the management of the swine barn and workers' involvement, which were not considered as a factor in the development of the BTA-AQP model. The poor NH_3 concentration predictions in April and CO_2 concentration predictions in February may be attributed to the relatively inaccurate ventilation rate estimations by the BTA model, which should be improved in future work (figure 5). The poor H_2S concentration predictions in July could partially be explained by the fact that some important variables were excluded in the H_2S predictive model, such as manure characteristics and surface temperature. The manure temperature may be an important variable affecting H_2S release in hot weather.

Moreover, in early July, some underestimated ventilation rates were observed at the beginning of a new swine growth cycle resulting in a corresponding higher predicted H_2S concentration.

The comparative boxplots of hourly actual vs. predicted NH_3, H_2S, and CO_2 emissions for each month in 2003, are illustrated in figure 3. Overall, the median, spread and skewness of the field collected and predicted gas emissions were similar except for February, April and December. Again, the poor forecasting performance in February and April were mainly due to the fact that the relatively inaccurate ventilation rate predictions, in comparison to other monthly fitted values, led to greater error in gas emission calculation. For the poor predictions in December, the reason could be the AQP model which was not able to estimate gas concentrations resulting from barn management and pig activity as previously outlined.

Furthermore, it was found that the BTA-AQP model with an additional variable, in-house manure level, could largely improve H_2S prediction accuracy. When in-house manure level was incorporated into the model, the overall average absolute error (AE=100%* $\left|$ predicted-measured $\right|$ /measured) dropped to 11% from an original 24% without manure depth considered. It should be noted that the data points which were outside the spread, as shown in figures 2 and 3, can be considered as potential outliers.

Table 1 summarizes the statistical performance of the BTA-AQP model for predicting hourly gas concentrations and emissions in 2003. The following statistical measures were employed to ensure the quality and reliability of the BTA-AQP model predictions. A more detailed description is given in Sun and Hoff (2010).

$$\text{Mean Absolute Error, MAE} = \frac{1}{N}\sum_{i=1}^{N}\left|P_i - O_i\right| \tag{1}$$

$$\text{Coefficient of Mass Residual, CMR} = \frac{\sum_{i=1}^{N} P_i - \sum_{i=1}^{N} O_i}{\sum_{i=1}^{N} O_i} \tag{2}$$

$$\text{Index of Agreement, IoA} = 1 - \frac{\sum_{i=1}^{N}(P_i - O_i)^2}{\sum_{i=1}^{N}(\left|O_i - \overline{O}\right| + \left|P_i - \overline{O}\right|)^2} \tag{3}$$

$$\text{Nash-Sutcliff Model Efficiency, NSEF} = \frac{\sum_{i=1}^{N}(O_i - \overline{O})^2 - \sum_{i=1}^{N}(P_i - O_i)^2}{\sum_{i=1}^{N}(O_i - \overline{O})^2} \tag{4}$$

Where N is the total number of observations, P_i is the predicted value of the *ith* observation, O_i is the observed value of the *ith* observation, and $\overline{O}$ is the mean of the observed values.

As shown in table 1, the annual predicted averages and standard deviations (SD) of gas concentrations and emissions were in very good agreement with the actual measurements. For all the parameters, the MAE/SD ratios were less than 0.5, indicating that the BTA-AQP models' performance for the residual variations was very good. The CMR values approximated to 0, meaning that there was no systematic under- or over- prediction by the BTA-AQP model. The IoA values were close to 1, implying excellent agreement between the observed and predicted values. The NSEF values were greater than 0.5, indicating that the simulated data matched the measured data very well. Therefore, the BTA-AQP model

was able to accurately predict indoor climate and gas concentrations and emissions from the monitored swine deep-pit building.

Long-term NH_3, H_2S, and CO_2 concentrations and emissions

A comparison was made between the TMY3 data set and the long-term mean weather data and the corresponding air quality predicted by the BTA-AQP model in order to investigate how the air quality values using a TMY3 data set followed actual long-term means (figures 4 to 7). The long-term period of time used in this study was selected from 2004 to 2008 due to the availability of a complete online weather data set in the region near the monitored swine facility. Hourly predictions were made using on-site weather data for each year (2004-2008, inclusive), with the monthly average minimum and maximum predictions determined. The maximum and minimum designations were determined by month and not year, e.g., the predicted minimum in January and the predicted minimum in February could have occurred in different years. The Des Moines International Airport was chosen as the TMY3 site, which is about 100 kilometers away from the swine facility used for field data collection, since it is the closest Class I site in the Iowa TMY3 data set. Class I stations are those with the lowest uncertainty in weather information. In addition to the predictions made with on-site weather data from 2004-2008 and the predictions using TMY3 weather data, the actual measured monthly averages from 2003 are given for completeness (figures 4 to 7).

Figure 4 illustrates the relationships among the long-term mean (i.e. on-site 5-year average data), the TMY3 generated values and 2003 actual field measurements for outside temperature. The minimum and maximum dashed lines represent the minimum and

maximum ranges of the outside temperature during the selected 5-year period (2004-2008). It was observed that the TMY3 data and 2003 field measurements fell within the min-max range but some noticeable differences between the TMY3 and the long-term means were evident especially in February, May, August, and December. The overall absolute error between those two data sets was 16.3% throughout the year. Also, the differences between 2003 field data and the long-term means can be seen in February, March, August, and September.

Figures 5 and 6 summarize monthly ventilation rate and indoor temperature estimated by the BTA model (Sun and Hoff, 2010) using the TMY3 data set and the on-site 2004-2008 weather data, respectively. The 2003 field measurements and the minimum and maximum ranges of the predicted ventilation rate and indoor temperature during the selected 5-year period were shown in figures 5 and 6 as well. The monthly ventilation rate predictions based on TMY3 data were higher than the long-term means during warm weather but closely matched the long-term means during cold weather conditions (figure 5). This probably was caused by the discrepancy in outdoor temperature between the TMY3 data set and the 2004-2008 weather data, i.e., relatively higher outdoor temperature using the TMY3 in the summer resulted in a higher estimated ventilation rate. Conversely, the predicted indoor temperatures were in good agreement with the long-term means (figure 6). The overall absolute error was less than 2.0%. Furthermore, the 2003 field measured ventilation rates fell into the ranges of min-max expect for January, February, and April while for all 12 months of the year, the 2003 field indoor temperatures were slightly higher than TMY3 predictions and long-term means. These differences between the 2003 actual data and TMY3 predictions could be due to different outside weather conditions and the forecasting error of the BTA model.

The monthly air quality predictions using the TMY3 data were compared with the averaged results of the 5-year period and the 2003 field measurements as illustrated in figure 7. It was found that: (1) the NH_3, H_2S, and CO_2 concentrations and emissions obtained by the TMY3 data set and the long-term air quality means were between the minimum and maximum values of the five individual year simulations, e.g., each of the five predicted data sets used one year weather data from 2004 to 2008; (2) the TMY3 predictions followed the long-term means well; and (3) although the majority of the 2003 field measurements were within the ranges of min-max of the predictions using on-site 2004-2008 weather data, some distinct differences between the actual data and the TMY3 predictions can be observed in figure 7, e.g., NH_3 emissions in January and April, H_2S concentrations in December, H_2S emissions in April, July and December, CO_2 concentrations in December, and CO_2 emissions in January, March and April. Again, these distinct differences were mainly attributed to different outside weather conditions and the forecasting error of the BTA model.

It can be further seen that the TMY3 values were within 6.0%, 7.0%, and 5.1% of the mean weather year (2004-2008) annual total for the NH_3, H_2S, and CO_2 concentrations respectively and 2.1%, 3.5%, and 2.6% of the mean weather year (2004-2008) annual total for the NH_3, H_2S, and CO_2 emissions respectively. These good agreements between the TMY3 data set predictions and the long-term means indicate that TMY3 data can be used in performing accurate long-term simulations of source air quality.

Table 2 gives the absolute errors between annual averaged predictions using the TMY3 data and the predictions using a single year weather data from 2004-2008. No major differences were observed between annual TMY3 predictions and any one single year. The minimum AE (2.0%) occurred with NH_3 emissions in 2004 while the maximum AE (11.1%)

appeared in H_2S concentration in the same year, which suggests that annual gas concentrations and emissions can be obtained by a TMY3 data set instead of an individual year weather data without resulting in large errors. These results show that a Class I TMY3 data set can be employed to evaluate annual air quality levels within an acceptable accuracy, especially for the livestock producers and environment researchers who might not be able to acquire complete and Class I level local weather information near a particular animal facility. However, it should be noted that the TMY3 data is not appropriate to estimate peak values for a particulate period of time.

Overall model error analysis and future work

The developed BTA-AQP model and TMY3 data can be used for accurately predicting indoor climate and long-term gas concentrations and emissions, but improvement in its accuracy should be made according to the following sources of error:

(1) Uncertainties in source air quality data. Since the source air quality data is important to develop the BTA-AQP model and evaluate the model predictive performance, more efforts should be made to maximize confidence, credibility, and consistency of the measured data;

(2) Prediction errors of the BTA model. As the number of assumptions in a model increases, the accuracy and relevance of the model diminishes. For example, the swine heat production data used in this research was from ASABE standards established decades ago. With improved genetics and feed management and diets, swine heat production (HP) has changed. Brown-Brandl el al. (2004) reported that the lean percent increase of 1.55% in the last 10 years has caused an increase in HP by approximately 15%. Future work is needed to collect new swine HP data from the latest literature;

(3) Prediction errors of the AQP model. The accuracy of the artificial neural network AQP model depends on the completeness of the data set and availability of various model input factors that significantly affect source air quality. The complete emission profiles should cover all possible swine production stages for a long period of time. In this study, one-year source air quality data was used that might not capture all of the relationships between gaseous concentrations and emissions and these input factors. More gas measurements are needed to expand the size of the data set. For the model input parameters, more important factors beyond indoor and outdoor temperatures, ventilation rate, swine growth cycle, and in-house manure storage level, should be considered and incorporated in the model. Added variables such as feed nutrient content, management practices, and manure temperature might prove to be important input variables. When pigs grow, the amount and composition of the feed intake change, as do the amount and composition of the manure. Thus, the amount of gas generation tends to increase. However, sharp decreases in the amount of daily nitrogen excretion were found when diet formulation changes were implemented. This adjustment process alleviates the amount of nitrogen in the manure converted to ammonia and other gases. Swine management practices are also vital factors to determine air quality levels. Good management practices can maintain proper environment requirements for the animals and decrease daily air emissions. Manure temperature might be a factor that may directly influence H_2S release; and,

(4) Bias error of the TMY3 and its limited application. Uncertainty values exist in the meteorological elements of the TMY3 data set (NSRDB, 2008). Additionally, TMY3 data is suitable for simulating solar energy conversion systems and building systems since each TMY3 month was selected according to five elements (global horizontal radiation, direct

normal radiation, dry bulb and dew point temperatures, and wind speed) which are the most important for solar energy and building systems. No literature has shown that the TMY3 data is suited to air quality predictions as well. Therefore, further research may focus on the development of new TMY data that is determined to be more appropriate for air quality simulations.

SUMMARY AND CONCLUSIONS

The over-arching goal of this study was to develop a building thermal analysis and air quality predictive (BTA-AQP) model to quantify indoor climate and long-term air quality (ammonia, hydrogen sulfide and carbon dioxide concentrations and emissions) from swine deep-pit buildings.

A comparison was made between the predicted and actual gas concentrations and emissions collected in 2003 in order to evaluate the accuracy of the BTA-AQP model estimates. It can be observed from the comparative boxplots that the median, spread and skewness of the field collected and predicted gas concentrations and emissions were similar. Poorer predictions in some of the months could be due to the relatively inaccurate ventilation rate predictions by the BTA model and the AQP model's inability in estimating gas concentrations resulting from barn management and pig activity. For all the predicted parameters, the MAE/SD ratios were less than 0.5; the CRM values approximated to 0; the IoA values were close to 1; and the NSEF values were greater than 0.5. These good model performance ratings indicated that the BTA-AQP model was able to accurately predict indoor climate and gas concentrations and emissions from swine deep-pit buildings.

The monthly air quality values estimated by the BTA-AQP model using TMY3 data were compared with those using 5-year on-site weather data. It was observed that the predictions using the TMY3 data followed the long-term mean patterns very well, which suggests that the TMY3 data can be used in performing accurate long-term simulations of source air quality. In addition, annual gas concentrations and emissions can be obtained using TMY3 data instead of an individual year weather data without resulting in large errors. These results demonstrate that a convenient approach to evaluate annual air quality levels within an acceptable accuracy is possible without long-term expensive on-site measurements. However, it should be noted that the TMY3 data is not appropriate to estimate peak values for a particulate period of time.

Improvement in the BTA-AQP model accuracy should be made according to four main sources of error: Uncertainties in air quality data; Prediction errors of the BTA model; Prediction errors of the AQP model, and Bias errors of the TMY3 data and its limited application.

ACKNOWLEDGEMENTS

The authors wish to acknowledge the USDA-IFAFS funding program for providing the funds required to collect the 2003 field data used in this research project and the USDA-Special Grants funding program for providing the funds for this specific research project. Their support is very much appreciated.

REFERENCES

Brown-Brandl, T.M., J.A. Nienaber, H. Xin and R. S. Gates. 2004. A literature review of swine heat and moisture production. *Trans. ASAE* 47(1): 259-270.

Dunning, T., and D.A. Freedman. 2008. Handbook of Social Science Methodology: Modeling selection effects. London: Sage.

Grivas, G. and A. Chaloulakou. 2006. Artificial neural network models for prediction of PM10 hourly concentrations, in the greater area of Athens, Greece. *Atmos. Environment* 40(7): 1216-1229.

Heber, A.J., J. Ni, T.T. Lim, P. Tao, A.M. Schmidt, J.A. Koziel, D.B. Beasley, S.J. Hoff, R.E. Nicolai, L.D. Jacobson and Y. Zhang. 2006. Quality assured measurements of animal building emissions: Gas concentrations. *J. Air and Waste Mgmt. Assoc.* 56(10): 1472-1483.

Hoff , S. J., D. S. Bundy, M. A. Nelson, B. C. Zelle, L. D. Jacobson, A. J. Heber, J. Ni, Y. Zhang, J. A. Koziel and D. B. Beasley. 2006. Emissions of ammonia, hydrogen sulfide, and odor before, during, and after slurry removal from a deep-pit swine finisher. *J. Air & Waste Mgmt. Assoc.* 56 (5): 581-590.

Hoff , S. J., D. S. Bundy, M. A. Nelson, B. C. Zelle, L. D. Jacobson, A. J. Heber, J. Ni, Y. Zhang, J. A. Koziel and D. B. Beasley. 2009. Real-time airflow measurement from mechanically ventilated animal buildings. *J. Air & Waste Mgmt. Assoc.* 59 (6): 683-694.

Hooyberghs, J., C. Mensink, G. Dumont, F. Fierens and O. Brasseur. 2005. A neural network forecast for daily average PM10 concentrations in Belgium. *Atmos. Environment* 39(18): 3279-3289.

Jacobson, L.D., H. Guo, D.R. Schmidt, R.E. Nicolai, J. Zhu and K.A. Janni. 2005. Development of the OFFSET model for determination of odor-annoyance-free

setback distances from animal production sites: Part I. Review and experiment. *Trans. ASABE* 48(6): 2259-2268.

NSRDB. 2008. Users manual for TMY3 data sets. Golden, Co: USDE National Renewable Energy Laboratory.

Pedersen, L. 2007. Use of different methodologies for thermal load and energy estimations in buildings including meteorological and sociological parameters. *Renewable and Sustainable Energy Review.* 11: 998-1007.

Sousa, S.I.V., F.G. Martins, M.C.M. Alvim-Ferraz and M.C. Pereira. 2007. Multiple linear regression and artificial neural network based on principal components to predict ozone concentrations. *Environ. Modeling and Software* 22(1): 97-103.

Sun, G. and S. J. Hoff. 2010. Prediction of indoor climate and long-term air quality using the BTA-AQP model: Part I. BTA model development and evaluation. *Trans. ASABE* 53(3):863-870.

Sun, G., S. J. Hoff, B. C. Zelle and M. A. Nelson. 2008. Development and comparison of backpropagation and generalized regression neural network models to predict diurnal and seasonal gas and PM_{10} concentrations and emissions from swine buildings. *Trans. ASABE* 51(2):685-694.

Yang, L., J. C. Lam, J. Liu and C. L. Tsang. 2008. Building energy simulation using multi-years and typical meteorological years in different climates. *Energy Convers. and Mgmt.*49:113-124.

Table 1. Statistical performance of the BTA-AQP models.[a]

Parameter	Actual ± S.D.	Predicted ± S.D.	MAE	CMR	IoA	NSEF
NH_3Con (ppm)	19.9 ± 6.8	20.5 ± 6.7	0.9	0.028	0.99	0.97
NH_3ER (kg d^{-1})	6.86 ± 2.04	6.38 ± 1.78	0.14	0.005	0.99	0.99
H_2SCon (ppb)	553 ± 260	560 ± 254	57	0.013	0.97	0.88
H_2SER (kg d^{-1})	0.473 ± 0.295	0.463 ± 0.295	0.056	-0.022	0.98	0.93
CO_2Con (ppm)	2636 ± 1618	2674 ± 1601	68	0.015	0.99	0.99
CO_2ER (kg d^{-1})	1226 ± 280	1143 ± 210	116	-0.068	0.83	0.52

[a] Con and ER indicate the concentrations and emissions, respectively.

Table 2. Comparison of predicted air quality using the TMY3 and a single year.[a]

Year	NH_3Con	NH_3ER	H_2SCon	H_2SER	CO_2Con	CO_2ER
2004	8.3%	2.0%	10.4%	3.5%	6.5%	3.1%
2005	6.5%	4.0%	7.1%	6.0%	5.4%	4.2%
2006	5.2%	3.7%	8.9%	7.1%	4.3%	6.0%
2007	5.6%	2.2%	7.3%	4.7%	5.5%	3.5%
2008	8.7%	4.6%	7.9%	6.7%	8.0%	4.8%

[a] Con and ER indicate concentrations and emissions, respectively.

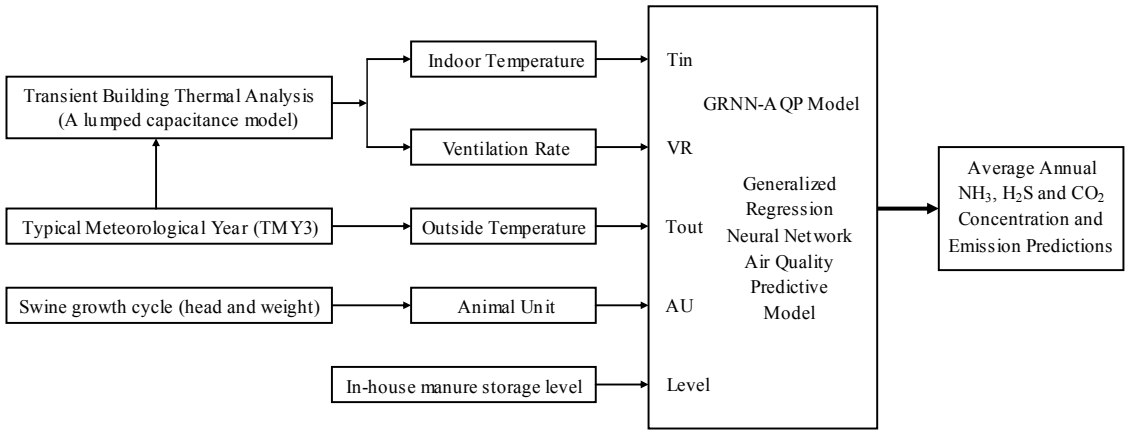

Figure 1. Scheme of the BTA-GRNN-AQP model (Tin: indoor temperature (^{o}C); VR: ventilation rate (m^3s^{-1}); AU: animal unit; Tout: outside temperature (^{o}C), Level: in-house manure storage level (m)).

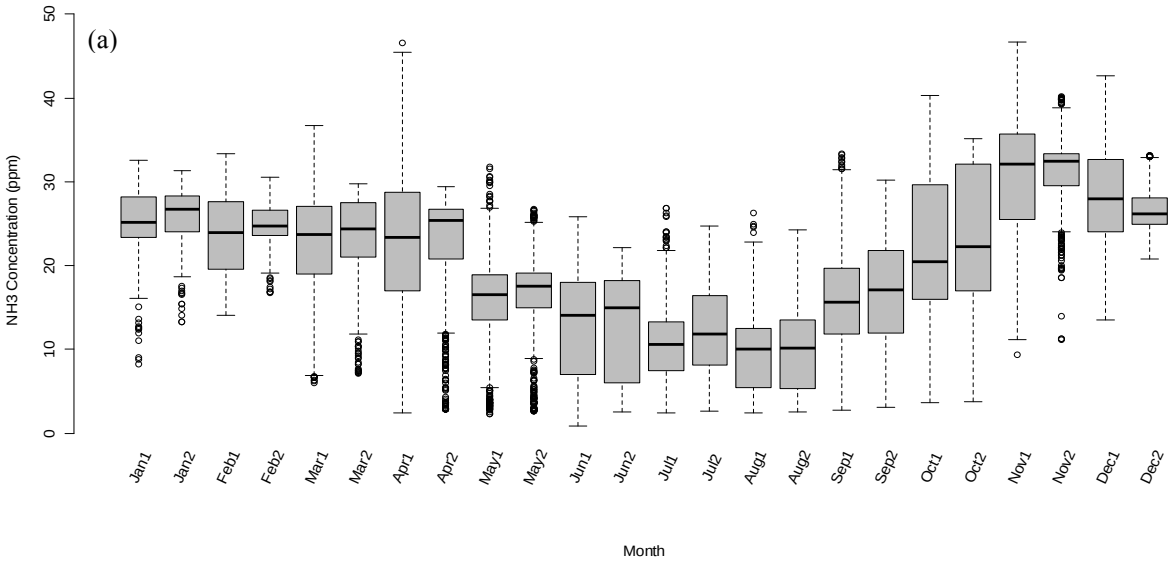

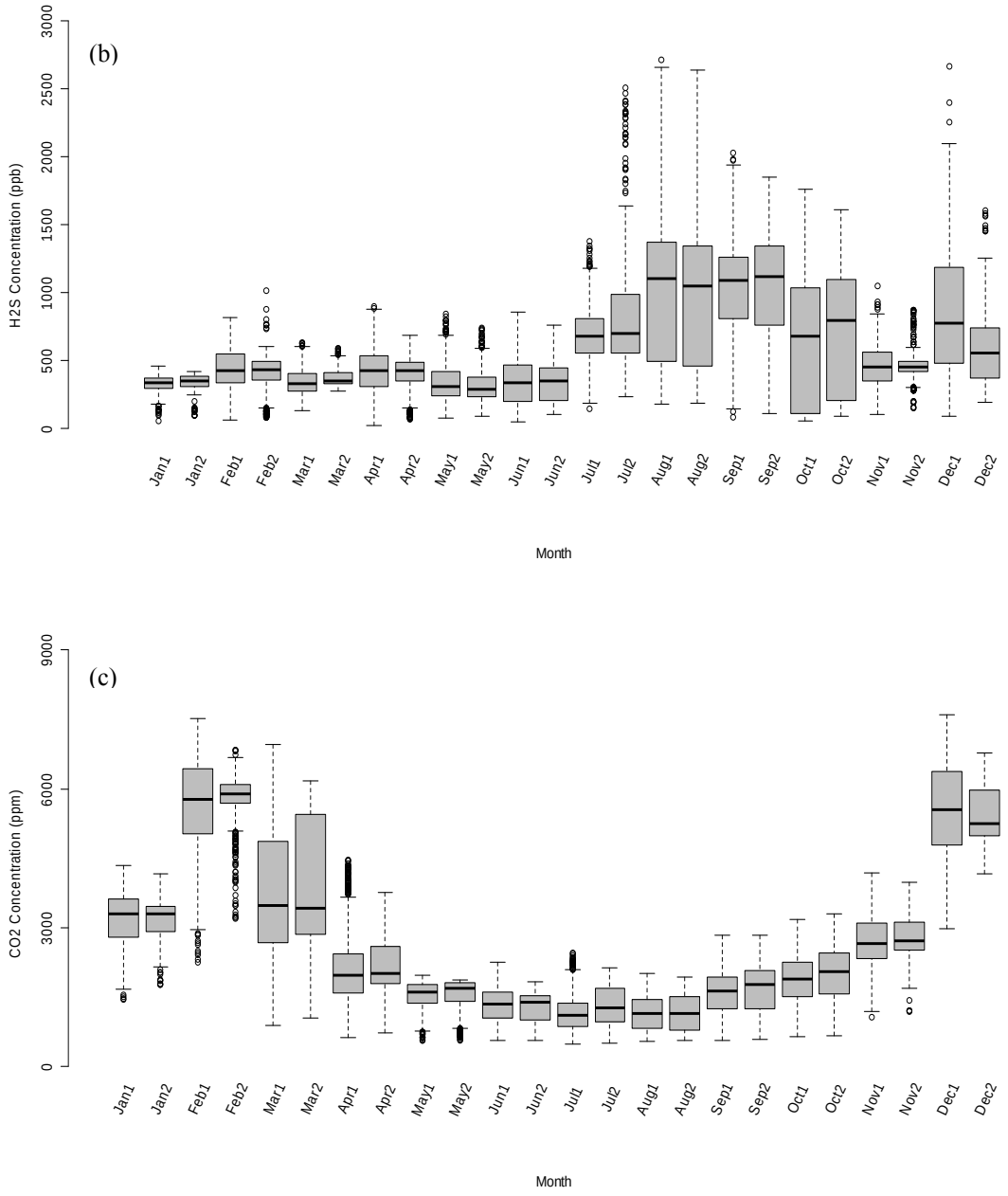

Figure 2. Actual vs. predicted hourly NH_3 (a), H_2S (b), and CO_2 (c) concentrations in 2003 (1: Actual; 2: Predicted; circles: Potential outliers).

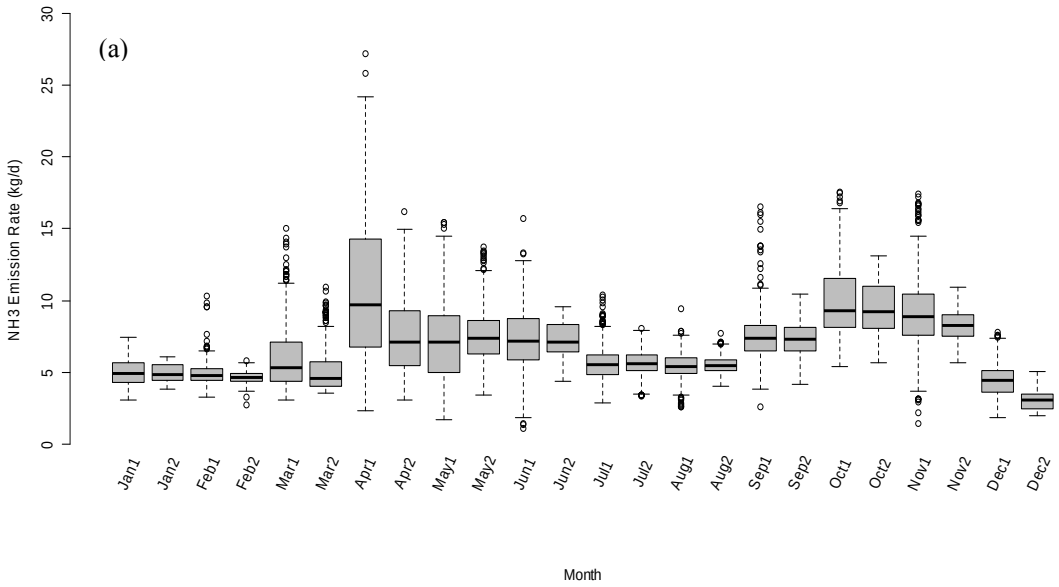
(a)
NH3 Emission Rate (kg/d)
0
5
10
15
20
25
30
Jan1
Jan2
Feb1
Feb2
Mar1
Mar2
Apr1
Apr2
May1
May2
Jun1
Jun2
Jul1
Jul2
Aug1
Aug2
Sep1
Sep2
Oct1
Oct2
Nov1
Nov2
Dec1
Dec2
Month

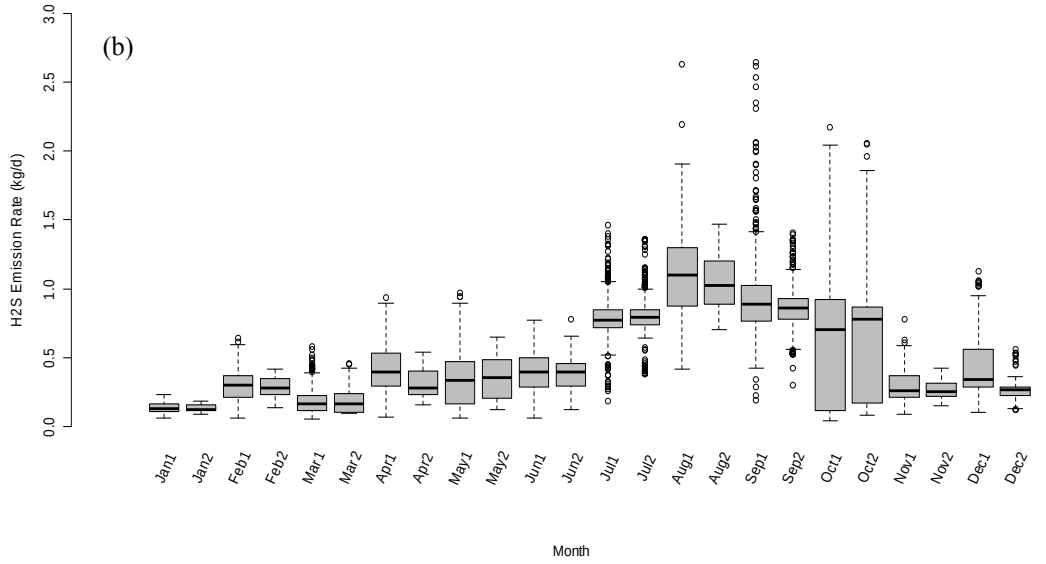
(b)
H2S Emission Rate (kg/d)
0.0
0.5
1.0
1.5
2.0
2.5
3.0
Jan1
Jan2
Feb1
Feb2
Mar1
Mar2
Apr1
Apr2
May1
May2
Jun1
Jun2
Jul1
Jul2
Aug1
Aug2
Sep1
Sep2
Oct1
Oct2
Nov1
Nov2
Dec1
Dec2
Month

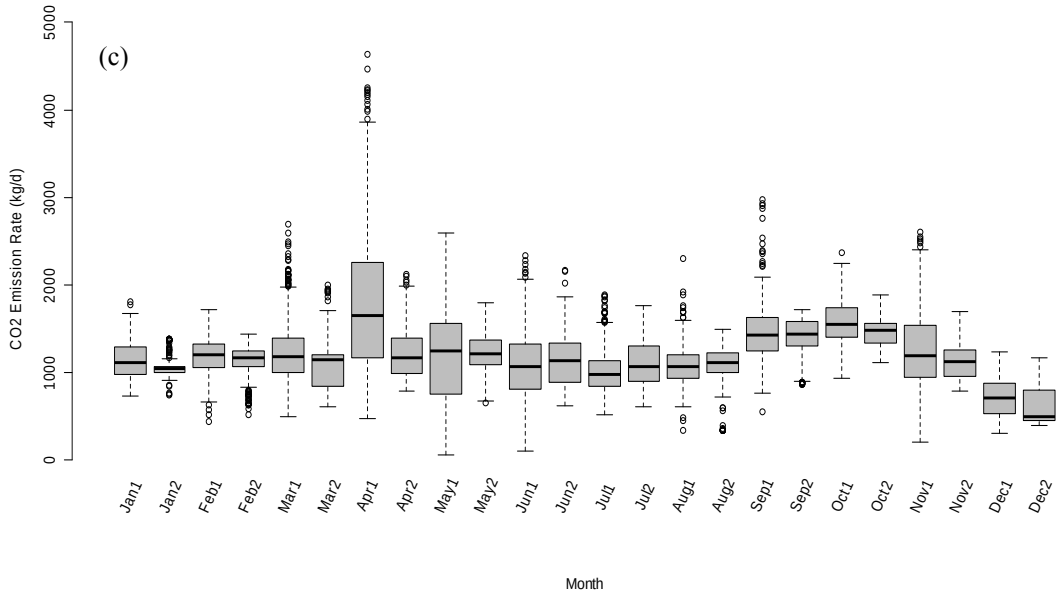

Figure 3. Actual vs. predicted hourly NH_3 (a), H_2S (b), and CO_2 (c) emissions in 2003 (1: Actual; 2: Predicted; circles: Potential outliers).

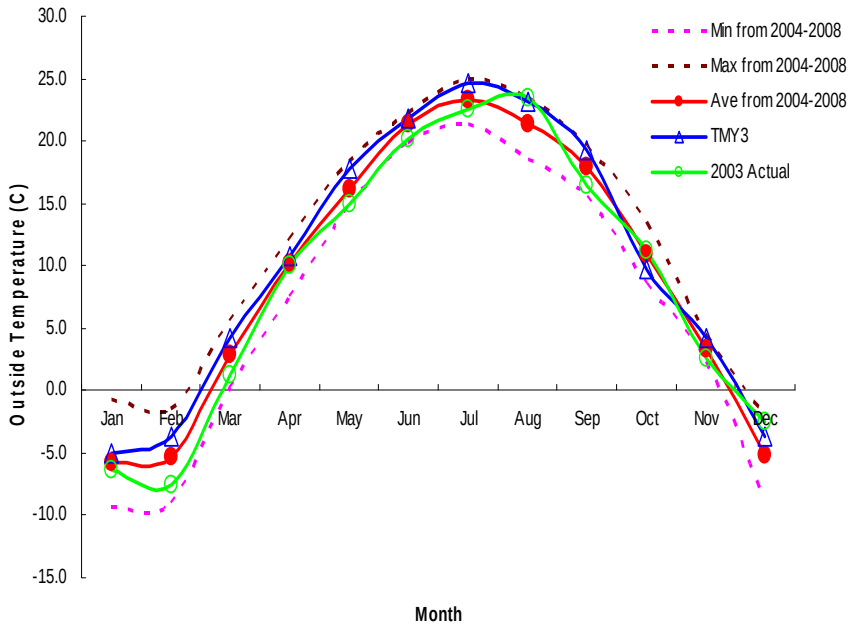

Figure 4. TMY3 vs. long-term means and 2003 field data for the outside temperature.

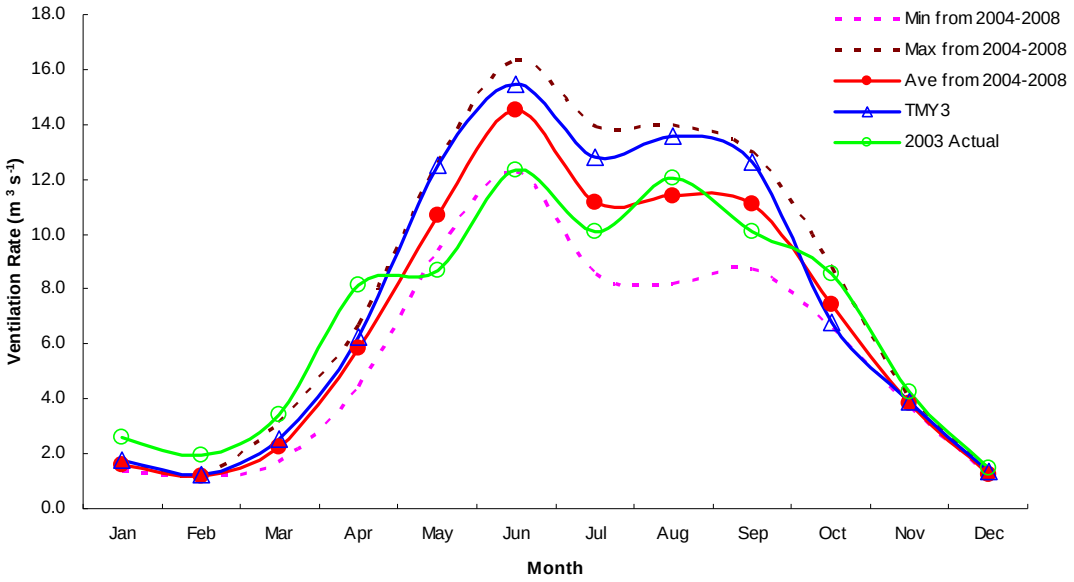

Figure 5. TMY3 predictions vs. long-term means and 2003 field data for the estimated ventilation rate.

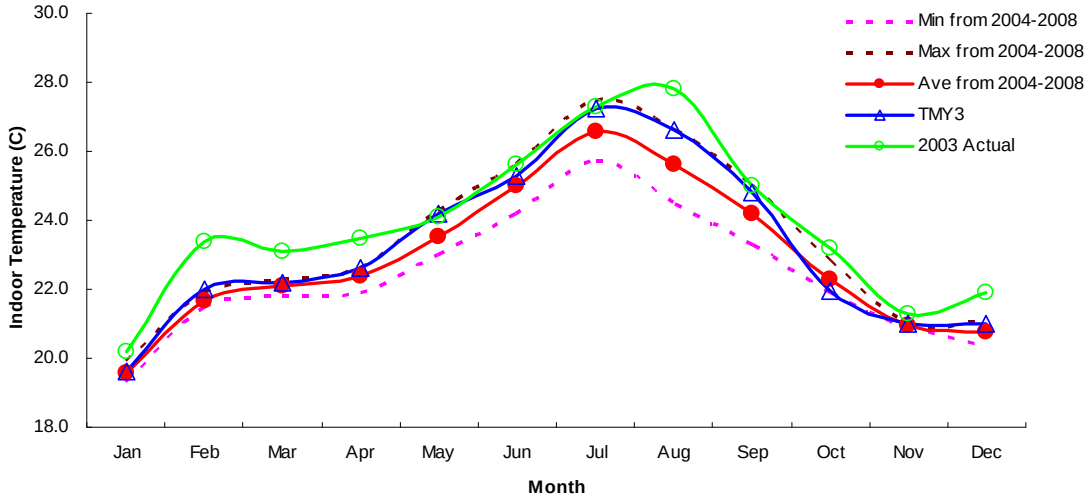

Figure 6. TMY3 predictions vs. long-term means and 2003 field data for the estimated indoor temperature.

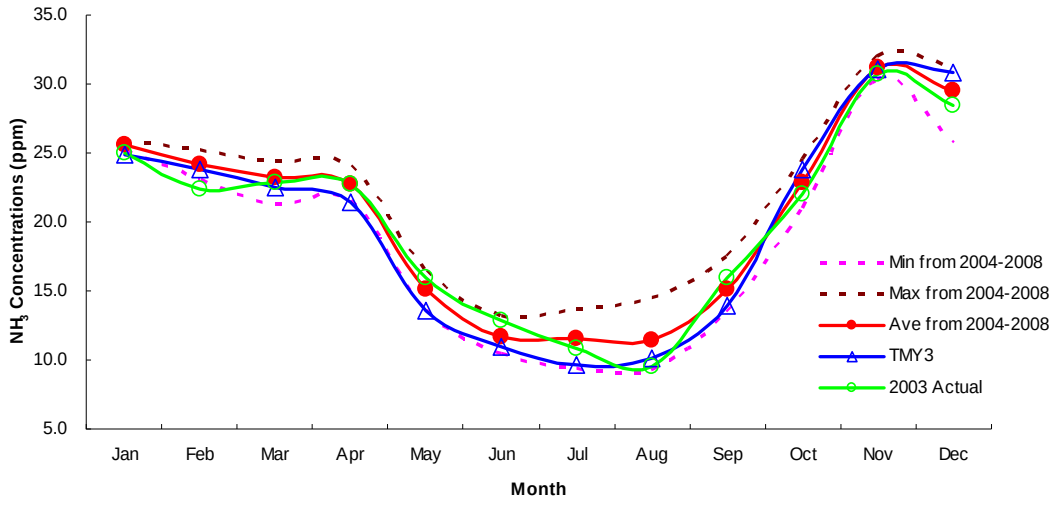
35.0
30.0
25.0
20.0
15.0
10.0
5.0
NH3 Concentrations (ppm)
Jan
Feb
Mar
Apr
May
Jun
Jul
Aug
Sep
Oct
Nov
Dec
Month
Min from 2004-2008
Max from 2004-2008
Ave from 2004-2008
TMY3
2003 Actual

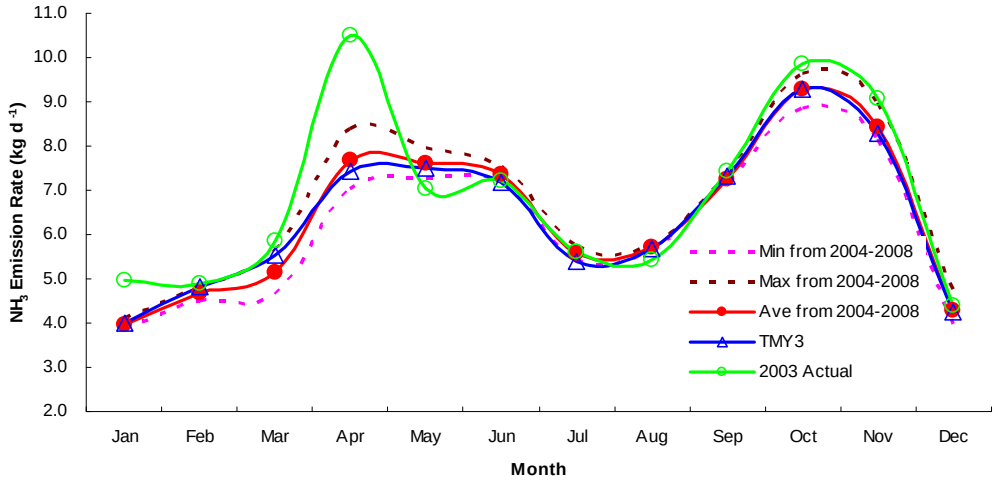
11.0
10.0
9.0
8.0
7.0
6.0
5.0
4.0
3.0
2.0
NH3 Emission Rate (kg d-1)
Jan
Feb
Mar
Apr
May
Jun
Jul
Aug
Sep
Oct
Nov
Dec
Month
Min from 2004-2008
Max from 2004-2008
Ave from 2004-2008
TMY3
2003 Actual

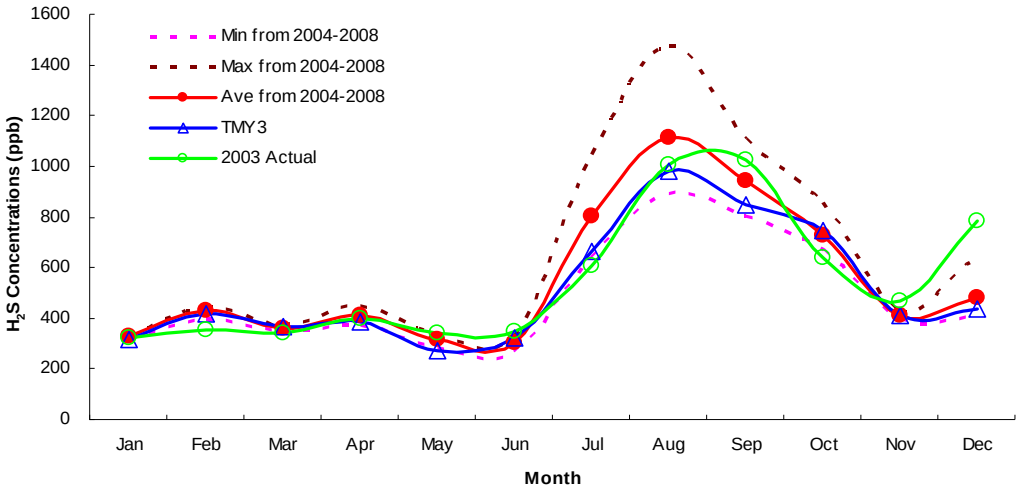
1600
1400
1200
1000
800
600
400
200
0
H2S Concentrations (ppb)
Min from 2004-2008
Max from 2004-2008
Ave from 2004-2008
TMY3
2003 Actual
Jan
Feb
Mar
Apr
May
Jun
Jul
Aug
Sep
Oct
Nov
Dec
Month

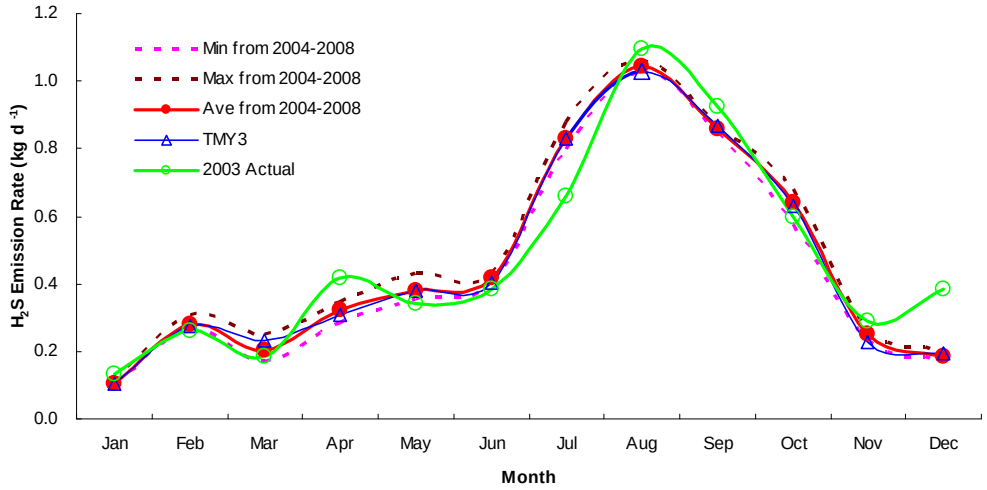
1.2
1.0
0.8
0.6
0.4
0.2
0.0
H2S Emission Rate (kg d -1)
Min from 2004-2008
Max from 2004-2008
Ave from 2004-2008
TMY3
2003 Actual
Jan
Feb
Mar
Apr
May
Jun
Jul
Aug
Sep
Oct
Nov
Dec
Month

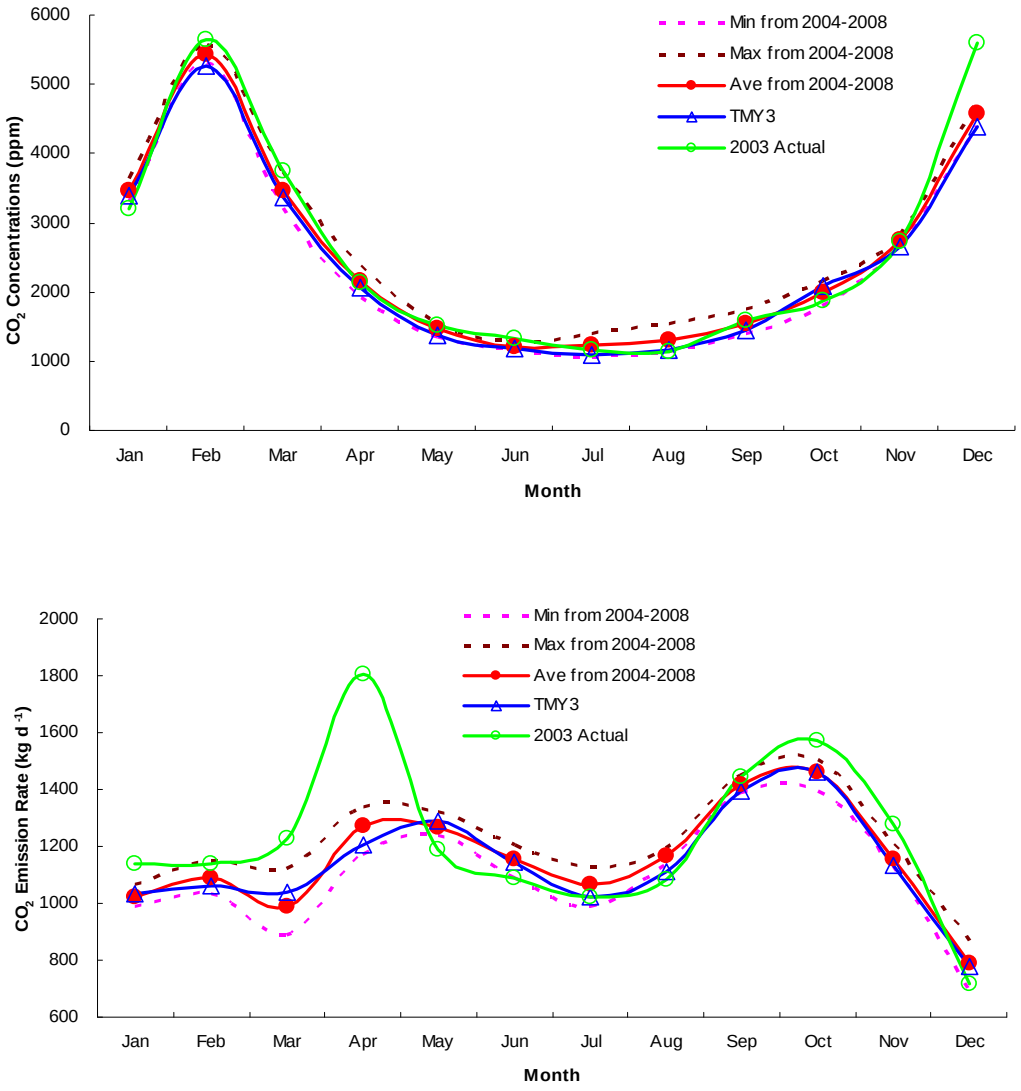

Figure 7. TMY3 predictions vs. long-term means and 2003 field data for the monthly air quality values (NH_3, H_2S and CO_2 concentrations and emissions).

CHAPTER 6. SIMULATED IMPACTS OF DIFFERENT HUSBANDRY MANAGEMENT PRACTICES AND GEOGRAPHICAL AREA ON LONG-TERM AIR QUALITY

A paper to be submitted to the Transaction of the American Society of Agricultural and Biological Engineers

G. Sun and S. J. Hoff

ABSTRACT

Simulated impacts of different husbandry management practices and geographical areas on long-term air quality have been studied using our proposed BTA-AQP (building thermal analysis-air quality predictive) model and statistical analysis methods with four scenarios: building heat loss factor (BHLF) scenario, barn set-point temperature (SPT) scenario, animal production schedule (APS) scenario, and geographical area (GA) scenario. The purpose was to help animal producers and environmental researchers understand the parameters influencing air quality and find a simple, inexpensive and effective abatement strategy to alleviate airborne pollution from livestock production facilities instead of numerous high-cost gas/odor control technologies. The predicted results indicated that (1) the BHLF scenario had a negligible effect on the source air quality; (2) the new SPT scenario was capable of reducing indoor gas levels during hot weather conditions while the corresponding gas emissions did not increase substantially. Thus, current barn set-point temperature strategies provide one method to decrease the risk of relatively high gas concentrations (especially H_2S concentration) inside the building and protect the health of

workers and animals; and (3) the new APS scenario had no significant effect on mean annual gas concentrations but could lead to a moderate decrease in mean annual gas emissions. Also, it was found that the GA factor, for the swine deep-pit barns with similar building characteristics and management practices, might have a large impact on indoor gas concentrations but very little effect on mean annual gas emissions.

Keywords. Simulated Impacts, Air Quality, Husbandry management practices, Geographical areas, Livestock.

INTRODUCTION

Source airborne pollutants within and from livestock production facilities are affected by barn characteristics, outdoor weather conditions, indoor climate, diurnal and seasonal effects, animal growth cycles, in-house storage levels, and barn management. Studying the impacts of these factors on air quality is very important for helping environmental researchers and animal producers understand the parameters influencing livestock air quality so that they might make wise decisions regarding the selection and implementation of odor and gas mitigation techniques.

Most recent studies have investigated the effects of several parameters, such as sampling sites, time of day, season, ambient air temperature, building ventilation rate, and flooring systems, on the odor and gas concentrations and emissions (OGCERs) for various animal facilities (Aarnink et al., 1995; Groot Koerkamp et al., 1998; Zhu et al., 1999; Ni et al., 2002; Gay et al., 2003; Jacobson et al., 2005; Guo et al., 2006; Hoff et al., 2006; Sun et al., 2008b, 2010c); few, however, have explored how husbandry management practices (e.g., the thermal insulation characteristic of an animal building, barn set-point temperature

scheme, and animal production schedule) and geographical factors impact long-term source air quality. It is reasonable to hypothesize that enforcing different animal management policies may be a simple, inexpensive and effective abatement strategy to reduce airborne pollution, although no evidence to support or refute this hypothesis was found in the literature.

Absence of evidence in the literature might be attributed to several factors. Firstly, testing the hypothesis is almost impossible in the field since actual animal buildings are not currently configured as laboratory testing rooms allowing changes to barn operational parameters for a period of time (e.g., from a couple of months to a year). Secondly, a laboratory testing room is inappropriate for use in hypothesis validation because it misses complexities in the real environment of animal buildings. Thirdly, conducting direct and long-term airborne contaminant measurements in different geographical areas is not practical due to complex experiment design, expensive monitoring system requirements, and high personal and management overhead.

On the contrary, the use of air quality predictive models could facilitate this type of hypothesis testing far more rapidly and economically than by field/lab experiment methods. Therefore, the objectives of this research were to (1) apply a validated building thermal analysis and air quality predictive (BTA-AQP) model (Sun and Hoff, 2010a and 2010b) to different husbandry management practices and geographical area scenarios, (2) compare the corresponding air quality profiles with those under normal barn management conditions, and (3) assess the simulated impacts of the new scenarios on long-term air quality (ammonia, hydrogen sulfide and carbon dioxide concentrations and emissions).

MATERIALS AND METHODS

Typical deep-pit swine building description

A mechanically ventilated deep-pit (2.4 m) swine finishing building, located in central Iowa, was used for this study. As shown in figure 1, this typical swine building was 60 m long and 13 m wide, designed to house 960 finishing pigs from ~20 to 120kg. Gas concentrations from an inside room site, wall and pit exhaust, and an outside location (background) were monitored via a mobile emission laboratory which contained a gas sampling system (GSS), a computer-based data acquisition system, gas analyzers, environmental instrumentation, standard gas calibration cylinders, and other supplies. A three-way solenoid system was used to automatically switch between 12 measuring locations with 10-min sampling intervals and sequentially delivered gas from each location to the gas analyzers. Thus, gas samples were taken during twelve, 120-min measurement cycles per day. Also, pertinent environment parameters (temperature, relative humidity, and static pressure) and total building ventilation rate were simultaneously measured. Data was stored on a 1-minute averaged basis for a total of 15-months, 12-months of which were used for previous model development (Sun and Hoff, 2010a and 2010b).

During cold-to-mild seasons, pit fans 1 and 2, side wall fan 3, and tunnel fans 4 and 5 (figure 1) combined with a series of 10 rectangular center-ceiling inlets were used to distribute fresh air and remove moisture, odors and aerosols within the building; while all the fans (except side wall fan 3) and an adjustable curtain at the opposing end wall were used to maintain suitable indoor environment under warm and hot weather. The total ventilation rate was obtained by recording the on/off status of four single-speed tunnel fans (fans 5, 6, 7, and

8) and the on/off status along with fan rpm levels for all variable speed fans (fans 1,2,3, and 4). The ventilation rate of each fan was measured *in situ* using a FANS unit (Gates et al., 2004) where calibration equations were developed as a function of static pressure and fan rpm levels for variable speed fans. Gas emission rates were determined by multiplying fan airflow rate by representative gas concentration differences between inlet and outlet for all fans operating at any given time. The maximum estimated uncertainty in ventilation rate and gas concentrations were ±7.2 % (Hoff et al., 2009) and ±5.0 %, respectively. These individual uncertainties led to an average uncertainty in emission rate of about ±9.0 %.

BTA-AQP model description

The building thermal analysis and air quality predictive (BTA-AQP) model developed by Sun and Hoff (2010a, 2010b) was utilized in this research to predict source air quality from swine deep-pit buildings with different animal management practices and geographical area scenarios.

The BTA model is capable of acquiring the transient behavior of ventilation rate and indoor air temperature according to the thermo-physical properties of a typical swine deep-pit building, set-point temperature scheme, fan staging scheme, transient outside temperature, and the heat fluxes from pigs and supplemental heaters. The obtained ventilation rate and resulting indoor air temperature combined with animal growth cycle, in-house manure storage level, and outdoor weather data were fed into the AQP model (Sun et al., 2008a) to calculate hourly ammonia, hydrogen sulfide and carbon dioxide concentrations and emission rates. The good model performance ratings and the graphical interpretations presented in Sun

and Hoff (2010a, 2010b) indicate that the BTA-AQP model is able to accurately predict indoor climate and air quality for the swine deep-pit building.

To better compare air quality results among different scenarios, a typical meteorological year (TMY3) database (NSRDB, 2008) was used instead of the single weather year data used for the field measurements that were ultimately used to develop the BTA-AQP model. TMY3 consists of a multi-year and long-term (30 years) average measured data series which represents a year of prevailing weather conditions for a specific location. The Des Moines (DSM) International Airport was selected as the TMY3 site in this research for the normal barn management scenario. This TMY3 site is about 100 kilometers away from the swine facility used for field data collection and was the closest Class I site (Class I site has the lowest uncertainty in weather information) in the Iowa TMY3 dataset. Moreover, the Dallas TMY3 weather data was employed to compute long-term air quality in Texas, used to test the geographical area (GA) factor component of this research.

Accuracy evaluation of simulated results

Due to lack of field measurements, evaluating the accuracy of model simulations under different scenarios is a challenge to model users. Regarding the ANN (artificial neural network)-based AQP model (Sun et al., 2008a), two important aspects including proper model training methods and high-quality training dataset, might be specially considered during the model development in order to gain reliable predicted values. In other words, these two aspects would have the model outputs approximate target values given new data that are not in the training set. Proper model training methods were presented in detail in Sun et al. (2008a), e.g., how to determine optimum values for the number of model layers and

neurons, type of activation functions and training algorithms, learning rates, momentum, and smoothing factors; while high-quality training datasets should possess three essential traits: a sufficiently large sample number, a representative subset, and complete information related to the target (Haykin, 1999).

The sufficient number of training samples for a given size neural network can be computed from the following:

$$N >= \log(n/(1-a)) * w/(1-a) \quad (1)$$

where

N = the number of training samples

n = the number of neurons in the network

a = the desired accuracy on the test set

w = the number of weights for the network

In this research, n, a, and w values were equal to 45, 90%, and 200, respectively. Thus, the minimum required sufficient number of training samples would be 5306. This study used a total of 7330 samples as the training dataset, which indicates that the AQP model contained sufficient information pertaining to livestock air quality. Furthermore, these training samples characterized nearly all cases of hourly air emission profiles and corresponding emission factors throughout the year and presented typical variation patterns of the air emissions and factors under different weather conditions, such as cold, mild, and warm weather. Meanwhile, the collected training data covered a wide range of outside temperatures from as low as -24 ^{o}C to as high as 36 ^{o}C and included two complete animal growth cycles, one was from small pigs (~20kg) entering the room in early February, 2003 to larger pigs (~120kg)

shipped to market at the end of June, 2003; the other was between the middle of July, 2003 (~20kg) and early December, 2003 (~120kg). The pigs of different ages experiencing cold-mild-warm seasons resulted in a range of set-point temperatures, fan staging schemes, and animal heat fluxes and supplemental heaters and thus influenced the indoor climate (e.g., ventilation rate and inside temperature) and gas concentrations and emissions. In general, these cases expand the representative samples in the training dataset and provide a solid basis for model generalization.

In addition to the above described two important aspects, another issue dealing with good model generalization is that a neural network performs very well using new testing data which are within the range of the training dataset. In other words, to ensure the accuracy of predictions, the cases from a new scenario should resemble known training data to a large extent. If the new testing data falls within the range of the training samples or are more or less surrounded by neighboring training cases, the predicted values by the AQP model are trustworthy; whereas, if new cases fall far outside the range of the training data, the predictions are scarcely reliable.

With the help of graphical presentations, a 3-D scatterplot (figure 2) illustrates the relationship between the Dallas site GA scenario vs. the training dataset to demonstrate whether the simulated Dallas results by the AQP model were dependable and therefore acceptable. The Dallas site data was selected as an example due to the fact that the difference between the Dallas cases and the training dataset was the largest among all the scenarios investigated in this research. Also, it should be pointed out that the air quality dataset has a five-dimensional input space so that it obviously could not be represented in a

3-D plot. This problem was solved using principle component analysis (PCA) technology, which is able to reduce the data dimensionality and transform a number of correlated variables into a smaller number of uncorrelated variables. The PCA results revealed that the fourth and fifth principle components (PC4 and PC5) were only responsible for about 3.76% and 5.44% of the total variance respectively, certainly the negligible factors; while the first three PCs (PC1~PC3) were able to explain more than 90% of the total variability, which suggested that it would be adequate to describe air quality data using the first three PCs (PC1~PC3 shown in figure 2) instead of the five original features.

As can be seen from the different viewing angles in figure 2, a majority of the data from the GA scenario (Dallas, TX) fell into the range of the training data and some cases were encircled by nearby training samples. Only a few of the Dallas site data were far removed from the training cases. To avoid viewing illusion that these two datasets looked closer than actual, the Bhattacharyya distance (B-distance) was employed to measure the similarity of their statistical distributions and determine the relative closeness of the two sample sets (Bhattacharyya, 1943). The closer B-distance is to 0, the more similar the two datasets become. The Bhattacharyya distance coefficient was equal to 0.1643 and indicated that the Dallas site data and the training samples seemed to overlap. Thus, it can be concluded that the new cases from the Dallas site scenario could bear much resemblance to the training data and the corresponding predictions by the AQP model would be reliable. Likewise, the new cases from the other scenarios (BHLF, SPT, APS) resembled the training data as well.

RESULTS AND DISCUSSION

Different animal management practices and geographical area scenarios were tested to evaluate their possible effects on long-term air quality. In total, twenty-four air quality predictions (six NH_3, H_2S, and CO_2 concentration and emission simulations per scenario) were made by the BTA-AQP model using four new scenarios: building heat loss factor (BHLF) scenario, barn set-point temperature (SPT) scenario, animal production schedule (APS) scenario, and geographical area (GA) scenario. The BHLF scenario assumed a 50% decline of current BHLF value, which means that the typical deep-pit swine grower/finisher building was on average double-insulated. The barn SPT scenario decreased the originally tested set-point temperature scheme by an average of 28.7% throughout the swine growth phase. The APS scenario would lead to a new animal growth cycle starting in mild weather instead of a warm or cold climate as was the case for the actual field measurements. For the GA scenario, Dallas, Texas was selected as a new sampling site.

Table 1 summarizes the mean annual simulated air quality values for the above four scenarios. The Des Moines (DSM) scenario (a typical swine deep-pit building located in Des Moines under normal barn management conditions) was considered the control against which other scenarios were compared. Side-by-side box plots were constructed for visually comparing features of sample distributions of the new scenarios and the DSM scenario. These boxplots can provide the comparison of the location, spread, and shape of the distributions by examining the relative positions of the median, the heights of the boxes which measure the interquartile ranges, the relative lengths of the whiskers, and the presence of outliers at either end of the whiskers.

BHLF scenario

The total building heat loss factor for the deep-pit swine building in Iowa monitored for this research was 965 W/^{o}C (Sun and Hoff, 2010a). The BHLF scenario used half of that value, i.e., 482 W/^{o}C to test this scenario.

From Table 1, the percentage difference in mean annual air quality data between the BHLF scenario and DSM scenario, calculated by (BHLF value-DSM value)/(DSM value), was very slight, within +/-1.5%. This can be also verified in Figure 3. The comparative boxplots of hourly gas predictions for each scenario show nearly the same median, spread, and skewness throughout the year, which suggests that those two datasets were generally distributed in the same way. Thus, the BHLF scenario had a negligible effect on the source long-term air quality ($p>0.05$).

Barn SPT scenario

Different set-point temperature curves used in animal buildings would result in changes of indoor climate during the animal production period possibly affecting air quality parameters. Figure 4 shows two different SPT curves: one was the SPT curve used in the field study (DSM scenario); the other was a new SPT curve, which decreased current SPT by an average of 28.7% throughout the growth cycle.

In Table 1, the SPT scenario reduced mean annual gas concentrations by -2.4% ~ -28.6% in comparison to those using the DSM scenario. Also, it can be seen that the largest decrease in gas concentrations was for H_2S (a -28.6% reduction). This large reduction was probably attributed to much higher ventilation rate as a result of the lowered set-point temperatures, especially during hot weather. Hence, increasing ventilation rate would be a significant way to expedite air exchange rate and substantially lower indoor H_2S level.

However, despite a large reduction in H_2S concentrations, the mean annual NH_3 and CO_2 concentrations did not follow this reduction pattern. Contrarily, their mean annual emissions increased slightly since the emission rate is the product of gas concentrations and the ventilation rate and there is an inverse relationship between them.

Figure 5 displays long-term hourly NH_3, H_2S, and CO_2 concentrations and emissions over 12 months for the SPT and DSM scenarios. Compared with the DSM scenario for each month, the SPT scenario shows a decreasing trend in the magnitudes of location (as measured by the median) of the gas concentration distributions throughout the year except for January, February, March and April. Additionally, the observed shapes of these concentration distributions during April to September appeared to be right-skewed with either long-right tails or outside values on the right-tail. The lower locations and right-skewed shapes indicated that the majority of predicted gas concentration data was highly concentrated in the very low range and only few high values fell into the upper range, i.e., the SPT scenario was capable of reducing indoor gas levels during most times under warm weather, due to higher ventilation rates. Meanwhile, the corresponding gas emissions did not increase significantly. Thus, current barn set-point temperature curves might be adjusted by setting a few degrees lower in warm season in order to reduce the risk of relatively high gas concentrations (especially H_2S concentrations) inside the building and protect the health of workers and animals.

APS scenario

For grower-finisher swine production operations, animal growth cycle indicates the growth period as pigs mature from approximately 20 to 120 kg inside the building. Typically, one complete animal growth cycle for grower-finisher pigs is ~140 days or about 4.5 months

and thus there are two complete growth cycles in a year. These two growth cycles started either in the winter or in the summer during field measurements. Pig weight determined indoor set point temperature and different SPT setting during different seasons would conceivably impact diurnal and seasonal air quality. To study the effect of animal production schedule on long-term air quality, a new swine production timetable was established and used in this research. The starting date of this new timetable was on the first day of April.

The percentage difference between the APS and DSM scenarios ranged from -2.2% to 5.2% for the mean annual gas concentrations and from -6.6% to -14.2% for the mean annual gas emissions (Table 1). The simulated results revealed that the new animal production schedule had no significant effect on gas concentrations ($p>0.05$) but could cause a moderate decrease in gas emissions. The ventilation rate variation resulting from the new schedule might account for this emission reduction.

Looking at the boxplots shown in Figure 6, the observed APS distributions of gas concentrations had different locations, spreads and shapes compared with those of the DSM scenario. For example, the median of the APS NH_3 concentration in February was larger than that of the DSM distribution. This may be due to two reasons: one was that larger pigs used for the APS scenario (87-105kg per pig) produced more gas/manure waste than the small pigs (20-38 kg per pig) in the DSM scenario; the other was that to maintain set-point temperature during cold weather, similar minimum ventilation rate was supplied for both scenarios. Hence, more gas accumulation inside the barn for the APS scenario resulted in much higher indoor NH_3 concentrations, while in July, the APS scenario shows an obvious pattern, i.e., low locations and a right-skewed shape with heavy tail, for all the gas concentrations. The possible explanation might be the lower set-point temperature and the

corresponding higher ventilation rate caused by the larger pigs during that time in the APS scenario. It can be further seen that for all the gas emissions, most APS emission distributions appeared to be similar to the DSM scenario distributions throughout the year expect for July, September and October. Again, the emission rate is a function of gas concentrations and the ventilation rate and there is an inverse relationship between them.

GA scenario

Different regions in the U.S have different temperature, relative humidity, wind speed and direction, rainfall frequency and intensity, solar energy, and barometric pressure. These climatic factors might significantly influence gas concentrations and emissions if the rates of gaseous emissions were measured in different areas of the country (e.g. northern, mid-western, and southern area). In this research, Dallas was used as a representative southern site to study the geographical area in warm weather on long-term livestock air quality.

Mean annual simulated NH_3, H_2S, and CO_2 concentrations decreased by -29.7%, -18.3%, and -27.3%, respectively (Table 1), in comparison to those in Des Moines. The relatively high temperature and large ventilation rates in Dallas most likely accounted for this large reduction in gas concentrations. However, due to the inverse relationship of gas concentrations and ventilation rate, the estimations of gas emissions did not present a similar pattern. The BTA-AQP model predicted only -4.2%, -12.8%, and 1.5% decline in the NH_3, H_2S, and CO_2 emissions, respectively.

From Figure 7, it is clearly observed that the medians of the Dallas gas concentration distributions during a majority of the time were much lower than those of the DSM scenario and their distributions were markedly shifted to the right of the locations, thus showing that most of Dallas gas concentrations were regarded as very low values compared with the DSM

distributions. For example, average monthly DSM NH_3 concentrations during the summer (June-September) were two times higher than the mean of the Dallas levels. Although there appeared to be a big difference between the DSM and Dallas scenarios for the gas concentration distributions, the boxplots of the gas emissions over 12 months looked very similar. This could be explained by the gas concentrations varying inversely with the ventilation rate and ambient temperature. Therefore, it may be concluded that, for swine deep-pit barns with similar building characteristics and management practices, different geographical area factor had a large impact on indoor gas concentrations but very little effect on mean annual gas emissions.

SUMMARY AND CONCLUSIONS

Studying the impacts of various important factors on air quality is vital for helping animal producers and environmental researchers understand the parameters influencing livestock air quality so that they might make wise decisions regarding the selection and implementation of gas/odor mitigation techniques. So far, few have evaluated the possible effects of different husbandry management practices and geographic area factors on long-term source air quality because it is a complex and difficult task in the field.

In this research, a total of twenty-four air quality predictions (six NH_3, H_2S, and CO_2 concentration and emission simulations per scenario) were made by our proposed BTA-AQP model using four new scenarios: building heat loss factor (BHLF) scenario, barn set-point temperature (SPT) scenario, animal production schedule (APS) scenario, and geographic area (GA) scenario. The specific conclusions are:

(1) The BHLF scenario used a 50% decline of current BHLF value (965 W/^{o}C), which had no effect on the source air quality;

(2) The new SPT scenario (decreased current set-point temperature by an average of 28.7% throughout the growth cycle) was capable of reducing indoor gas levels during most of the time under warm weather, due to higher required ventilation rates. The corresponding gas emissions did not increase substantially. Hence, current barn set-point temperature curves might be adjusted lower in warm seasons in order to reduce the risk of relatively high gas concentrations (especially H_2S concentrations) in the building and protect the health of workers and animals;

(3) The new animal production schedule, which started pigs in the barn in mild weather (April 1), had no significant effect on mean annual gas concentrations but could cause a moderate decrease in mean annual gas emissions;

(4) Different geographical areas could have a large impact on indoor gas concentrations and ventilation rate but very little effect on mean annual gas emissions since the emission rate is a function of gas concentrations and the ventilation rate and there is an inverse relationship between them.

It should be noted that the simulated results were speculative by the model predictions. Although a great deal of effort has been made to guarantee the accuracy of predicted values, some of the results in the scenarios are still incompletely understood. However, these outcomes could enrich our present knowledge in order to be prepared for future research.

ACKNOWLEDGEMENTS

The authors wish to acknowledge the USDA-IFAFS funding program for providing

the funds required to collect the field data used in this research project and the USDA-Special Grants funding program for providing the funds for this specific research project. Their support is very much appreciated.

REFERENCES

Aarnink, A. J. A., and A. Elzing. 1998. Dynamic model for ammonia volatilization in housing with partially slatted floors, for fattening pigs. *Livestock Prod. Sci.* 53(2): 153-169.

Bhattacharyya, A. 1943. On a measure of divergence between two statistical populations defined by their probability distributions. Bull. Calcutta Math. Soc. 35: 99-109.

Gates, R. S., K. D. Casey, H. Xin, E. F. Wheeler, and J. D. Simmons. 2004. Fan assessment numeration system (FANS) design and calibration specifications. *Trans. ASAE* 47(5): 1709-1715.

Gay, S.W.; Schmidt, D.R.; Clanton, C.J.; Janni, K.A.; Jacobson, L.D.; Weisberg, S. Odor, total reduced sulphur, and ammonia emissions from animal housing facilities and manure storage units in Minnesota. *Applied Eng. in Agric.* 2003, *19*, 347-360.

Groot Koerkamp, P.W.G.; Metz, J.H.M.; Uenk, G.H.; Phillips, V.R.; Holden, M.R.; Sneath, R.W.; Short, J.L.; White, R.P.; Hartung, J.; Seedorf, J.; Schroder, M.; Linkert, K.H.; Pedersen, S.; Takai, H.; Johnsen, J.O; Wathes, C.M. Concentrations and emissions of ammonia in livestock buildings in northern Europe; *J. Agric. Eng. Res.* 1998, *70*, 79-95.

Guo, H.; Dehod, W.; Agnew, J.; Laguë, C.; Feddes, J. R.; Pang, S. Annual odor emission rate from different types of swine production buildings; *Trans. ASABE* 2006, *49*, 517-525.

Haykin, S. 1999. *Neural Networks, a comprehensive foundation*. Upper Saddle River, NJ: Prentice Hall.

Hoff, S. J., D. S. Bundy, M. A. Nelson, B. C. Zelle, L. D. Jacobson, A. J. Heber, J. Ni, Y. Zhang, J. A. Koziel, and D. B. Beasley. 2006. Emissions of ammonia, hydrogen sulfide, and odor before, during, and after slurry removal from a deep-pit swine finisher. *J. Air Waste Mgmt. Assoc.* 56(5): 581-590.

Hoff, S.J., D.S. Bundy, M.A. Nelson, B.C. Zelle, L.D. Jacobson, A.J. Heber, J. Ni, Y. Zhang, J.A. Koziel, D.B. Beasley. 2009. Real-time airflow rate measurements from mechanically ventilated animal buildings. *J. Air and Waste Mgmt. Assoc.* 59: 683-694.

Jacobson, L. D., H. Guo, D. R. Schmidt, R. E. Nicolai, J. Zhu, and K. A. Janni. 2005. Development of the OFFSET model for determination of odor-annoyance-free setback distances from animal production sites: Part I. Review and experiment. *Trans. ASABE* 48(6): 2259-2268.

Ni, J.; Heber, A. J.; Lim, T. T.; Diehl, C. A.; Duggirala, R. K; Haymore, B. L. Hydrogen sulfide emission from two large pig-finishing buildings with long-term high-frequency measurements. *J. Agric. Sci*. 2002, *138*, 227-236.

NSRDB. 2008. Users manual for TMY3 data sets. Golden, Co: USDE National Renewable Energy Laboratory.

Sun, G., S. J. Hoff, B. C. Zelle and M. A. Nelson. 2008a. Development and comparison of backpropagation and generalized regression neural network models to predict diurnal and seasonal gas and PM_{10} concentrations and emissions from swine buildings. *Trans. ASABE* 51(2):685-694.

Sun, G., H. Guo, J. Peterson, B. Predicala, and C. Laguë. 2008b. Diurnal odor , ammonia, hydrogen sulfide and carbon dioxide emission profiles of confined swine grower/finisher rooms. *Journal of the Air and Waste Management Association.* 58 (11):1434-1448.

Sun, G. and S. J. Hoff. 2010a. Prediction of indoor climate and long-term air quality using the BTA-AQP model: Part I. BTA model development and evaluation. *Trans. ASABE* 53(3): 863-870.

Sun, G. and S. J. Hoff. 2010b. Prediction of indoor climate and long-term air quality using the BTA-AQP model: Part II. Overall model evaluation and application. *Trans. ASABE* 53(3): 871-881.

Sun, G., H. Guo, and J. Peterson. 2010c. Seasonal odor , ammonia, hydrogen sulfide and carbon dioxide concentrations and emissions from swine grower-finisher rooms. *Journal of the Air and Waste Management Association*. 60 (4): 471-480.

Zhu, J.; Jacobson, L.; Schmidt, S.; Nicolai, R. Daily variations in odor and gas emissions from animal facilities; *Applied Eng. in Agric.* 1999, *16*, 153-158.

Table 1.Mean annual air quality simulations using different management practices and geographical area scenarios.*

Parameter		DSM	BHLF	SPT	APS	GA
NH_3 Concentration (ppm)	Mean	19.5	19.4	19.0	20.5	13.7
	SD	9.1	9.0	11.1	10.3	9.1
	%	-	-0.3%	-2.4%	5.2%	-29.7%
NH_3 Emission (kg/d)	Mean	6.65	6.66	7.08	6.21	6.93
	SD	2.52	2.60	4.07	2.01	2.44
	%	-	0.2%	6.5%	-6.6%	4.2%
H_2S Concentration (ppb)	Mean	519	510	370	534	424
	SD	368	364	271	524	330
	%	-	-1.7%	-28.6%	3.1%	-18.3%
H_2S Emission (kg/d)	Mean	0.469	0.475	0.419	0.403	0.530
	SD	0.346	0.347	0.360	0.306	0.411
	%	-	1.3%	-10.7%	-14.2%	12.8%
CO_2 Concentration (ppm)	Mean	2334	2341	2084	2282	1696
	SD	1335	1345	1084	1061	1124
	%	-	0.3%	-10.7%	-2.2%	-27.3%
CO_2 Emission (kg/d)	Mean	1176	1194	1217	1084	1159
	SD	360	366	698	332	375
	%	-	1.5%	3.5%	-7.8%	-1.5%

* DSM, BHLF, SPT, APS and Dallas indicate average annual air quality in Des Moines, air quality changed by different Building Heat Loss Factor, Set-point Temperature, Animal Production Schedule and Geographical Area (Dallas), respectively. % means the percentage difference between the Des Moines and different scenarios.

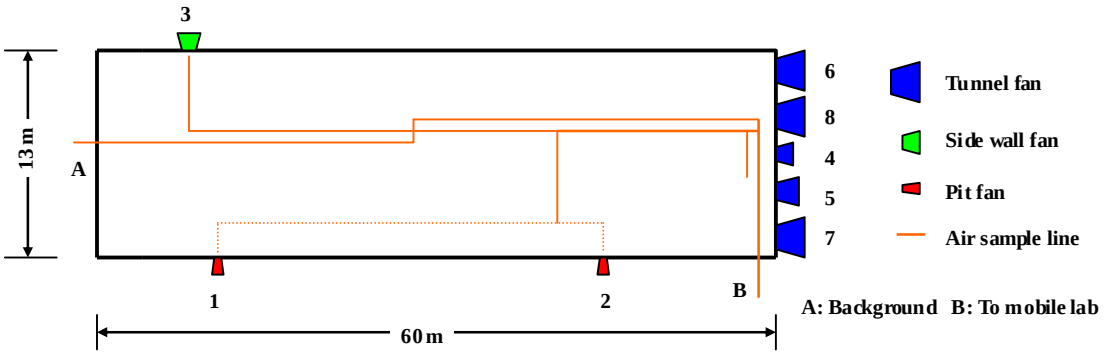

Figure 1. Layout of typical deep-pit swine finishing building.

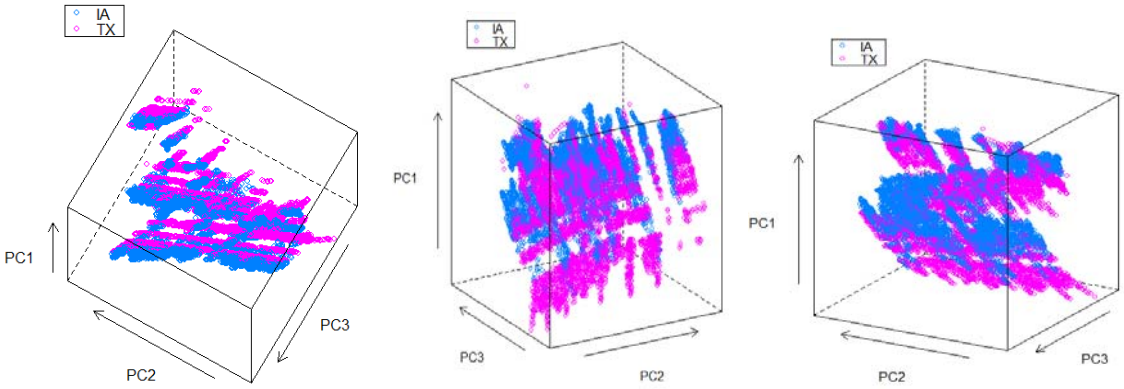

Figure 2. The 3-D scatterplots of Dallas site cases vs. the training dataset from different viewing angles (IA: the training data sampled in Iowa; TX: new cases predicted by the BTA model at Dallas site, TX).

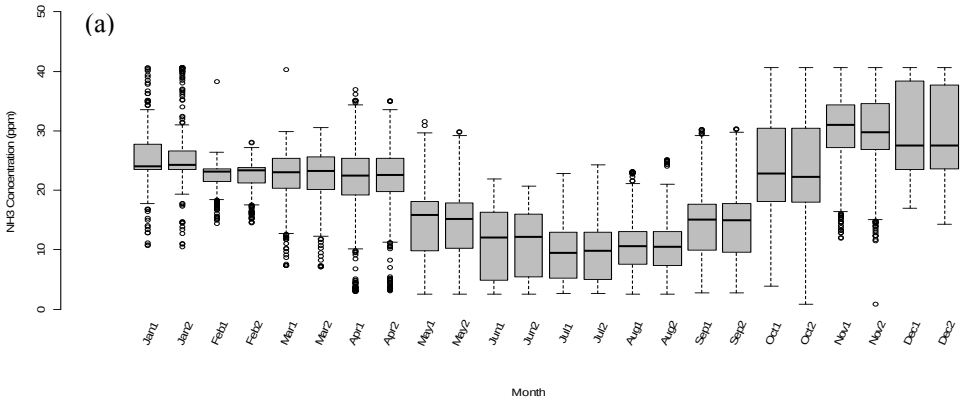
(a)
NH3 Concentration (ppm)
0
10
20
30
40
50
Jan1
Jan2
Feb1
Feb2
Mar1
Mar2
Apr1
Apr2
May1
May2
Jun1
Jun2
Jul1
Jul2
Aug1
Aug2
Sep1
Sep2
Oct1
Oct2
Nov1
Nov2
Dec1
Dec2
Month

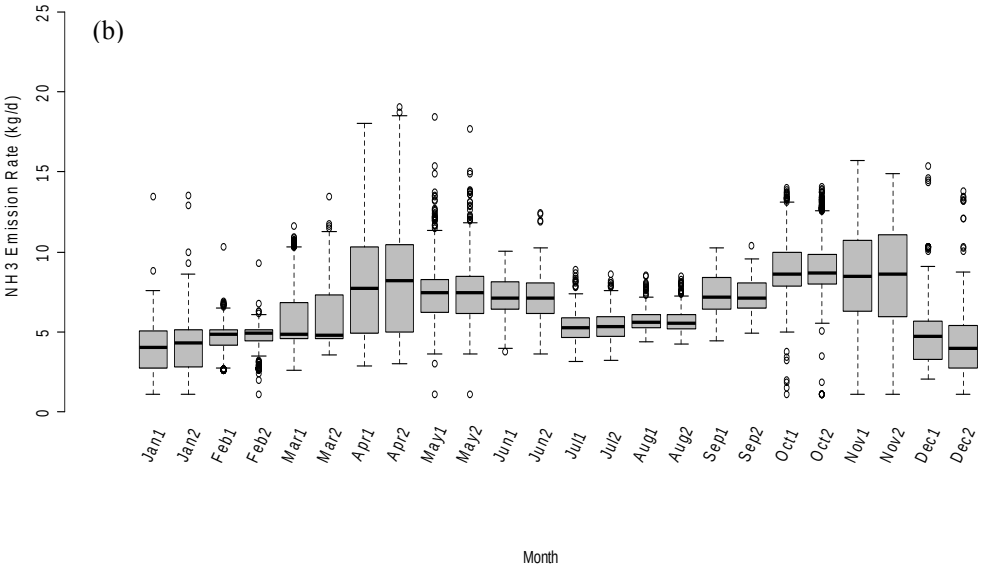
(b)
NH3 Emission Rate (kg/d)
0
5
10
15
20
25
Jan1
Jan2
Feb1
Feb2
Mar1
Mar2
Apr1
Apr2
May1
May2
Jun1
Jun2
Jul1
Jul2
Aug1
Aug2
Sep1
Sep2
Oct1
Oct2
Nov1
Nov2
Dec1
Dec2
Month

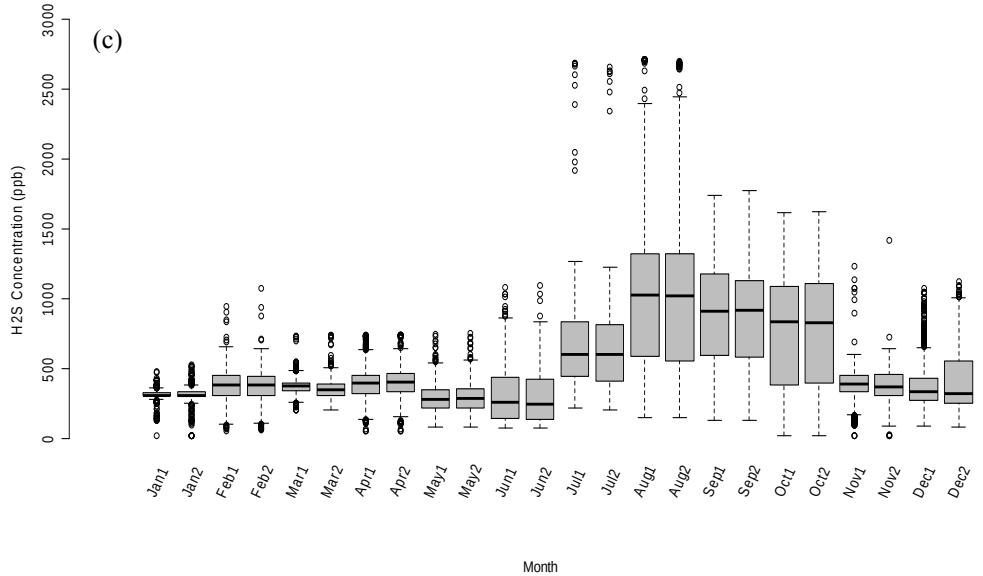
(c)
H2S Concentration (ppb)
0
500
1000
1500
2000
2500
3000
Jan1
Jan2
Feb1
Feb2
Mar1
Mar2
Apr1
Apr2
May1
May2
Jun1
Jun2
Jul1
Jul2
Aug1
Aug2
Sep1
Sep2
Oct1
Oct2
Nov1
Nov2
Dec1
Dec2
Month

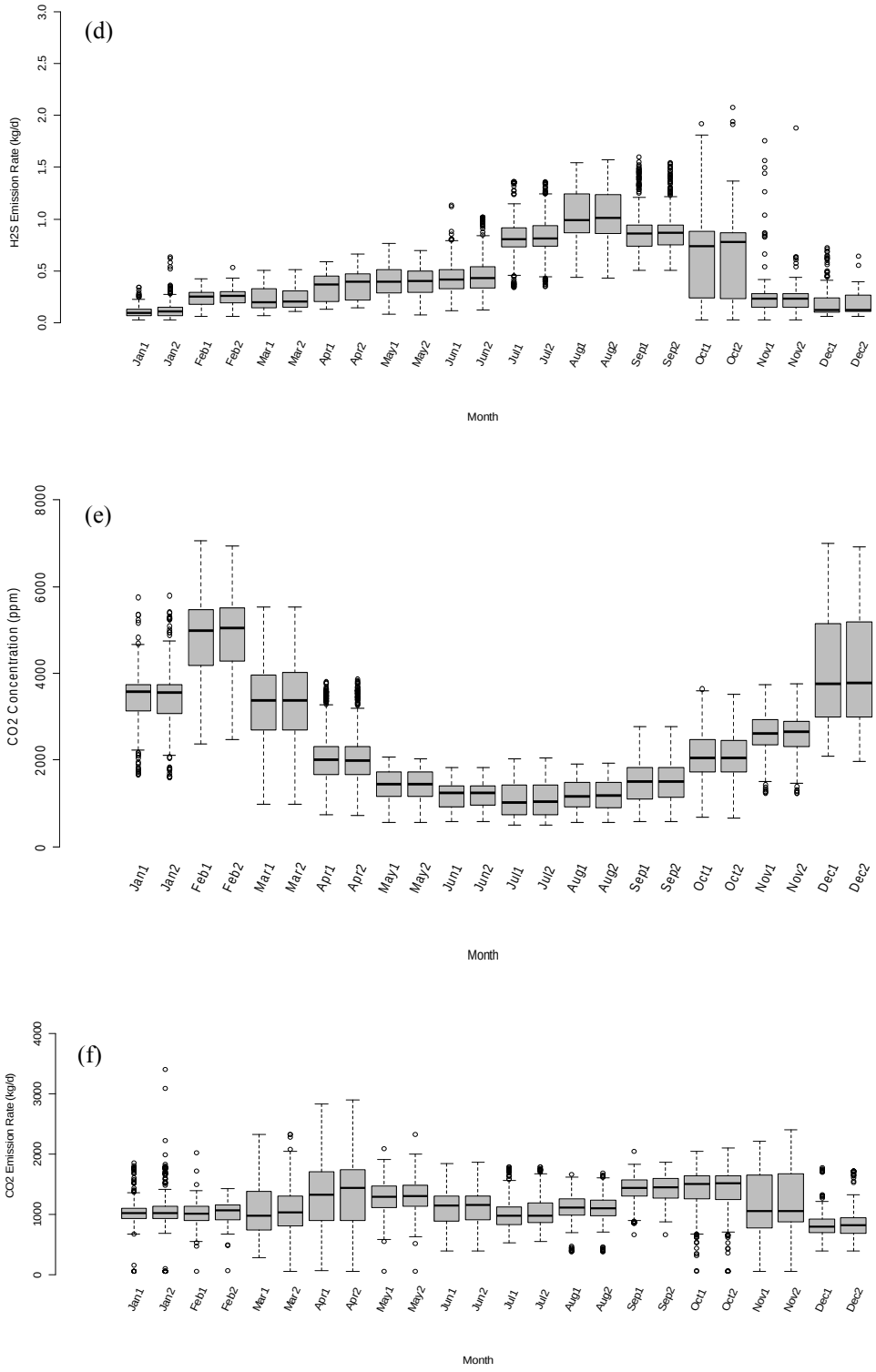

Figure 3. Long-term hourly NH_3, H_2S and CO_2 concentrations (a, c, e) and emissions (b, d, f) for the DSM and BHLF scenarios (1: DSM scenario; 2: BHLF scenario; circles: Potential outliers).

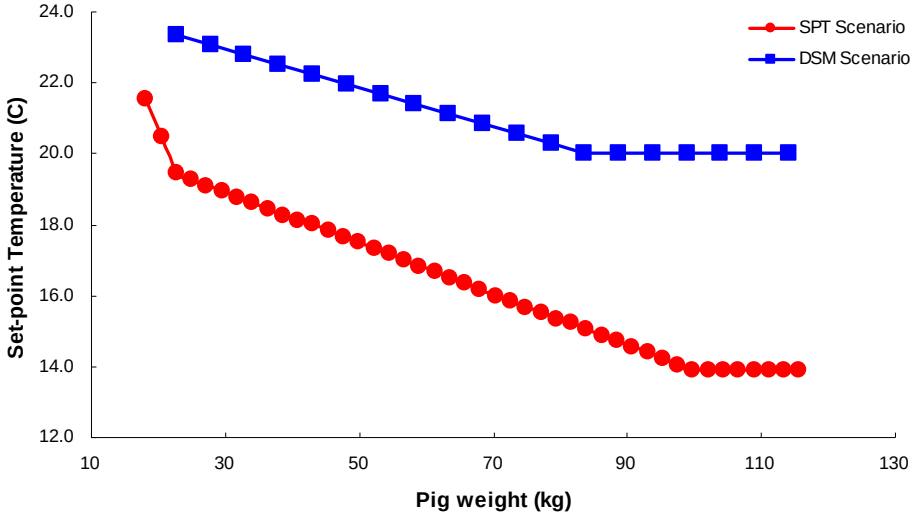

Figure 4. The set-point temperature curves with the SPT scenario and DSM scenario.

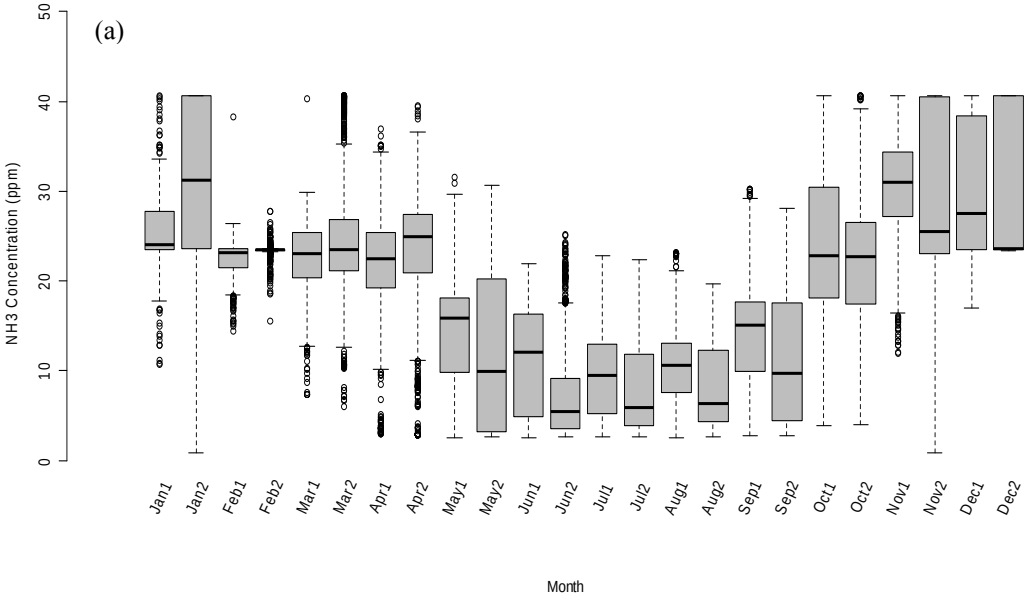

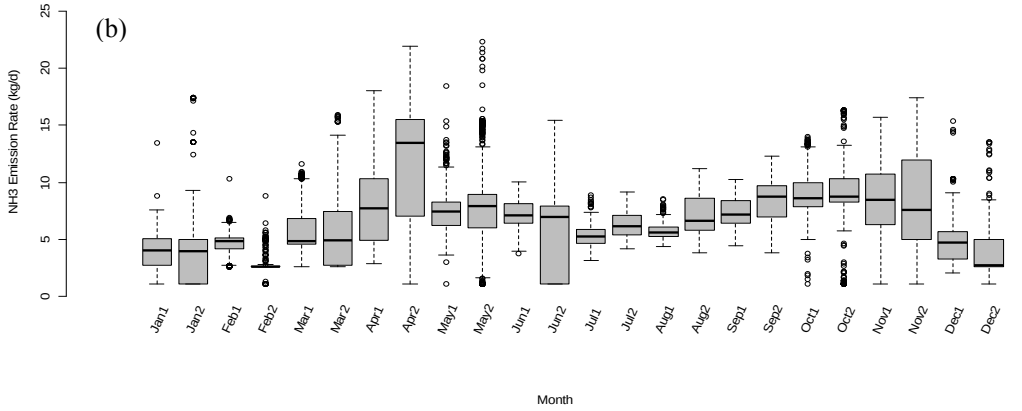
(b)
NH3 Emission Rate (kg/d)
0
5
10
15
20
25
Jan1
Jan2
Feb1
Feb2
Mar1
Mar2
Apr1
Apr2
May1
May2
Jun1
Jun2
Jul1
Jul2
Aug1
Aug2
Sep1
Sep2
Oct1
Oct2
Nov1
Nov2
Dec1
Dec2
Month

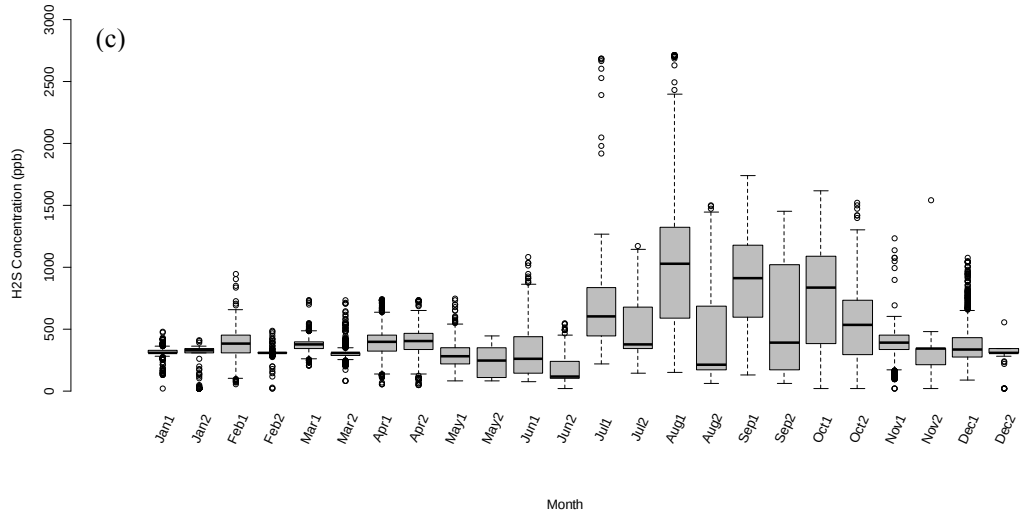
(c)
H2S Concentration (ppb)
0
500
1000
1500
2000
2500
3000
Jan1
Jan2
Feb1
Feb2
Mar1
Mar2
Apr1
Apr2
May1
May2
Jun1
Jun2
Jul1
Jul2
Aug1
Aug2
Sep1
Sep2
Oct1
Oct2
Nov1
Nov2
Dec1
Dec2
Month

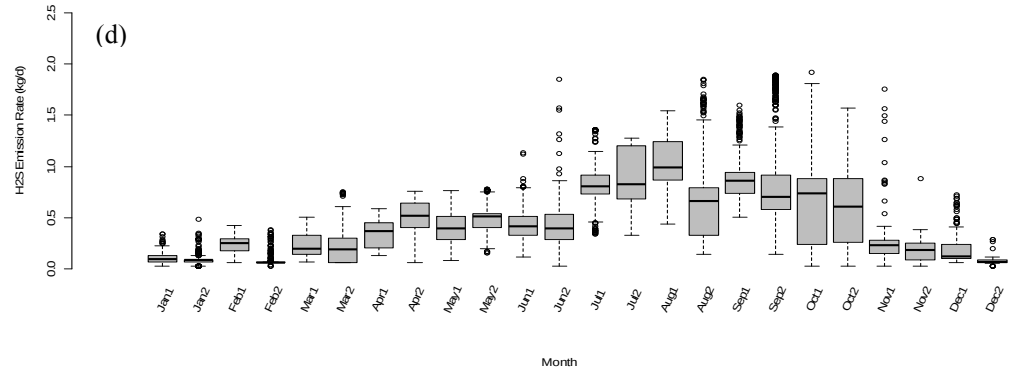
(d)
H2S Emission Rate (kg/d)
0.0
0.5
1.0
1.5
2.0
2.5
Jan1
Jan2
Feb1
Feb2
Mar1
Mar2
Apr1
Apr2
May1
May2
Jun1
Jun2
Jul1
Jul2
Aug1
Aug2
Sep1
Sep2
Oct1
Oct2
Nov1
Nov2
Dec1
Dec2
Month

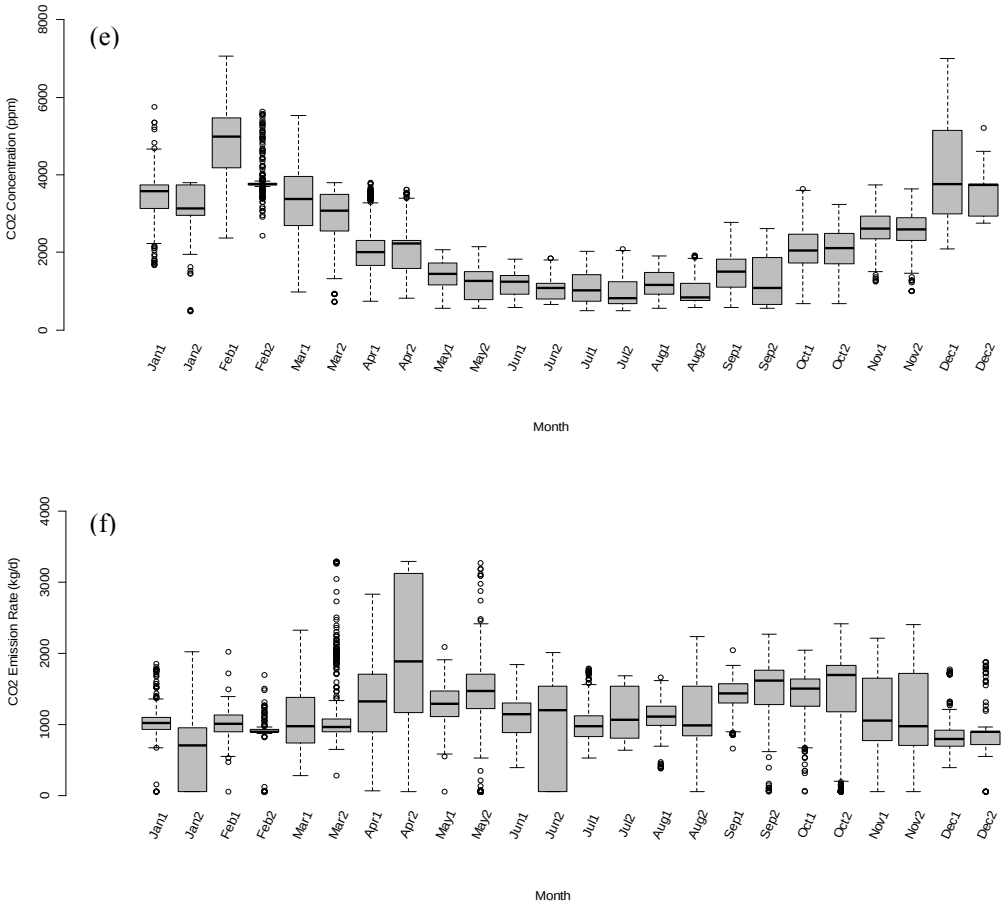

Figure 5. Long-term hourly NH_3, H_2S and CO_2 concentrations (a, c, e) and emissions (b, d, f) for the DSM and SPT scenarios (1: DSM scenario; 2: SPT scenario; circles: Potential outliers).

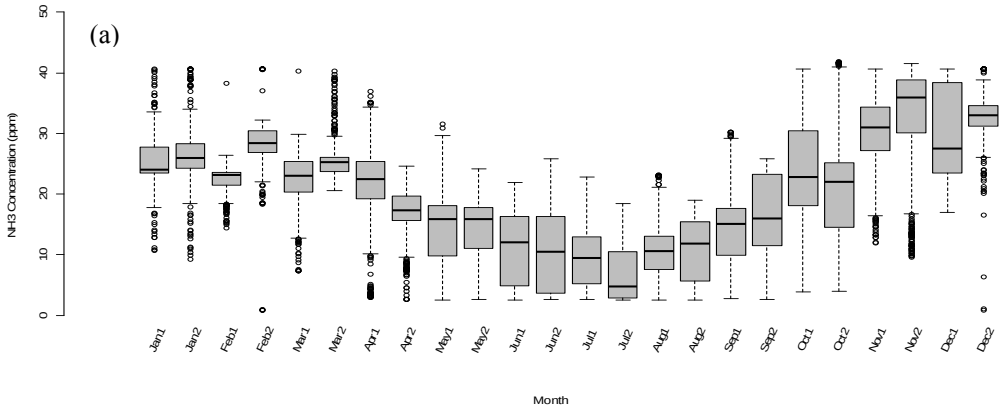

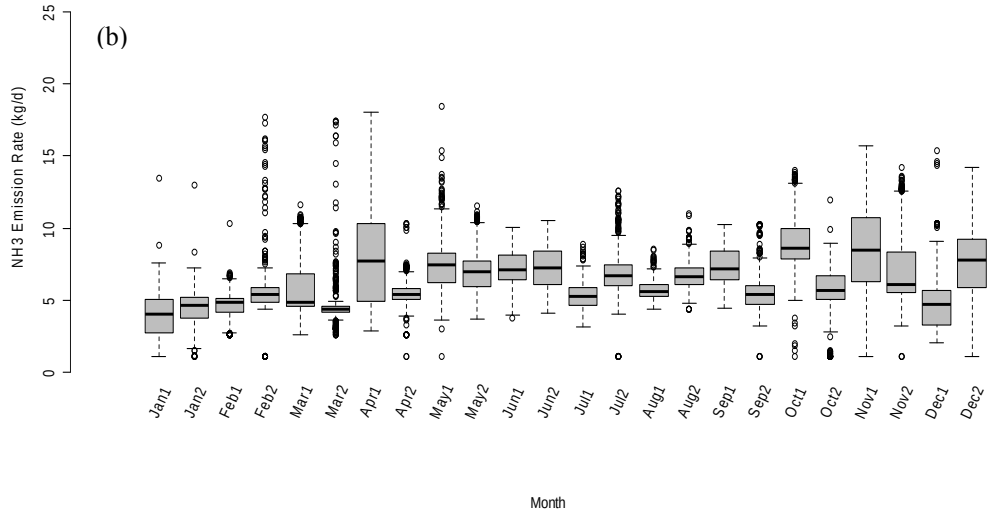
(b)
NH3 Emission Rate (kg/d)
0
5
10
15
20
25
Jan1
Jan2
Feb1
Feb2
Mar1
Mar2
Apr1
Apr2
May1
May2
Jun1
Jun2
Jul1
Jul2
Aug1
Aug2
Sep1
Sep2
Oct1
Oct2
Nov1
Nov2
Dec1
Dec2
Month

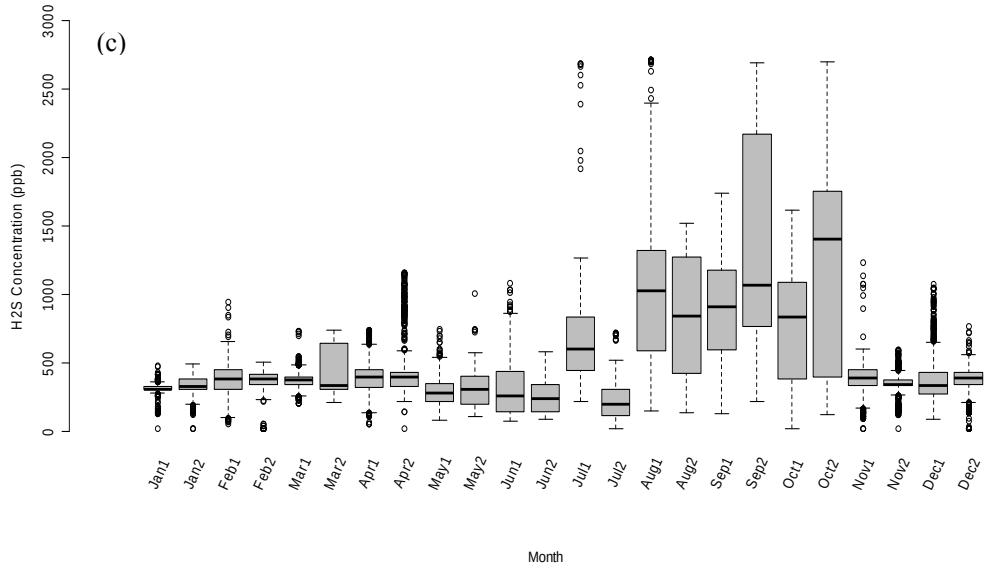
(c)
H2S Concentration (ppb)
0
500
1000
1500
2000
2500
3000
Jan1
Jan2
Feb1
Feb2
Mar1
Mar2
Apr1
Apr2
May1
May2
Jun1
Jun2
Jul1
Jul2
Aug1
Aug2
Sep1
Sep2
Oct1
Oct2
Nov1
Nov2
Dec1
Dec2
Month

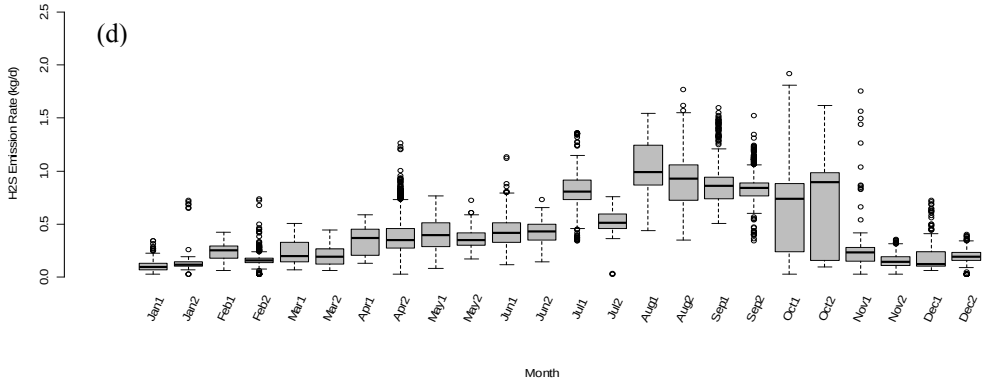
(d)
H2S Emission Rate (kg/d)
0.0
0.5
1.0
1.5
2.0
2.5
Jan1
Jan2
Feb1
Feb2
Mar1
Mar2
Apr1
Apr2
May1
May2
Jun1
Jun2
Jul1
Jul2
Aug1
Aug2
Sep1
Sep2
Oct1
Oct2
Nov1
Nov2
Dec1
Dec2
Month

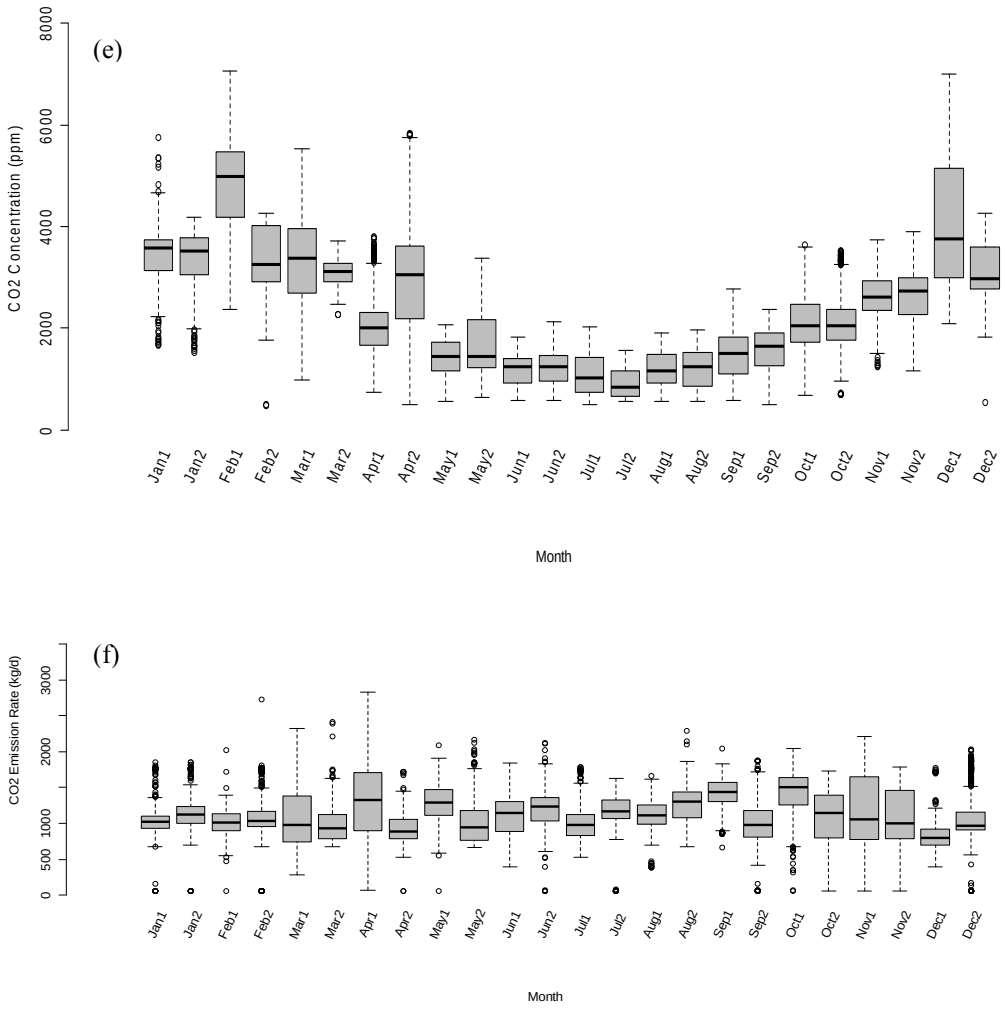

Figure 6. Long-term hourly NH_3, H_2S and CO_2 concentrations (a, c, e) and emissions (b, d, f) for the DSM and APS scenarios (1: DSM scenario; 2: APS scenario; circles: Potential outliers).

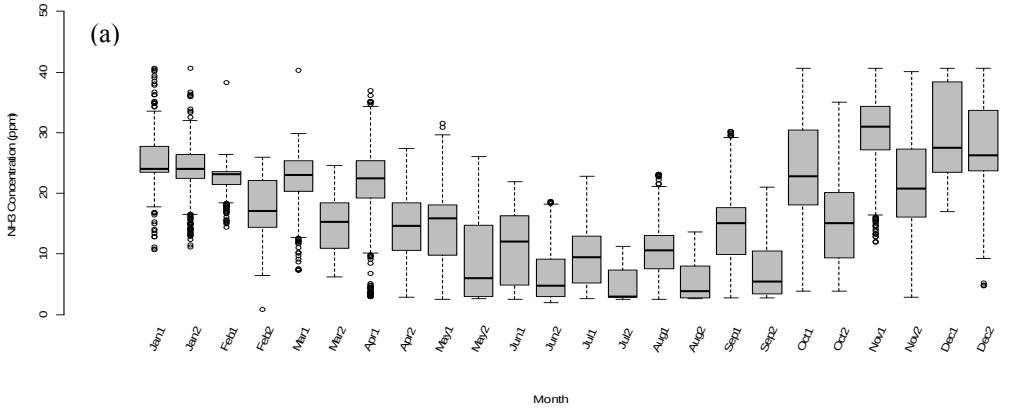

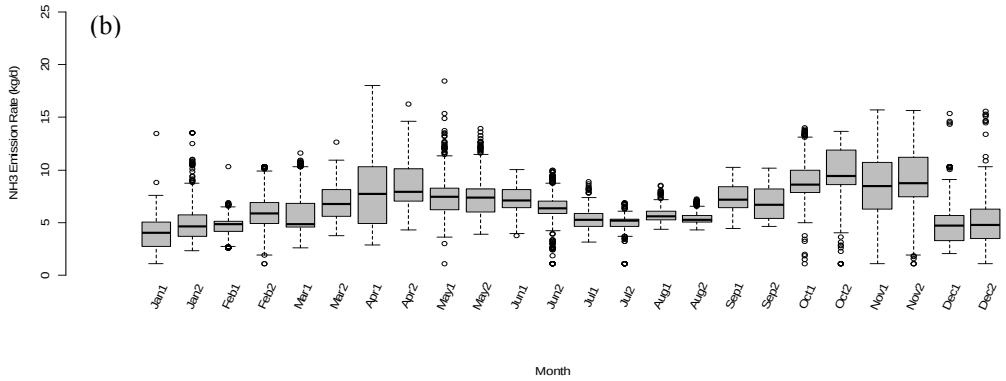
(b)
NH3 Emission Rate (kg/d)
0
5
10
15
20
25
Jan1
Jan2
Feb1
Feb2
Mar1
Mar2
Apr1
Apr2
May1
May2
Jun1
Jun2
Jul1
Jul2
Aug1
Aug2
Sep1
Sep2
Oct1
Oct2
Nov1
Nov2
Dec1
Dec2
Month

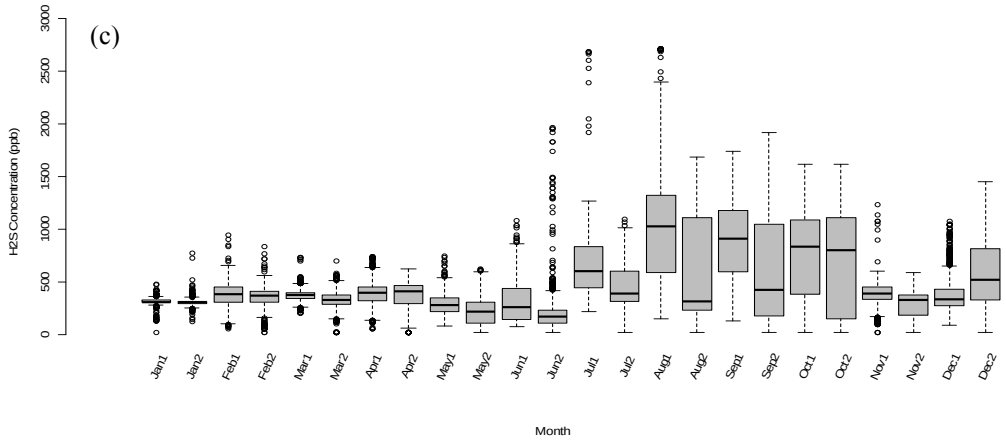
(c)
H2S Concentration (ppb)
0
500
1000
1500
2000
2500
3000
Jan1
Jan2
Feb1
Feb2
Mar1
Mar2
Apr1
Apr2
May1
May2
Jun1
Jun2
Jul1
Jul2
Aug1
Aug2
Sep1
Sep2
Oct1
Oct2
Nov1
Nov2
Dec1
Dec2
Month

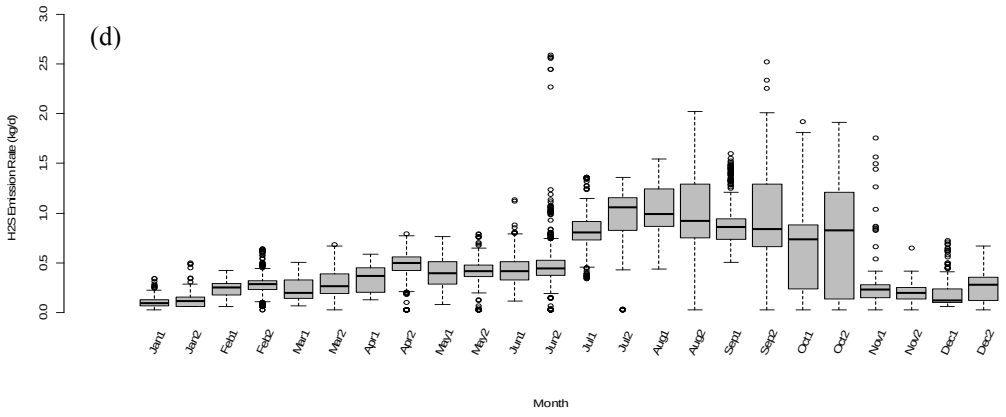
(d)
H2S Emission Rate (kg/d)
0.0
0.5
1.0
1.5
2.0
2.5
3.0
Jan1
Jan2
Feb1
Feb2
Mar1
Mar2
Apr1
Apr2
May1
May2
Jun1
Jun2
Jul1
Jul2
Aug1
Aug2
Sep1
Sep2
Oct1
Oct2
Nov1
Nov2
Dec1
Dec2
Month

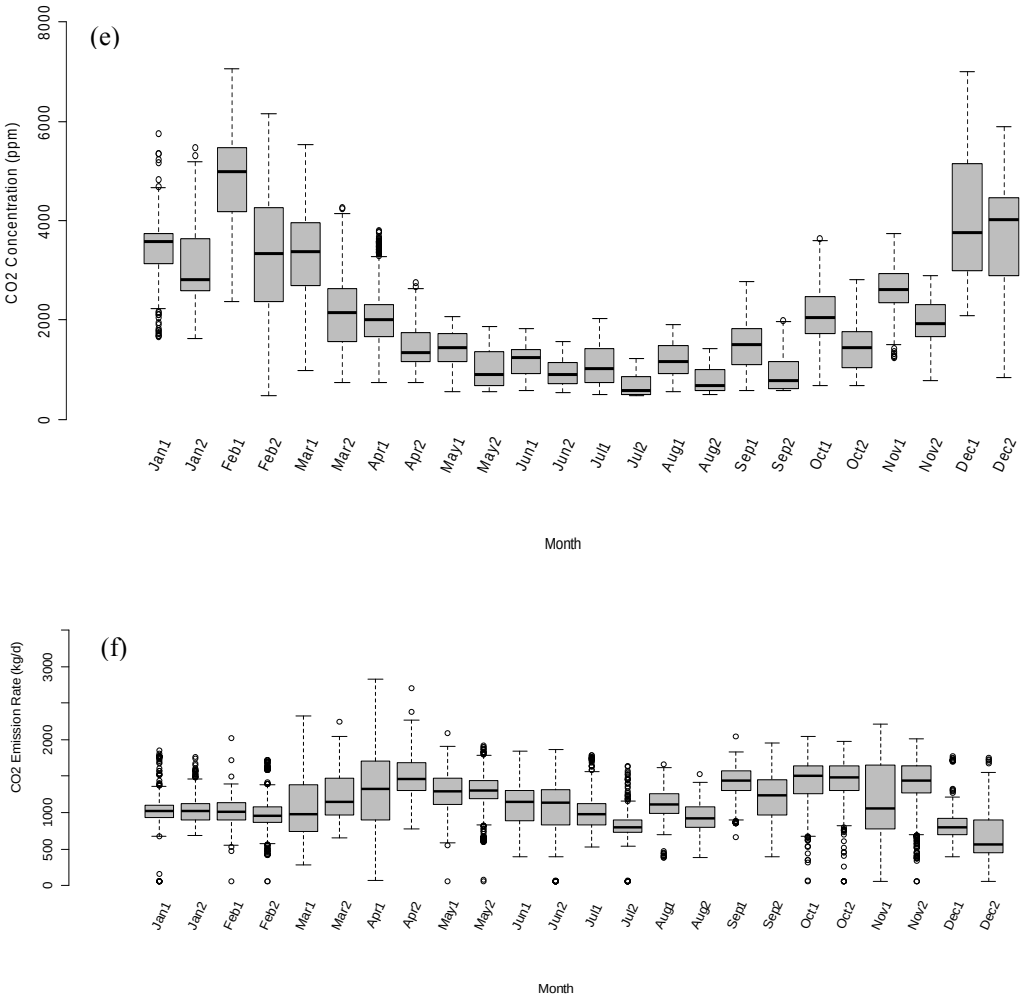

Figure 7. Long-term hourly NH_3, H_2S and CO_2 concentrations (a, c, e) and emissions (b, d, f) for the DSM and Dallas scenarios (1: DSM scenario; 2: Dallas scenario; circles: Potential outliers).

CHAPTER 7. GENERAL CONCLUSIONS

SUMMARY AND CONCLUSIONS

The major conclusions drawn from this research are:

1. Four significant contributors (outdoor temperature, animal units, total building ventilation rate, and indoor temperature) to the AQP models have been identified using a multivariate statistical analysis method. Also, in-house deep-pit manure level is a significant variable for H_2S. The purpose of introducing fewer uncorrelated variables to the AQP models is to reduce model structure complexity, eliminate model over-fitting problems, and minimize field monitoring costs without sacrificing model predictive accuracy.

2. The backpropagation and generalized regression neural network based AQP models were developed to predict diurnal and seasonal gas and PM_{10} concentrations and emissions from swine deep-pit finishing buildings. It was found that the obtained forecasting results of the neural network models were in good agreement with actual field measurements, with coefficient of determination values between 81.2% and 99.5% and very low values of systemic performance indices. The promising results from this work indicated that artificial neural network technologies were capable of accurately modeling source air quality within and emissions from these livestock production facilities. Also, the process of constructing, training, and simulating the BP network models was very complicated. Likewise, determining the best values for several network parameters, such as the number of layers and neurons, type of activation functions and training algorithms, learning rates, and momentum, were difficult. The effective way of obtaining good BP modeling results was to use some

trial-and-error methods and thoroughly understand the theory of backpropagation. Conversely, for the GRNN models, there was only one parameter (the smoothing factor) that needed to be adjusted experimentally. Moreover, the BP network performance was very sensitive to randomly assigned initial values. However, this problem was not faced in GRNN simulations. The GRNN approach did not require an iterative training procedure as in the backpropagation method. The local minima problem was also not faced in the GRNN simulations. Other significant characteristics of the GRNN in comparison to the BPNN were the excellent approximation ability, fast training time, and exceptional stability during the prediction stage. Thus, the GRNN technology outperformed BP, which has been demonstrated in this study. It can be recommended that a generalized regression neural network be used instead of a backpropagation neural network in source air quality modeling.

3. A lumped capacitance model (BTA model) was built to study the transient behavior of indoor air temperature and ventilation rate according to the thermo-physical properties of a typical swine building, the set-point temperature scheme, fan staging scheme, transient outside temperature, and the heat fluxes from pigs and supplemental heaters. The obtained indoor air temperature and ventilation rate developed from the BTA model could then be combined with animal growth cycle, in-house manure storage level, and field meteorological data to predict indoor air quality and emissions based on the generalized regression neural network (AQP model). The purpose was to acquire accurate estimates of significant input parameters required for the AQP model without relying on expensive field measurements. It was found that the performance of the BTA model for predicting indoor climate (ventilation rate and indoor air temperature) was very good in terms of the statistical analysis and graphical presentations.

The air quality predictive (AQP) model used was based on the generalized regression neural network. A comparison was made between the predicted and actual gas concentrations and emissions collected in 2003 in order to evaluate the accuracy of the BTA-AQP model estimates. It can be observed from the comparative boxplots that the median, spread and skewness of the field collected and predicted gas concentrations and emissions were similar. Poorer predictions in some of the months could be due to the relatively inaccurate ventilation rate predictions by the BTA model and the AQP model's inability in estimating gas concentrations resulting from barn management and pig activity. For all the predicted parameters, the MAE/SD ratios were less than 0.5; the CMR values approximated to 0; the IoA values were close to 1; and the NSEF values were greater than 0.5. These good model performance ratings indicated that the BTA-AQP model was able to accurately predict indoor climate and gas concentrations and emissions from swine deep-pit buildings for a specific year.

In addition, the monthly air quality values estimated by the BTA-AQP model using TMY3 data were compared with those using 5-year on-site weather data. It was observed that the predictions using the TMY3 data followed the long-term mean patterns very well, which suggests that the TMY3 data can be used in performing accurate long-term simulations of source air quality. In addition, annual gas concentrations and emissions can be obtained using TMY3 data instead of an individual year weather data without resulting in large errors. These results demonstrate that a convenient approach to evaluate annual air quality levels within an acceptable accuracy is possible without long-term expensive on-site measurements. However, it should be noted that the TMY3 data is not appropriate to estimate peak values for a particulate period of time.

4. A total of twenty-four air quality predictions (six NH_3, H_2S, and CO_2 concentration and emission simulations per scenario) were made by our proposed BTA-AQP model using four new scenarios: building heat loss factor (BHLF) scenario, barn set-point temperature (SPT) scenario, animal production schedule (APS) scenario, and geographical area (GA) scenario. The specific conclusions are: (1) The BHLF scenario used a 50% decline of current BHLF value (965 W/^{o}C), which had no effect on the source air quality; (2) The new SPT scenario (decreased current set-point temperature by an average of 28.7% throughout the growth cycle) was capable of reducing indoor gas levels during most of time under warm weather, due to the high ventilation rate. While, the corresponding gas emissions did not increase substantially. Hence, current barn set-point temperature curves might be adjusted by setting a few degrees lower in warmer seasons in order to reduce the risk of relatively high gas concentrations (especially H_2S concentrations) in the building and protect the health of workers and animals; (3) The new animal production schedule starting on the first day of April had no significant effect on mean annual gas concentrations but could cause a moderate decrease in mean annual gas emissions; and (4) Different geographical area factor could have a large impact on indoor gas concentrations and ventilation rate but very little effect on mean annual gas emissions since the emission rate is a function of gas concentrations and the ventilation rate and there is an inverse relationship between them.

It should be noted that the simulated results were speculative by the model predictions. Although a great deal of effort had been made to guarantee the accuracy of predicted values, some of the results in the scenarios are still incompletely understood. However, these outcomes could enrich our present knowledge in order to be prepared for future research.

RECOMMENDATIONS FOR FUTURE RESEARCH

The following are recommended for future research to improve prediction accuracy of the BTA-AQP model:

1. Uncertainties in source air quality data. Since the source air quality data is important to develop the BTA-AQP model and evaluate the model predictive performance, more efforts should be made to maximize confidence, credibility, and consistency of the measured data;

2. Prediction errors of the BTA model. As the number of assumptions in a model increases, the accuracy and relevance of the model diminishes. For example, the swine heat production data used in this research was from ASABE standards established decades ago. With improved genetics and feed management and diets, swine heat production (HP) has changed. Brown-Brandl el al. (2004) reported that the lean percent increase of 1.55% in the last 10 years has caused an increase in HP by approximately 15%. Future work is needed to collect new swine HP data from the latest literature;

3. Prediction errors of the AQP model. The accuracy of the artificial neural network AQP model depends on the completeness of the data set and availability of various model input factors that significantly affect source air quality. The complete emission profiles should cover all possible swine production stages for a long period of time. In this study, one-year source air quality data was used that might not capture all of the relationships between gaseous concentrations and emissions and these input factors. More gas measurements are needed to expand the size of the data set. For the model input parameters, more important factors beyond indoor and outdoor temperatures, ventilation rate, swine growth cycle, and in-house manure storage level, should be considered and incorporated in the model. Added variables such as feed nutrient content, management practices, and manure temperature

might prove to be important input variables. When pigs grow, the amount and composition of the feed intake change, as do the amount and composition of the manure. Thus, the amount of gas generation tends to increase. However, sharp decreases in the amount of daily nitrogen excretion were found when diet formulation changes were implemented. This adjustment process alleviates the amount of nitrogen in the manure converted to ammonia and other gases. Swine management practices are also vital factors to determine air quality levels. Good management practices can maintain proper environment requirements for the animals and decrease daily air emissions. Manure temperature might be a factor that may directly influence H_2S release; and,

4. Bias error of the TMY3 and its limited application. Uncertainty values exist in the meteorological elements of the TMY3 data set (NSRDB, 2008). Additionally, TMY3 data is suitable for simulating solar energy conversion systems and building systems since each TMY3 month was selected according to five elements (global horizontal radiation, direct normal radiation, dry bulb and dew point temperatures, and wind speed) which are the most important for solar energy and building systems. No literature has shown that the TMY3 data is suited to air quality predictions as well. Therefore, further research may focus on the development of new TMY data that is determined to be more appropriate for air quality simulations.

APPENDIX A. SENSIBLE HEAT PRODUCTION PROCEDURES

The sensible heat fluxes from the pigs were calculated by multiplying sensible heat production (SHP/kg) at a specific temperature by the total pig mass, which included three main steps: (1) obtaining the average mass of a pig (kg) and indoor air temperature at Δt = 0.01 hr; (2) calculating sensible heat production per pig based on the indoor temperature and data from ASABE standards (Albright, 1990); and finally (3) calculating total sensible heat production. Figure A.1 shows five different SHP curves (30kg, 50kg, 70kg, 90kg, and 110kg) as a function of indoor air temperature and are representative of the SHP curves used in the BTA model.

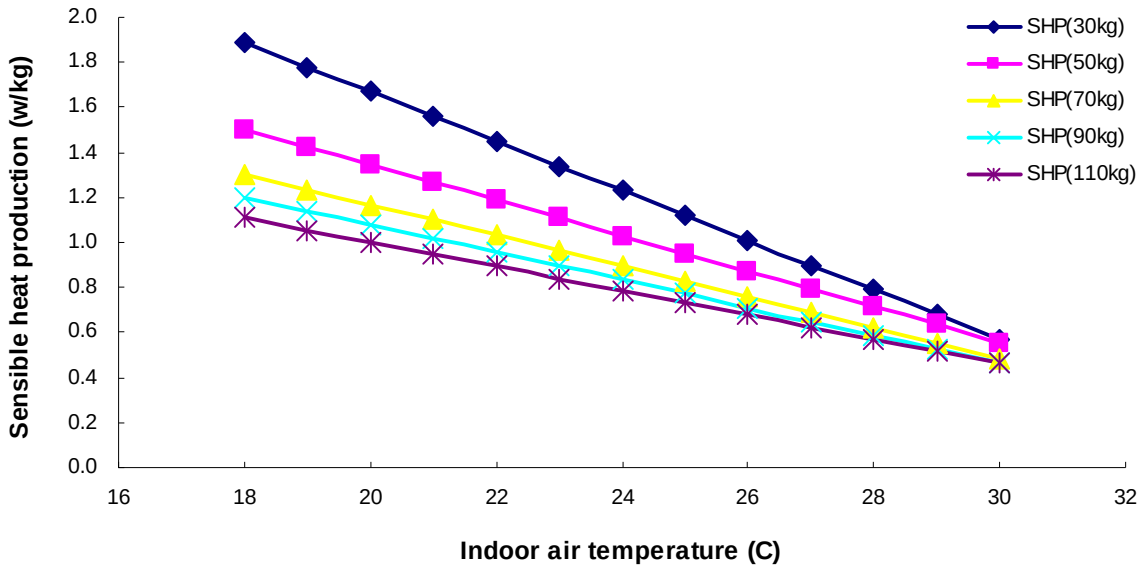

Figure A.1. Five different SHP curves (30kg, 50kg, 70kg, 90kg, and 110kg) as a function of indoor air temperature.

APPENDIX B. APECAB DAILY DATA

The following table summarizes the daily average field collected data used to compare with the developed BTA-AQP model presented in this thesis. In total, 1-minute averages were originally collected but for the sake of space, only the daily averages are shown.

Date	Outdoor T	Outside RH	Inventory	Mass	AU	Airflow	Indoor T	Exhaust T	Exhaust RH	NH_3Con	H_2SCon	CO_2Con	PM_{10}Con	NH_3ER	H_2SER	CO_2ER	PM_{10}ER
2003	°C	%		kg/pig		m^3/s	°C	°C	%	ppm	ppb	ppm	mg/m^3	kg/d	kg/d	kg/d	kg/d
1-Jan	-3.6	60	565	116	131.4	2.6	20	17.3	37	15.0	87	2790	260	2.73	0.033	801	0.060
2-Jan	-5.3	70	565	117	132.2	2.5	20.1	18	38	15.3	88	2910	277	2.56	0.030	775	0.061
3-Jan	-5.8	69	565	118	133.0	2.7	20.2	18	37	14.4	85	2880	279	2.76	0.033	888	0.066
4-Jan	0.3	86	565	118	133.8	2.6	20.6	18.7	43	15.7	95	2670	270	3.62	0.043	759	0.062
5-Jan	-1.4	91	565	119	134.6	2.5	20.4	18.5	45	16.4	91	2710	250	3.53	0.039	714	0.055
6-Jan	-3.0	80	565	120	135.2	2.6	20.6	18.5	41	15.6	80	2710	284	2.82	0.029	746	0.062
7-Jan	3.2	68	565	120	136.0	2.9	21.3	19.6	38	14.6	73	2250	261	3.75	0.041	685	0.065
8-Jan	6.4	48	565	121	136.4	3.6	21.5	19.8	36	14.9	76	1930	261	3.39	0.042	657	0.068
6-Feb	-13.7	78	897	28	50.0	2.3	23	22.1	65	14.4	97	6170	350	4.08	0.086	1580	0.071
7-Feb	-15.2	72	897	29	51.2	2.4	23	22.1	64	15.6	113	6380	364	3.54	0.090	1730	0.075
8-Feb	-7.9	69	897	29	52.6	2.3	23.2	22.6	68	16.2	179	6190	289	3.94	0.131	1700	0.058
9-Feb	-10.4	76	897	30	54.0	2.4	23.2	22.4	69	19.8	204	6570	280	4.02	0.151	1890	0.060
10-Feb	-12.7	61	897	31	55.4	2.3	23.1	22.1	69	17.3	170	6320	269	4.33	0.179	1640	0.054
11-Feb	-7.9	69	897	32	56.6	2.3	23	22.3	66	18.2	262	5650	264	3.94	0.187	1490	0.053
12-Feb	-9.1	57	897	32	58.0	2.4	23.2	22.1	68	18.5	241	6170	257	4.21	0.194	1620	0.052
13-Feb	-2.6	61	897	33	59.4	2.8	23.6	22.5	66	20.3	257	5190	226	4.75	0.200	1720	0.058
14-Feb	-1.8	86	897	34	60.8	2.3	22.8	20.9	69	24.0	370	4690	235	-	-	1330	0.047
15-Feb	-7.8	79	897	35	62.0	2.4	22.7	19.8	65	21.7	347	4730	280	4.67	0.203	1290	0.057
16-Feb	-11.6	76	897	35	63.4	2.4	23.2	21.1	68	23.2	386	5730	261	5.27	0.253	1500	0.055
17-Feb	-9.1	84	897	36	64.8	3.2	22.7	21	69	25.3	392	5550	249	6.57	0.273	1980	0.070
18-Feb	-0.8	83	897	37	66.2	2.7	23.6	21.9	67	23.4	421	4730	190	5.56	0.247	1330	0.048
19-Feb	-2.1	75	897	38	67.6	2.4	23.6	21.9	66	26.4	399	5160	185	5.23	0.207	1330	0.040
20-Feb	3.2	70	897	38	68.8	2.5	24.1	22.6	62	23.7	393	4440	156	5.64	0.188	1280	0.035
21-Feb	1.5	79	897	39	70.2	2.9	24.3	22.5	61	25.2	-	4310	151	5.50	-	1380	0.039
22-Feb	-4.4	77	897	40	71.6	2.3	23	21.4	65	27.8	-	5110	163	5.49	-	1310	0.032
23-Feb	-10.9	72	897	41	73.0	2.3	22.6	20.8	65	29.9	472	5670	214	5.54	0.183	1510	0.043
24-Feb	-16.6	69	897	41	74.2	2.5	22.4	20.3	60	25.7	438	5410	242	5.13	0.195	1480	0.053
25-Feb	-16.4	74	897	42	75.6	2.8	22.5	20.4	65	28.9	397	6300	247	6.36	0.231	2060	0.063
26-Feb	-11.0	71	897	43	77.0	2.6	23.1	21	63	27.2	404	5710	239	5.47	0.199	1680	0.056
27-Feb	-5.6	68	897	44	78.2	2.8	23.5	21.2	59	23.6	243	4930	232	4.90	0.151	1510	0.064
28-Feb	-2.7	70	897	44	79.6	2.9	23.8	21.4	56	20.8	301	4690	185	5.09	0.160	1460	0.047
1-Mar	-1.9	87	897	45	81.0	2.4	24.3	21.9	61	24.5	344	4710	635	4.38	0.123	1270	0.044
2-Mar	-11.9	56	897	46	82.4	2.3	23.2	20.6	60	21.5	322	5210	850	4.22	0.138	1380	0.060
3-Mar	-5.1	80	897	47	83.8	2.9	23.4	20.9	61	-	367	5210	923	-	0.185	1790	0.062
4-Mar	-12.1	83	897	47	85.2	2.3	22.9	20.5	63	-	-	5380	924	-	-	1400	0.044
5-Mar	-14.0	68	897	48	86.4	2.6	23.2	20.3	61	-	-	5510	911	-	-	1610	0.060
6-Mar	-8.2	86	897	49	87.8	3.1	22.7	19.3	60	26.5	446	-	899	5.96	0.234	-	0.064
7-Mar	-5.9	83	897	50	89.2	2.9	24.2	21	57	20.4	261	4630	701	4.45	0.178	1480	0.062
8-Mar	-10.2	83	897	50	90.4	2.5	23.7	20.8	60	22.7	304	5210	925	4.22	0.133	1490	0.049
9-Mar	-14.4	62	897	51	91.8	2.4	23.3	20.4	61	26.5	407	5740	804	4.76	0.124	1580	0.053
10-Mar	-10.8	66	897	52	93.2	2.9	23.5	20.6	61	28.3	444	5600	858	5.88	0.194	1940	0.064
11-Mar	0.1	71	897	53	94.4	3.4	24.3	21.6	55	21.6	338	3970	887	5.90	0.217	1600	0.068
12-Mar	0.9	88	897	54	96.0	3.2	24.5	20.7	55	17.9	272	3610	881	5.73	0.132	1350	0.069
13-Mar	1.5	84	897	54	97.4	3.6	24.6	21	54	18.3	288	3490	865	6.44	0.156	1510	0.075
14-Mar	4.4	86	897	55	98.6	3.8	24.6	21.4	53	16.7	100	3060	723	6.15	0.063	1440	0.073
15-Mar	11.3	74	897	56	100.0	5.9	25.7	23.6	49	13.0	84	2290	666	6.32	0.106	1440	0.101
16-Mar	14.1	74	897	57	101.4	7.6	26	24.2	49	-	-	-	527	-	-	-	0.129
17-Mar	13.6	73	897	57	102.6	7.5	26.2	24.2	48	-	-	-	592	-	-	-	0.125
18-Mar	10.8	81	897	58	104.0	4	25	22	52	-	-	-	916	-	-	-	0.081
19-Mar	4.3	90	897	59	105.4	2.7	24.2	20.3	54	-	-	-	922	-	-	-	0.063
20-Mar	3.4	95	897	59	106.6	3.9	24.3	20.6	54	-	-	-	908	-	-	-	0.085
21-Mar	2.9	79	897	60	108.0	3.4	24.4	20.6	51	-	-	-	925	-	-	-	0.081
22-Mar	5.9	65	897	61	109.4	5.4	24.5	21.6	43	-	-	-	645	-	-	-	0.115
23-Mar	10.9	53	897	62	110.8	7.5	25.2	23	39	-	-	-	728	-	-	-	0.153
24-Mar	11.4	53	897	62	112.0	5.7	25.1	22.6	41	-	-	-	911	-	-	-	0.112
25-Mar	7.9	46	897	63	113.4	5.9	24.3	21.9	38	-	-	-	925	-	-	-	0.155
26-Mar	7.5	62	897	64	114.8	5.2	24.4	21.2	42	16.4	240	2350	923	8.23	0.324	1400	0.124
27-Mar	6.9	90	897	65	116.2	3.8	24.4	20.7	52	16.1	225	2440	922	6.56	0.181	1130	0.090
28-Mar	1.5	85	897	66	117.6	3.7	24.4	20.4	51	21.4	282	3210	924	7.28	0.195	1460	0.106
29-Mar	0.7	71	897	66	118.8	3.3	24.1	20.3	48	22.0	294	3400	920	7.02	0.222	1360	0.106
30-Mar	1.5	59	896	67	120.0	4.4	23.9	20.7	44	21.4	341	3240	924	8.14	0.262	1680	0.123
31-Mar	9.0	52	895	68	121.4	6.7	24.5	22.3	41	17.8	294	2470	909	8.68	0.363	1630	0.169

T: Temperature; RH: Relative humidity; AU: Animal unit; Con: Concentration; ER: Emission rate.

Date	Outdoor T	Outside RH	Inventory	Mass	AU	Airflow	Indoor T	Exhaust T	Exhaust RH	NH_3Con	H_2SCon	CO_2Con	PM_{10}Con	NH_3ER	H_2SER	CO_2ER	PM_{10}ER
2003	°C	%		kg/pig		m^3/s	°C	°C	%	ppm	ppb	ppm	mg/m^3	kg/d	kg/d	kg/d	kg/d
1-Apr	18.5	38	895	69	122.8	11.5	27.1	26	33	-	229	1330	191	-	0.373	1290	0.191
2-Apr	18.0	50	895	69	124.2	12.1	26.8	25.6	40	-	290	1300	232	-	0.427	1280	0.272
3-Apr	12.3	71	895	70	125.4	7.9	25.6	22.7	46	12.2	-	1600	291	8.02	-	1200	0.234
4-Apr	-1.1	94	895	71	126.8	3.5	24	19.4	51	-	-	-	345	-	-	-	0.109
5-Apr	-3.0	82	895	72	128.2	3.3	23.9	19.9	49	23.5	433	3790	366	7.22	0.303	1540	0.111
6-Apr	-0.5	80	894	72	129.4	2.4	23.4	18.7	50	22.4	415	3700	391	5.34	0.226	1020	0.082
7-Apr	-1.8	93	894	73	130.6	2.7	23.3	18.9	51	19.9	369	3560	381	5.44	0.237	1110	0.094
8-Apr	-2.2	79	894	74	132.0	3.6	23.4	19.9	47	20.1	336	3460	400	7.12	0.293	1500	0.130
9-Apr	1.1	70	894	75	133.4	4.8	23.5	20.6	43	18.7	259	3130	376	7.64	0.289	1660	0.171
10-Apr	8.7	54	894	75	134.8	7.1	24.5	22.7	38	14.4	283	2270	370	8.23	0.367	1500	0.256
11-Apr	12.1	51	894	76	136.2	8.1	25.5	23.6	37	11.8	263	-	-	7.44	0.364	-	-
12-Apr	12.6	42	894	77	137.4	8.2	25.7	23.7	35	11.7	282	1800	-	7.58	0.402	1450	-
13-Apr	14.8	48	893	78	138.8	9.5	26.3	24.3	37	10.5	266	1660	-	6.79	0.374	1270	-
14-Apr	21.9	47	893	78	140.0	18.9	28.8	28.1	38	8.3	-	1090	-	6.50	-	1390	-
15-Apr	22.4	51	893	79	141.4	18.7	28	27.7	43	5.6	192	912	337	5.42	0.409	1330	0.563
16-Apr	13.4	87	893	80	142.6	8.9	26.6	24.2	55	14.3	-	1600	286	8.34	-	1480	0.209
17-Apr	5.3	87	893	81	144.0	4.4	23.7	19.4	50	13.4	-	2070	442	6.16	-	1120	0.177
18-Apr	6.7	91	893	81	145.4	4	24	19.2	52	14.0	446	2070	428	6.49	0.289	1050	0.145
19-Apr	10.0	95	893	82	146.8	6.1	24.2	21	57	15.8	473	1760	304	8.67	0.412	1360	0.175
20-Apr	7.2	91	892	83	147.8	4.6	24.1	20.2	53	16.1	443	1920	374	7.43	0.360	1140	0.157
21-Apr	9.9	71	891	84	149.2	6.6	25.3	22.2	47	17.2	555	1790	350	7.36	0.455	1370	0.222
22-Apr	10.5	55	891	85	150.6	7.5	26.4	24	41	24.6	621	1880	344	7.79	0.473	1340	0.229
23-Apr	12.7	51	891	85	152.0	8.8	26.4	23.8	40	19.4	602	1700	283	8.45	0.577	1570	0.230
24-Apr	9.3	79	891	86	153.2	5.4	24.3	20.8	51	16.5	-	1810	288	8.05	-	1190	0.113
25-Apr	13.4	49	891	87	154.6	8.9	25.5	23.6	39	14.4	440	1620	315	9.28	0.579	1580	0.245
26-Apr	15.0	51	891	87	155.8	10.7	25.4	23.8	38	13.4	327	1390	308	8.62	0.464	1430	0.312
27-Apr	16.4	54	891	88	157.2	11.3	26.1	24.7	41	13.1	325	1280	274	9.04	0.498	1330	0.275
28-Apr	15.7	44	891	89	158.6	10.5	26.6	24.7	37	14.8	323	1430	290	9.79	0.442	1570	0.274
29-Apr	11.2	60	891	90	160.0	8.3	24.4	21.9	45	17.8	327	1680	320	11.40	0.454	1750	0.232
30-Apr	10.5	95	891	91	161.4	4.8	24.3	21.7	57	17.6	254	1670	386	8.23	0.204	953	0.148
1-May	12.7	74	891	91	162.6	3.6	25.8	23.5	49	16.7	376	1560	516	4.58	0.182	589	0.161
2-May	13.3	69	891	92	164	4.1	27.3	24.5	46	17.3	392	1540	472	3.75	0.183	403	0.162
3-May	13.2	70	891	93	165.4	4	27.1	24.4	46	15.8	378	1590	423	3.71	0.184	543	0.140
4-May	9.9	86	890	94	166.6	3.7	25.6	21.7	53	16.5	-	-	415	5.37	-	-	0.117
5-May	11.0	87	890	94	167.8	4	24.4	22.1	55	12.4	421	1650	436	4.58	0.267	760	0.149
6-May	13.5	77	890	95	169.2	3.8	25.9	23.9	50	12.4	367	-	471	3.68	0.219	-	0.153
7-May	13.7	84	890	96	170.6	6.7	26.3	24.3	52	11.2	314	1500	368	5.10	0.299	1040	0.189
8-May	10.2	93	890	97	171.8	6.7	24.9	21.9	56	12.2	-	1780	280	6.83	-	1300	0.166
9-May	15.5	78	890	97	173.2	10.6	26.5	25	53	9.8	366	1390	259	6.28	0.464	1460	0.235
10-May	11.2	88	890	98	174.6	9.1	26.2	23.5	53	13.2	295	1710	298	7.15	0.328	1710	0.245
11-May	8.6	81	889	99	175.8	7	24.3	20.9	51	10.9	246	1770	331	6.35	0.320	1510	0.207
12-May	13.0	60	889	100	177.2	8.6	26.5	23.9	43	10.2	315	1610	325	5.40	0.352	1410	0.250
13-May	14.6	70	889	100	178.4	10.4	26.3	24.4	47	9.9	289	1470	256	6.62	0.403	1600	0.235
14-May	15.7	79	889	101	179.8	11.4	28.1	26.1	49	10.4	252	1440	249	6.03	0.332	1580	0.242
15-May	13.0	84	889	102	181.2	10.3	28	25.2	49	13.2	248	1580	298	6.81	0.282	1580	0.271
16-May	14.3	72	889	103	182.4	11.1	28	25.6	46	12.9	271	1500	277	7.58	0.350	1610	0.268
17-May	16.3	68	889	103	183.8	13.2	28.3	26.3	45	11.6	245	1350	269	7.41	0.335	1610	0.296
18-May	18.3	74	889	104	184.4	13.4	28.5	26.8	51	11.0	-	-	248	7.75	-	-	0.272
19-May	16.8	83	822	103	169.4	11.2	27.4	26.1	56	12.1	-	-	227	8.05	-	-	0.215
30-May	21.1	53	618	108	133	16.2	28.2	27.3	40	9.8	284	984	250	6.99	0.417	838	0.379
31-May	16.8	45	618	108	134	10.1	27.8	25.6	35	12.8	394	1210	229	5.70	0.344	954	0.185
1-Jun	17.9	52	618	109	134.8	10.9	27.6	25.6	40	12.5	400	1260	277	6.73	0.419	993	0.250
2-Jun	11.9	79	618	110	135.6	5.6	25.8	22.2	52	16.8	425	-	283	-	-	-	0.127
3-Jun	13.7	77	618	111	136.6	7.7	26.2	23.5	51	15.6	440	-	335	6.09	0.369	-	0.245
4-Jun	16.8	67	618	111	137.4	9.4	26.8	25	47	13.0	455	-	326	6.58	0.478	-	0.282
5-Jun	17.7	67	618	112	138.4	10.8	26.8	25.3	48	11.5	383	-	321	5.85	0.404	-	0.317
6-Jun	16.1	83	618	113	139.2	10	27.4	25.6	53	14.1	384	-	292	7.15	0.414	-	0.256
10-Jun	20.3	76	628	115	144.2	11.2	27.5	26.4	57	11.0	282	-	111	6.35	0.365	-	0.103

T: Temperature; RH: Relative humidity; AU: Animal unit; Con: Concentration; ER: Emission rate.

Date	Outdoor T	Outside RH	Inventory	Mass	AU	Airflow	Indoor T	Exhaust T	Exhaust RH	NH_3Con	H_2SCon	CO_2Con	PM_{10}Con	NH_3ER	H_2SER	CO_2ER	PM_{10}ER
2003	°C	%		kg/pig		m^3/s	°C	°C	%	ppm	ppb	ppm	mg/m^3	kg/d	kg/d	kg/d	kg/d
12-Jul	24.2	83	933	36	67	8.8	28.5	27.4	57	12.0	-	1310	100	5.80	-	1040	0.075
13-Jul	25.5	84	933	37	68.4	10.5	28.7	28	58	10.8	-	1240	104	5.88	-	1030	0.096
14-Jul	26.7	90	933	38	70	13.9	29.5	28.8	63	8.8	-	1000	88	6.19	-	1130	0.097
15-Jul	27.0	83	933	38	71.4	12.8	29.5	28.6	59	8.9	-	1020	75	6.29	-	1140	0.083
16-Jul	24.6	90	933	39	73	10.9	28.6	27.6	62	10.3	-	1250	94	5.61	-	1040	0.083
17-Jul	28.9	88	933	40	74.6	17.1	30.2	29.6	66	7.3	-	948	63	5.97	-	1170	0.091
18-Jul	26.1	90	933	41	76	12.3	29.4	28.6	63	9.4	-	1020	61	6.71	-	1160	0.066
19-Jul	25.1	89	933	42	77.6	11.2	28.5	27.5	62	9.8	-	1160	89	5.90	-	1100	0.081
20-Jul	25.9	97	933	42	79	12.7	29.3	28.5	69	8.5	-	1060	54	6.19	-	1220	0.059
21-Jul	23.3	91	933	43	80.6	10.5	28.5	27.4	60	10.6	-	1260	61	6.30	-	1400	0.055
22-Jul	22.1	85	933	44	82	9	27.8	26.2	54	11.5	-	1360	99	5.82	-	1210	0.076
23-Jul	22.8	80	933	45	83.6	8.8	28	26.3	51	11.3	-	1430	112	5.59	-	1170	0.080
24-Jul	23.1	84	933	46	85.2	9.9	28	26.7	54	10.3	-	1370	111	-	-	-	0.094
25-Jul	27.8	82	933	47	86.8	16.1	29.5	28.9	55	6.6	-	887	98	5.21	-	1070	0.132
26-Jul	31.4	82	933	47	88.2	21.2	31	31	61	4.4	-	685	89	5.22	-	969	0.159
27-Jul	25.9	99	932	48	89.6	13	29.8	28.8	66	7.2	-	917	35	5.44	-	1070	0.036
28-Jul	27.1	84	932	49	91	13.4	29.1	28.2	58	7.3	-	983	54	5.35	-	1140	0.059
29-Jul	26.6	82	932	50	92.6	12.9	28.8	27.7	58	7.3	-	1080	69	5.08	-	1160	0.070
30-Jul	26.0	89	932	51	94.2	13.6	28.8	28.1	61	6.9	-	990	51	5.20	-	1120	0.058
31-Jul	26.3	-	932	51	95.8	15.2	28.8	28.3	59	6.8	-	989	56	5.46	-	1090	0.072
1-Aug	26.5	-	932	52	97.2	-	29.1	-	56	8.0	-	973	55	-	-	-	-
2-Aug	24.3	-	932	53	98.8	10.9	-	27.3	56	9.8	521	1120	61	5.99	0.627	956	0.053
3-Aug	23.9	-	931	54	100	9.8	-	27.3	57	10.2	535	1160	59	5.42	0.575	884	0.045
4-Aug	24.7	-	930	55	101.6	10.8	-	27.2	56	9.1	473	1160	67	5.30	0.571	961	0.053
5-Aug	20.2	-	930	55	103.2	10	-	26.4	62	10.6	547	1270	61	6.63	0.738	1230	0.053
6-Aug	25.1	-	930	56	104.6	12.7	-	27.8	60	8.6	444	1190	54	6.16	0.664	1320	0.056
7-Aug	26.6	-	930	57	106.2	14.4	-	28.4	58	8.4	443	1150	52	6.58	0.740	1330	0.060
8-Aug	25.9	-	930	58	107.6	13.4	-	28.1	57	9.3	495	1170	57	7.02	0.779	1340	0.064
9-Aug	25.4	-	930	59	109.2	13.3	-	27.8	56	9.7	498	1200	66	6.97	0.741	1320	0.072
10-Aug	24.3	-	930	59	110.6	12.7	-	27.9	59	10.2	555	1270	65	7.18	0.789	1370	0.070
11-Aug	25.8	-	930	60	112.2	14.9	-	28.2	59	9.1	484	1110	50	7.18	0.788	1280	0.061
12-Aug	24.2	-	930	61	113.8	13.3	-	27.5	58	9.8	563	1170	67	7.42	0.888	1360	0.072
13-Aug	25.3	-	930	62	115.2	14.5	-	27.9	59	8.6	470	1110	65	6.75	0.776	1300	0.076
14-Aug	26.4	-	930	63	116.8	16.6	-	28.5	63	7.6	451	1040	90	6.78	0.812	1330	0.132
15-Aug	28.5	-	930	64	118.2	19.6	-	29.6	62	6.5	393	972	71	6.34	0.770	1230	0.106
16-Aug	30.3	-	930	64	119.8	19.7	-	30.4	61	6.0	376	937	57	6.16	0.768	1130	0.093
17-Aug	29.9	-	928	65	121.2	19.8	-	30.5	61	5.7	378	916	54	5.93	0.785	1070	0.089
18-Aug	30.8	-	927	66	122.4	20.1	-	30.8	67	5.8	381	791	50	6.31	0.813	1040	0.088
19-Aug	29.5	-	927	67	124	20	-	30.3	68	5.2	376	808	51	5.79	0.813	1060	0.087
20-Aug	29.8	-	927	68	125.4	21	-	30.6	64	5.1	342	828	48	6.09	0.816	1150	0.087
21-Aug	27.8	-	927	69	127	16.3	-	29.3	59	6.6	462	1020	45	6.03	0.850	1310	0.063
22-Aug	24.5	-	927	69	128.6	13.5	-	27.6	55	8.2	560	1200	75	6.20	0.835	1340	0.080
23-Aug	25.0	-	927	70	130	15.5	-	27.8	52	8.0	512	1130	93	6.38	0.824	1300	0.113
24-Aug	29.8	-	926	71	131.4	20.5	-	30.3	57	5.8	344	909	90	6.54	0.789	1280	0.157
25-Aug	30.2	-	926	72	133	20.2	-	30.9	56	5.9	370	899	79	6.51	0.801	1110	0.143
2-Sep	19.1	72	924	78	144.8	14.5	27.4	26.3	51	9.2	524	1230	110	6.46	0.768	1290	0.134
3-Sep	19.0	67	924	79	146.2	11.3	27.7	26.5	48	10.9	584	1390	97	7.54	0.836	1540	0.095
4-Sep	17.0	67	924	80	147.8	11.1	27.3	25.5	46	12.5	645	1470	111	7.67	0.798	1490	0.099
5-Sep	18.7	65	924	81	149.2	15	27.6	26.3	45	11.2	552	1330	140	8.10	0.795	1410	0.177
6-Sep	21.7	63	924	82	150.8	17.4	28.6	27.6	47	9.7	497	1120	110	7.63	0.795	1410	0.167
7-Sep	22.0	61	923	82	152.2	17.4	28.8	27.9	45	8.8	443	1080	103	7.44	0.748	1320	0.151
8-Sep	21.7	62	922	83	153.6	17.2	28.2	27.7	46	8.6	443	1090	105	7.56	0.776	1350	0.153
9-Sep	21.7	66	922	84	155	16.7	28.2	27.4	49	9.4	498	1120	100	7.70	0.847	1420	0.138
10-Sep	23.9	64	922	85	156.4	17.5	29.2	28.5	52	7.8	414	994	96	7.22	0.770	1320	0.137
11-Sep	22.8	79	922	86	158	15.5	28.9	28.3	59	8.8	494	1070	64	7.73	0.875	1430	0.082
12-Sep	18.8	77	922	86	159.4	13.1	27.3	26.7	54	10.3	579	1280	56	7.95	0.904	1560	0.066
13-Sep	16.7	84	922	87	161	10.5	26.4	25.3	56	13.2	634	1480	60	8.84	0.880	1640	0.055
14-Sep	15.0	65	921	88	162.4	9.9	26.9	24.9	44	14.4	652	1540	106	8.73	0.831	1540	0.092
15-Sep	17.2	60	920	89	163.6	13	27	25.3	42	12.4	526	1390	147	8.32	0.716	1470	0.186
16-Sep	20.5	66	920	90	165.2	16.7	27.7	26.8	49	10.1	446	1130	128	8.64	0.779	1340	0.205
17-Sep	22.8	61	920	91	166.6	16.4	28.6	28	49	8.6	344	1000	89	7.71	0.631	1280	0.128
18-Sep	16.4	80	920	91	168.2	11	27.2	25.3	52	12.9	529	1380	91	8.70	0.750	1490	0.090
19-Sep	11.0	67	920	92	169.8	8.1	25.9	22.9	43	17.3	687	1740	125	8.79	0.759	1490	0.085
20-Sep	13.4	64	920	93	171.2	9.7	25.8	23.3	41	14.8	586	1690	118	8.29	0.708	1450	0.096
21-Sep	12.4	91	920	94	172.8	8.8	25.7	22.9	54	16.3	667	1740	86	9.53	0.838	1690	0.065
22-Sep	13.4	77	920	95	174.2	9.4	26.5	24	49	14.7	633	1680	93	8.62	0.779	1680	0.078
23-Sep	14.4	64	920	96	175.8	11.2	25.8	23.5	43	13.7	598	1570	117	8.36	0.762	1480	0.119
24-Sep	14.9	55	920	96	177.4	10.2	26.5	24.5	40	13.5	606	1610	102	8.19	0.780	1650	0.092
25-Sep	10.1	61	920	97	178.8	8.3	25.5	22.4	39	15.5	626	1820	140	7.95	0.663	1620	0.101
26-Sep	12.6	72	920	98	180.2	9.2	25.6	22.7	47	14.7	595	1680	108	8.49	0.709	1750	0.085
27-Sep	10.4	66	920	99	181.8	8.4	25.2	21.9	44	16.5	627	1800	118	8.72	0.704	1730	0.087
28-Sep	9.3	61	917	100	182.8	7.9	25.3	21.8	41	16.6	572	1800	151	8.48	0.632	1640	0.107
29-Sep	8.0	61	916	100	184	7.2	24.9	21.5	38	16.8	516	1950	174	6.75	0.455	1480	0.112
30-Sep	6.9	57	916	101	185.6	6.6	24.6	20.9	37	17.2	516	2050	192	-	-	-	0.114

T: Temperature; RH: Relative humidity; AU: Animal unit; Con: Concentration; ER: Emission rate.

Date	Outdoor T	Outside RH	Inventory	Mass	AU	Airflow	Indoor T	Exhaust T	Exhaust RH	NH_3Con	H_2SCon	CO_2Con	PM_{10}Con	NH_3ER	H_2SER	CO_2ER	PM_{10}ER
2003	°C	%		kg/pig		m^3/s	°C	°C	%	ppm	ppb	ppm	mg/m^3	kg/d	kg/d	kg/d	kg/d
1-Oct	5.1	56	916	102	187.0	6.3	24.3	20.5	36	18.9	506	2170	208	7.72	0.448	1500	0.118
2-Oct	5.8	55	916	103	188.4	6.8	24.3	20.8	36	19.4	509	2190	214	8.33	0.494	1530	0.132
3-Oct	13.6	51	916	104	190.0	9.6	26.3	23.7	38	14.3	433	1660	132	8.34	0.529	1740	0.111
4-Oct	14.1	54	916	105	191.6	10.8	26.6	24.1	37	13.3	461	1630	149	7.56	0.544	1660	0.135
5-Oct	16.7	55	912	105	192.4	12.5	27	25.2	39	10.8	424	1450	125	7.40	0.580	1640	0.135
6-Oct	18.0	53	911	106	193.6	15.5	27.1	25.8	38	9.6	377	1320	151	7.37	0.592	1550	0.217
7-Oct	18.8	62	911	107	195.0	16.6	26.9	26	44	8.3	355	1210	139	6.97	0.591	1540	0.208
8-Oct	19.3	69	911	108	196.6	15.7	27.2	26.1	48	-	355	1170	151	-	0.626	1450	0.210
9-Oct	20.7	66	911	109	198.0	15.7	27.5	26.8	48	-	318	1090	128	-	0.563	1360	0.183
10-Oct	17.9	74	911	110	199.6	12.7	26.9	25.5	50	-	379	1260	110	-	0.597	1510	0.126
11-Oct	15.0	84	911	111	202.0	10.4	26.6	24.7	54	-	497	1520	100	8.14	0.645	1640	0.091
12-Oct	12.5	60	909	111	202.0	9.9	26.1	23.1	40	-	537	1610	154	-	0.611	1560	0.136
13-Oct	11.4	73	908	112	204.0	8.6	25.9	22.3	45	-	541	1640	123	-	0.608	1580	0.090
14-Oct	11.3	67	908	112	204.0	8.4	26	22.4	42	-	496	1600	123	-	-	_	0.093
15-Oct	8.2	73	908	113	206.0	6.7	24.8	20.9	43	-	521	1760	121	-	0.521	1310	0.068
16-Oct	5.3	70	908	115	208.0	5.3	24.6	19.9	43	-	-	2070	147	-	-	1260	0.071
17-Oct	7.5	67	908	116	210.0	7.3	24.8	21.4	40	-	-	2010	153	-	-	1490	0.100
18-Oct	15.4	61	908	116	210.0	12.5	26.7	25	40	-	425	1560	119	-	0.550	1590	0.121
19-Oct	18.2	54	907	116	210.0	14.7	27.2	26.2	38	-	367	1330	143	-	0.554	1420	0.193
20-Oct	18.6	55	658	111	146.6	13.5	26.7	25	40	-	581	1140	121	-	1.150	1030	0.170
21-Oct	14.4	52	556	112	124.4	8.6	24.9	22.4	40	15.8	897	1350	130	7.17	0.973	1070	0.094
22-Oct	13.7	62	556	113	125.2	9	24.2	21.8	42	18.4	2270	1440	-	9.22	3.750	1120	-
23-Oct	10.5	60	556	113	126.0	6.3	24.6	21.7	41	25.0	93	1670	146	9.20	0.070	1030	0.080
24-Oct	9.1	78	556	114	127.0	4.8	24.2	20.6	48	26.0	93	1920	136	9.01	0.065	1000	0.057
25-Oct	5.7	64	556	115	127.8	4.3	23.7	20.3	43	29.6	83	2070	130	7.51	0.047	940	0.050
26-Oct	1.9	68	555	115	128.2	2.8	23.4	19.8	44	32.2	86	2560	158	6.86	0.037	852	0.039
27-Oct	4.0	77	554	116	129.0	3.2	23.6	20.5	46	31.9	75	2460	159	-	-	-	0.045
28-Oct	6.4	68	554	117	130.0	2.7	23.7	20.5	45	27.3	61	2190	130	5.52	0.024	696	0.030
29-Oct	3.4	73	554	118	130.8	2.4	23.4	19.6	44	33.7	72	2500	167	6.45	0.029	735	0.035
30-Oct	8.3	77	554	119	131.6	5.1	24	21.1	45	27.1	80	1960	123	8.12	0.048	959	0.050
31-Oct	4.8	77	554	120	133.0	3.2	23.8	20.6	46	31.6	86	2300	153	7.23	0.039	850	0.044
1-Nov	1.8	76	554	120	133.2	2.8	23.6	20.4	45	38.6	117	2890	158	7.99	0.051	955	0.038
2-Nov	4.1	92	553	121	133.8	2.9	23.8	20.6	48	36.7	139	2570	150	7.84	0.057	890	0.039
3-Nov	4.1	94	552	122	134.6	2.9	23.6	20	49	32.7	125	2510	138	7.17	0.060	857	0.036
4-Nov	4.1	91	552	123	135.4	3.3	23.7	20.5	50	34.0	179	2510	111	7.57	0.082	964	0.032
5-Nov	-0.9	82	552	123	136.2	2.9	23.3	20.2	47	40.1	279	3210	152	8.08	0.117	1120	0.039
6-Nov	-2.4	72	552	124	137.0	3	23.2	20	43	39.4	316	3160	165	7.68	0.137	1120	0.044
7-Nov	-3.1	75	552	125	137.8	2.9	23.2	20	44	39.2	390	3350	174	7.39	0.155	1130	0.046
8-Nov	-5.5	63	552	126	138.8	2.6	22.3	19	43	37.3	421	3650	189	6.89	0.164	1070	0.044
9-Nov	-0.8	66	552	125	138.2	2.5	22.1	19.1	44	31.1	420	3090	163	5.96	0.182	836	0.038
23-Dec	-3.5	85	1030	29	59.0	1.8	23.7	22.8	64	28.4	355	5450	62	4.93	0.136	1120	0.010
24-Dec	-6.9	86	1030	29	60.6	2.1	23.6	22.6	63	34.5	460	6040	82	5.53	0.180	1370	0.017
25-Dec	-2.9	79	1030	30	62.2	1.9	23.4	22.1	64	35.7	548	5320	85	5.06	0.252	1100	0.015
26-Dec	2.5	79	1030	31	63.4	1.9	23.6	22.3	59	27.7	594	4410	63	4.13	0.277	885	0.011
27-Dec	7.5	83	1020	32	64.8	2	24.2	23.2	60	20.1	553	3870	46	3.50	0.273	884	0.008
28-Dec	2.1	73	1020	33	66.4	2.5	24.8	24.1	58	21.3	752	4770	58	5.01	0.367	1260	0.014
29-Dec	-2.6	80	1020	33	68.0	1.9	24.1	23.1	64	27.2	955	5710	45	4.62	0.395	1240	0.008
30-Dec	-0.6	76	1020	34	69.6	2.1	23.9	22.8	64	28.7	854	5380	50	4.72	0.376	1240	0.010
31-Dec	-3.8	73	1020	35	71.0	2.3	23.9	22.7	64	27.2	867	5270	64	5.12	0.417	1330	0.014

T: Temperature; RH: Relative humidity; AU: Animal unit; Con: Concentration; ER: Emission rate.

Date	Outdoor T	Outside RH	Inventory	Mass	AU	Airflow	Indoor T	Exhaust T	Exhaust RH	NH_3Con	H_2SCon	CO_2Con	PM_{10}Con	NH_3ER	H_2SER	CO_2ER	PM_{10}ER
2004	°C	%		kg/pig		m^3/s	°C	°C	%	ppm	ppb	ppm	mg/m^3	kg/d	kg/d	kg/d	kg/d
1-Jan	1.3	82	1020	36	72.6	2.2	24.1	22.6	63	26.3	754	4870	53	4.41	0.335	1220	0.009
2-Jan	2.4	91	1020	36	73.8	2.4	24.6	23.4	63	27.4	742	4890	35	4.78	0.371	1310	0.007
3-Jan	-5.7	72	1020	37	75.4	1.8	24.4	23.2	61	27.3	773	5710	66	4.18	0.277	1250	0.012
4-Jan	-8.4	74	1020	38	76.8	1.5	23.9	22.6	61	32.1	820	5890	37	3.66	0.205	1060	0.005
5-Jan	-16.0	66	1020	38	78.4	1.9	24.1	22.3	56	32.9	-	5810	49	4.43	-	1200	0.008
6-Jan	-12.8	59	1020	39	80.0	1.9	23.5	22	56	38.0	-	6270	47	5.47	-	1260	0.008
7-Jan	-10.1	71	1020	40	81.4	1.9	23.7	22	59	41.5	-	6640	44	5.65	-	1390	0.008
8-Jan	-5.3	85	1020	41	83.0	2.2	24.5	22.6	58	38.1	567	5920	52	6.32	0.245	1420	0.011
9-Jan	-7.7	80	1020	41	84.4	2.4	24.7	22.8	57	37.3	605	5800	65	6.14	0.257	1540	0.014
10-Jan	-4.8	87	1020	42	86.0	2.3	25.1	23.4	56	34.3	618	5820	63	6.10	0.281	1660	0.013
11-Jan	1.7	81	1020	43	87.6	3.5	25.2	23.1	50	24.7	477	4120	64	7.12	0.349	1660	0.021
12-Jan	0.2	81	1020	44	89.0	3.4	25.2	22.8	48	21.5	458	4120	68	6.75	0.347	1730	0.022
13-Jan	-2.0	77	1020	44	90.6	3.2	25	22.5	49	23.6	492	4760	65	6.59	0.357	-	0.019
14-Jan	-1.9	75	1020	45	92.0	3.2	25.2	22.5	51	22.3	491	4650	62	6.22	0.324	1820	0.019
15-Jan	-4.6	75	1020	46	93.6	2.7	25	22	51	26.6	553	5090	76	6.00	0.317	1700	0.019
16-Jan	-0.4	85	1020	47	95.2	3.3	24.8	20.9	52	24.7	478	4420	65	7.23	0.390	1830	0.020
17-Jan	-0.4	87	1020	47	96.6	3.3	25.1	22.4	51	21.7	428	4250	-	7.28	0.385	1720	-
18-Jan	-13.9	64	1020	48	98.2	2.1	24.4	21.7	53	32.7	520	5540	-	5.18	0.185	1400	-
19-Jan	-13.9	66	1020	49	99.8	2.1	24.5	21.3	56	43.2	-	6570	-	6.48	-	1690	-
20-Jan	-8.4	77	1020	50	101.2	2.4	24.4	21.7	55	42.6	-	6040	-	7.48	-	1750	-
21-Jan	-3.3	72	1020	50	102.8	3.2	25.1	22.2	49	29.9	538	4750	-	7.34	0.310	1780	-
22-Jan	-13.7	55	1020	51	104.2	2.4	24	21.6	53	34.9	551	5500	-	5.99	0.213	1590	-
23-Jan	-1.5	63	1020	52	105.8	2.9	24.9	22.9	48	33.5	494	4420	-	6.98	0.282	1450	-
24-Jan	-7.5	61	1020	53	107.4	2.7	24.1	21	50	32.8	601	4670	-	6.86	0.307	1510	-
25-Jan	-6.3	55	1020	53	109.0	1.7	23.2	20.3	53	40.2	638	4780	-	5.03	0.194	987	-
26-Jan	-7.5	89	1020	54	110.4	2.2	24.1	21.9	53	33.2	507	4720	-	5.83	0.222	1240	-
27-Jan	-17.2	78	1020	55	112.0	2.3	23.3	22.2	54	33.5	413	5070	-	5.76	0.156	1420	-
28-Jan	-20.1	73	1020	56	113.4	2	23	22.4	57	41.5	-	6140	-	5.60	-	1380	-
29-Jan	-20.7	73	1020	56	115.0	2	23.2	22.5	57	37.4	-	6090	-	4.97	-	1470	-
30-Jan	-21.8	72	1020	57	116.6	2.1	23.3	21.7	55	32.1	-	6050	-	4.77	-	1490	-
31-Jan	-15.6	67	1020	58	118.0	2.1	23.3	18.8	54	33.5	-	-	-	4.78	-	-	-
1-Feb	-8.4	86	1020	59	119.6	2.9	23.9	17.6	52	29.2	-	-	-	6.47	-	-	-
2-Feb	-6.9	90	1020	59	121.2	3.3	24.5	21.1	49	22.3	552	4240	-	6.10	0.325	1640	-
3-Feb	-17.5	71	1020	60	122.6	2.9	23.9	21.3	52	26.6	576	5060	-	5.69	0.281	1710	-
4-Feb	-12.6	70	1020	61	124.2	2.8	23.8	17.6	52	32.7	588	4930	-	6.46	0.271	1730	-
5-Feb	-5.8	83	1020	62	125.6	3	23.5	13.8	51	23.2	522	3800	-	5.70	0.309	1470	-
6-Feb	-7.0	88	1020	62	127.2	3.2	24.5	21.3	48	21.5	554	4200	-	5.60	0.332	1630	-
7-Feb	-14.2	82	1020	63	128.8	2.9	24.3	22.5	50	24.6	570	5050	-	5.47	0.306	1740	-
9-Feb	-4.5	82	1020	65	131.8	3.3	24.4	21.8	44	19.1	492	3920	-	6.25	0.402	1550	-
10-Feb	-8.4	81	1020	65	133.4	3	23.9	21.5	47	22.8	571	4200	-	6.03	0.378	1480	-
11-Feb	-6.9	81	1020	66	134.8	3.3	24	21.4	44	21.7	502	4190	-	6.40	0.386	1610	-
12-Feb	-11.4	83	1020	67	136.4	3.1	24.1	21.5	46	25.6	527	4800	-	7.09	0.384	1820	-
13-Feb	-9.1	74	1020	68	138	3.1	24.7	22.9	47	29.7	581	4860	-	7.89	0.378	1850	-
14-Feb	-10.4	80	1020	68	139.4	3.1	24.1	20.7	45	24.6	466	4430	-	7.41	0.369	1630	-
15-Feb	-15.0	65	1020	69	141	3	23.7	19.5	47	32.6	483	4930	-	7.98	0.308	1780	-
16-Feb	-8.7	82	1020	70	142.6	2.9	23.7	20.3	47	32.0	488	4570	-	8.24	0.336	1580	-
17-Feb	-7.5	92	1020	71	144	3.2	23.7	20.9	46	24.2	402	4240	-	7.20	0.337	1560	-
18-Feb	-0.6	85	1020	71	145.6	3.4	24.3	21	43	19.6	342	3370	-	6.66	0.294	1300	-
19-Feb	0.9	91	1020	72	147	3.5	24.2	20.4	44	16.9	283	3010	-	7.26	0.312	1280	-
20-Feb	0.9	92	1020	73	148.6	-	24.5	21	46	16.8	294	3020	-	-	-	-	-
21-Feb	0.5	86	1020	74	150	3.4	24.2	20.4	43	16.8	297	2930	-	6.10	0.255	1190	-
22-Feb	2.7	90	1020	74	151.6	3.2	24.4	20.6	45	17.6	311	2940	-	6.09	0.264	1100	-
23-Feb	0.9	92	1020	75	153	3.5	24.4	20.5	46	17.4	282	3010	-	6.39	0.253	1240	-
24-Feb	0.5	85	1020	76	154.6	3.6	23.9	19.4	45	17.5	301	2990	-	7.08	0.283	1310	-
25-Feb	0.4	84	1020	77	156.2	3.7	24	19	44	18.4	291	3020	-	7.34	0.287	1300	-
26-Feb	1.3	84	1020	77	157.6	3.2	24	20.1	43	19.2	268	2870	-	6.35	0.226	1100	-
27-Feb	2.7	82	1020	78	159.2	3.3	24.1	20.7	43	19.4	254	2720	-	6.85	0.233	1110	-
28-Feb	5.4	76	1020	79	160.8	3.1	24.7	21.8	42	20.5	273	2520	-	6.21	0.207	902	-
29-Feb	7.3	79	1020	80	162.2	3.7	25	22.5	44	20.9	276	2350	-	6.64	0.221	981	-

T: Temperature; RH: Relative humidity; AU: Animal unit; Con: Concentration; ER: Emission rate.

Date	Outdoor T	Outside RH	Inventory	Mass	AU	Airflow	Indoor T	Exhaust T	Exhaust RH	NH_3Con	H_2SCon	CO_2Con	PM_{10}Con	NH_3ER	H_2SER	CO_2ER	PM_{10}ER
2004	°C	%		kg/pig		m^3/s	°C	°C	%	ppm	ppb	ppm	mg/m^3	kg/d	kg/d	kg/d	kg/d
1-Mar	5.9	92	1020	80	163.8	5.1	25	22	48	21.3	281	2410	-	9.52	0.330	1500	-
2-Mar	2.6	88	1020	81	165.2	4.2	24.5	21.2	45	21.2	263	2630	-	8.43	0.290	1360	-
3-Mar	2.1	93	1020	82	166.8	3.9	24.2	20.9	45	20.4	282	2740	-	8.04	0.312	1290	-
4-Mar	2.9	96	1020	83	168.4	4.6	24.3	20.6	46	18.5	275	2520	-	9.04	0.356	1440	-
5-Mar	2.8	92	1010	84	169.4	4.2	24.2	20.9	46	18.2	263	2490	-	8.15	0.313	1260	-
6-Mar	5.1	78	1010	84	170.6	5.8	24	21.6	42	-	-	-	-	-	-	-	-
7-Mar	2.7	71	1010	85	172.2	4.9	23.8	20	41	-	-	-	963	-	-	-	0.427
8-Mar	4.2	74	1010	86	173.6	5.7	24	20.9	41	18.1	250	2470	859	8.82	0.318	1690	0.448
9-Mar	2.8	80	1010	87	175.2	5.2	23.4	20.1	41	16.8	259	2450	820	8.13	0.302	1570	0.399
10-Mar	3.9	77	1010	87	176.6	5	23.8	20.4	42	18.8	297	2660	824	8.18	0.320	1520	0.382
11-Mar	-4.7	65	1010	88	178.2	3.7	23.1	18.9	43	21.7	306	3500	1090	7.77	0.272	1510	0.366
12-Mar	-2.5	64	1010	89	179.6	4.6	23.2	19.6	39	20.9	329	3260	946	8.00	0.306	1760	0.411
13-Mar	5.6	67	1010	90	181.2	5	23.8	20.6	41	17.9	318	2630	798	8.05	0.341	1560	0.374
14-Mar	3.1	66	1010	90	182.6	5.6	23.7	20.1	39	17.9	286	2670	786	9.38	0.359	1860	0.448
15-Mar	-1.3	90	1010	91	184.2	4.3	23.3	18.7	44	21.4	288	3300	-	10.10	0.347	1880	-
16-Mar	-0.9	87	1010	92	185.8	4.9	23.6	19.6	42	22.5	322	3280	892	10.80	0.386	1970	0.393
17-Mar	1.7	88	1010	93	187.2	5.5	23.9	20.1	42	22.3	326	3030	798	12.00	0.430	2060	0.404
18-Mar	3.3	84	1010	93	188.8	5.7	24	20.3	44	22.4	329	2660	814	11.50	0.411	1860	0.439
19-Mar	7.2	75	1010	94	190	6.2	25.8	22.9	44	25.5	423	2590	913	10.90	0.387	1770	0.542
20-Mar	6.9	59	1010	95	191.4	8.3	26.5	23.4	38	22.7	357	2350	777	11.20	0.368	2300	0.563
21-Mar	-1.9	64	1010	96	193	5.1	23.8	19.8	39	23.6	286	2970	1020	10.70	0.332	1890	0.487
22-Mar	1.2	59	1010	96	194.4	5.7	23.9	20.3	38	24.3	308	2940	936	11.20	0.346	2040	0.489
23-Mar	8.5	61	1010	97	196	7.5	25.2	22.2	38	19.1	286	2190	803	10.00	0.358	1770	0.540
24-Mar	15.9	73	1010	98	197.6	13.5	26.2	24.7	47	-	283	1380	-	-	0.408	1730	-
25-Mar	16.5	89	1010	99	199.2	12.3	26	25.6	56	-	255	1400	371	-	0.411	1780	0.390
26-Mar	16.7	90	1010	99	199.6	11.9	27.1	26.2	56	-	224	1570	321	-	0.363	1890	0.334
27-Mar	16.0	93	946	99	186.8	10.4	27	25.9	57	-	210	1640	328	-	0.277	1670	0.299
28-Mar	9.0	84	921	99	183	8.3	25.1	22.1	49	-	-	2050	591	-	-	2130	0.440
29-Mar	7.4	73	921	100	184.4	7.7	24.9	21.4	42	-	-	2150	533	-	-	1970	0.378
30-Mar	1.3	77	921	101	185.8	5.3	23.3	19.1	44	23.0	-	2820	717	11.40	-	1890	0.345
31-Mar	3.1	69	921	102	187	7.1	23.6	19.9	40	23.0	-	2680	589	13.30	-	2260	0.367
1-Apr	6.3	63	921	102	188.6	7.7	24.4	21.1	38	21.8	-	2370	603	12.60	-	2120	0.405
2-Apr	8.9	49	920	102	188.4	7.8	25.2	22.1	34	23.7	-	2240	599	13.00	-	2050	0.414
3-Apr	7.3	51	796	101	161	8	24.4	20.9	36	21.7	-	2170	576	13.30	-	2080	0.408
4-Apr	6.7	45	745	102	151.6	7.7	24.7	21.5	33	22.9	-	2330	652	12.80	-	2080	0.448
5-Apr	11.2	46	745	103	152.8	9.3	24.7	22.4	32	21.6	265	1860	515	13.90	0.343	1760	0.425
6-Apr	14.6	44	745	103	153.8	8.7	25.4	23.5	33	22.8	278	1630	372	12.90	0.337	1590	0.282
7-Apr	13.5	40	745	104	154.8	8.3	25.2	23.3	31	22.1	280	1560	373	11.10	0.297	1330	0.261
8-Apr	9.2	48	745	105	156	7	24	21.6	34	17.2	213	1410	413	8.67	0.229	1040	0.254
9-Apr	8.7	42	744	105	156.8	6.5	23.6	21.2	33	17.7	230	1500	460	8.41	0.229	1040	0.260
10-Apr	4.2	48	744	106	158	5.5	23.1	20.1	35	17.9	235	1650	537	7.74	0.216	1010	0.268
11-Apr	3.2	39	744	107	159	5.5	23	20.2	33	20.4	-	1920	593	7.96	-	1110	0.287
12-Apr	5.2	44	744	108	160	6	23.2	20.3	33	17.4	233	1720	582	8.62	0.254	1160	0.315
13-Apr	6.7	41	744	108	161	6.5	23.8	21.3	32	19.0	246	1730	636	7.76	-	1170	0.343
14-Apr	12.3	40	744	109	162.2	9.1	24.7	22.7	30	-	-	-	615	-	-	-	0.533
15-Apr	15.4	49	744	110	163.2	9.9	25.1	23.4	37	-	-	-	522	-	-	-	0.493
16-Apr	19.5	55	743	110	163.4	13.7	27.3	26	37	-	-	-	488	-	-	-	0.590
17-Apr	19.1	72	593	109	129.6	13.7	27.3	26	49	-	-	-	221	-	-	-	0.244
18-Apr	21.4	68	531	110	116.8	16	26.3	26	53	9.3	62	765	270	9.60	0.131	-	0.388
19-Apr	11.3	76	531	111	117.6	7.7	24.6	21.9	47	18.3	183	1360	348	8.44	0.190	-	0.236
20-Apr	10.3	91	531	111	118.4	5	24	20.7	52	22.6	154	1620	320	7.31	0.129	803	0.140
21-Apr	11.1	76	531	112	119	5.2	24.2	21.8	48	-	-	-	363	-	-	-	0.143
22-Apr	11.1	75	531	113	119.8	5	24.1	22	47	-	-	-	406	-	-	-	0.170

T: Temperature; RH: Relative humidity; AU: Animal unit; Con: Concentration; ER: Emission rate.

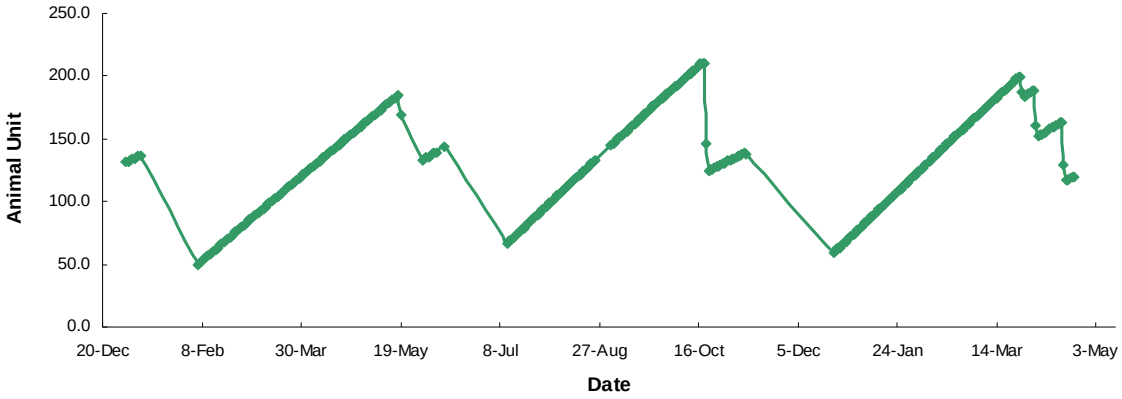

Figure B.1. Three complete animal growth cycles from Jan, 2003 to April, 2004.

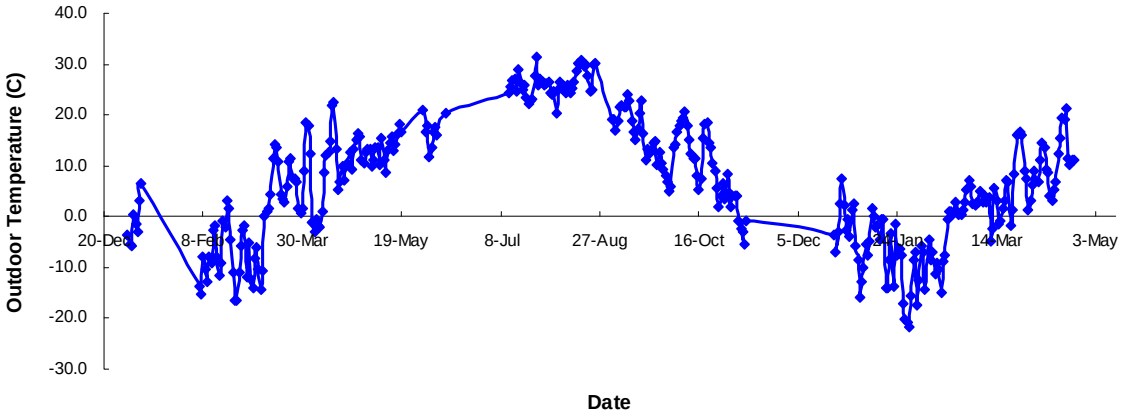

Figure B.2. Daily outdoor temperature from Jan, 2003 to April, 2004.

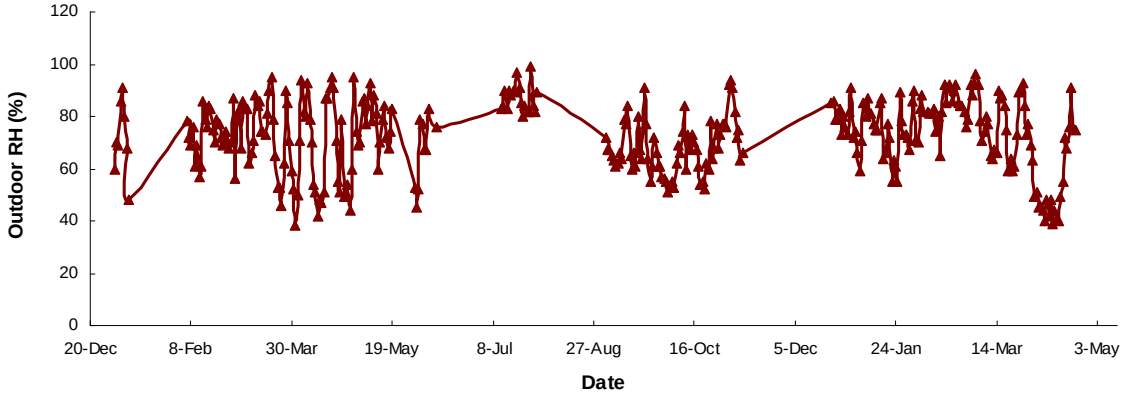

Figure B.3. Daily outdoor RH from Jan, 2003 to April, 2004.

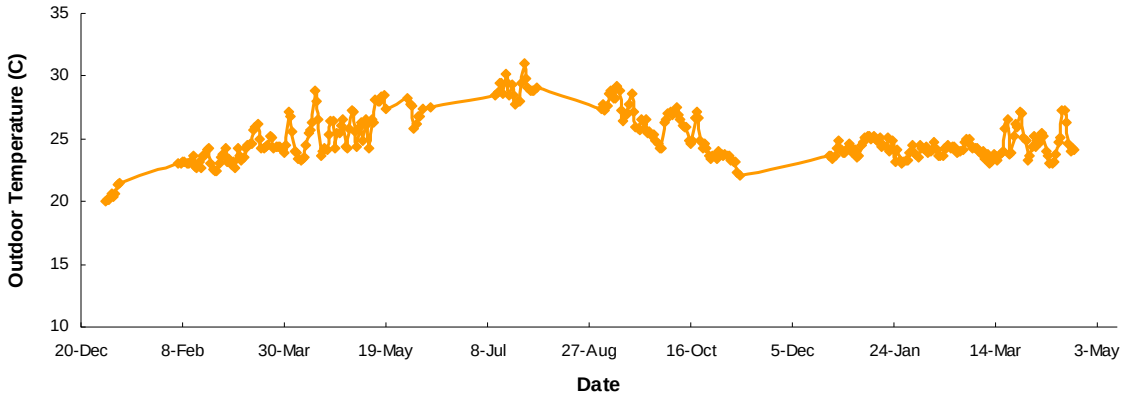

Figure B.4. Daily indoor air temperature from Jan, 2003 to April, 2004.

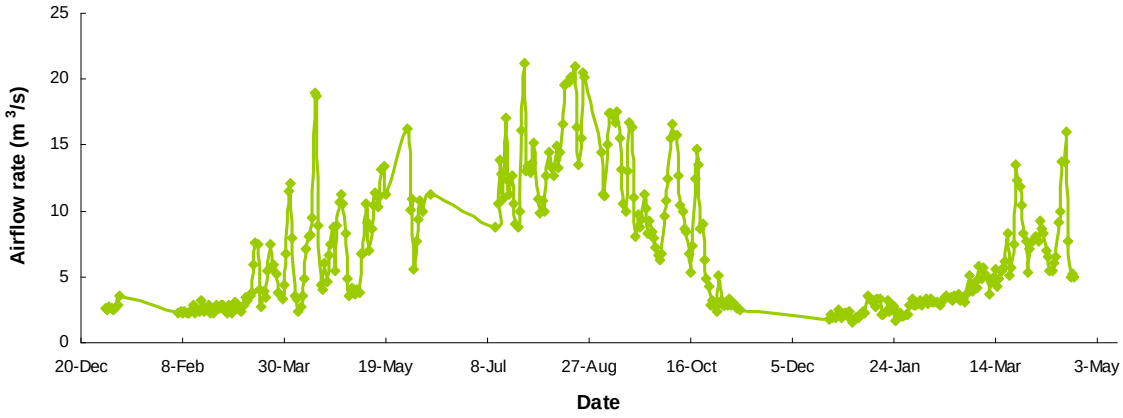

Figure B.5. Daily airflow rate from Jan, 2003 to April, 2004.

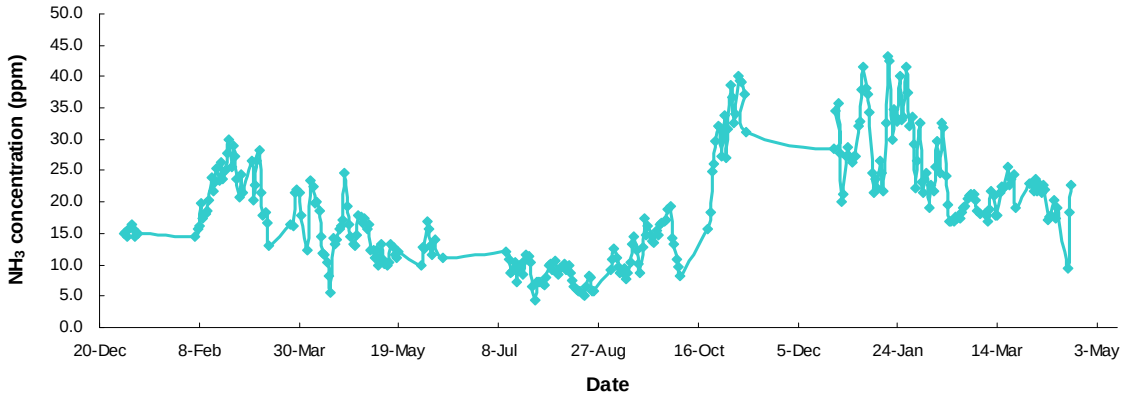

Figure B.6. Daily NH_3 concentration from Jan, 2003 to April, 2004.

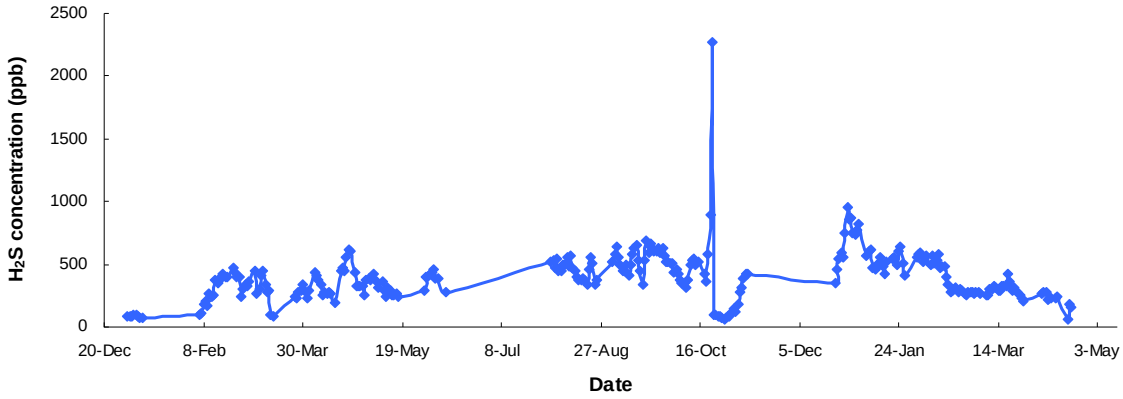

Figure B.7. Daily H_2S concentration from Jan, 2003 to April, 2004.

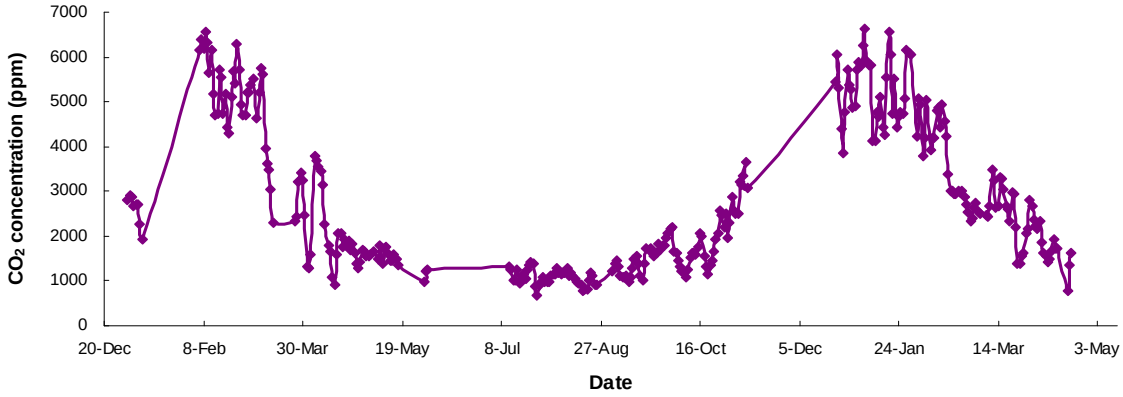

Figure B.8. Daily CO_2 concentration from Jan, 2003 to April, 2004.

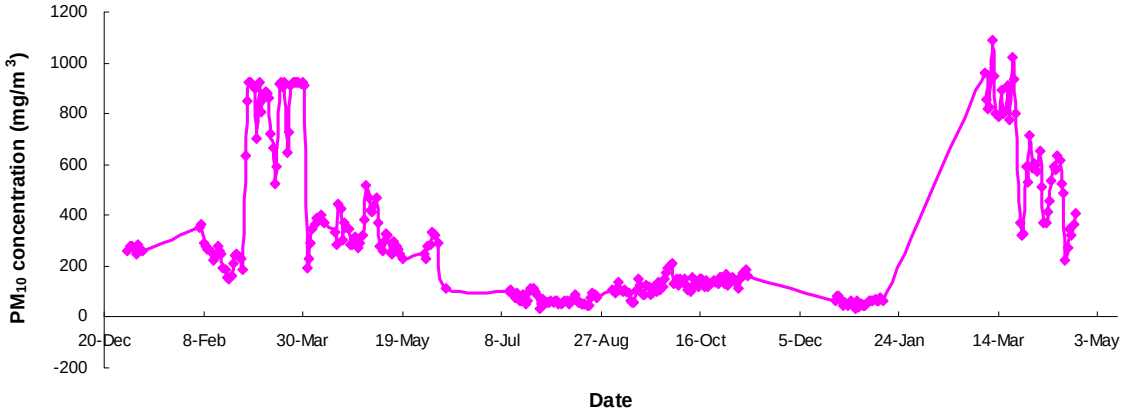

Figure B.9. Daily PM_{10} concentration from Jan, 2003 to April, 2004.

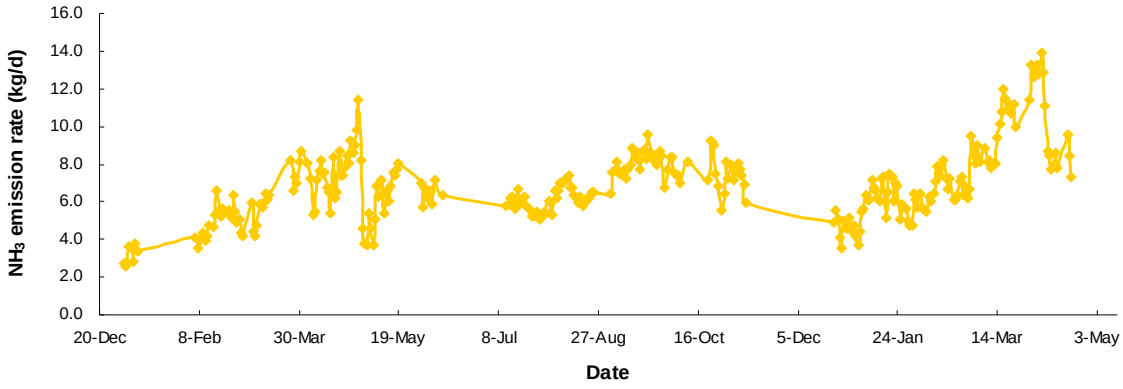

Figure B.10. Daily NH_3 emission rate from Jan, 2003 to April, 2004.

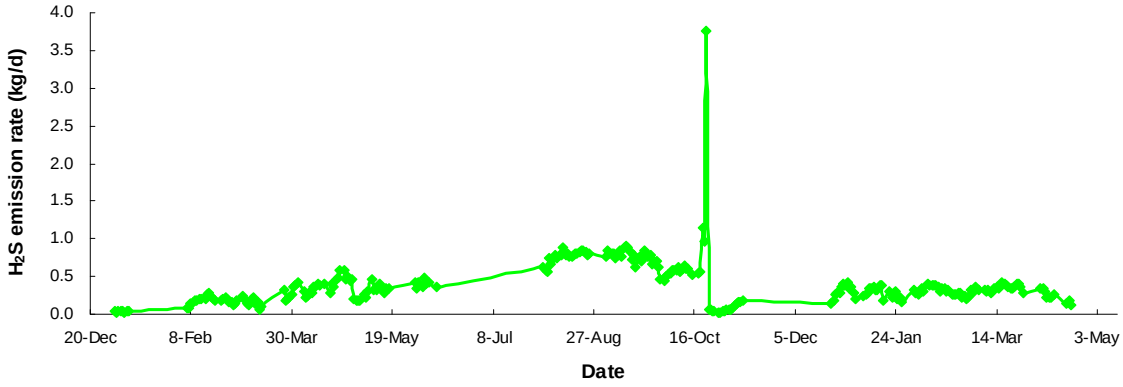

Figure B.10. Daily H_2S emission rate from Jan, 2003 to April, 2004.

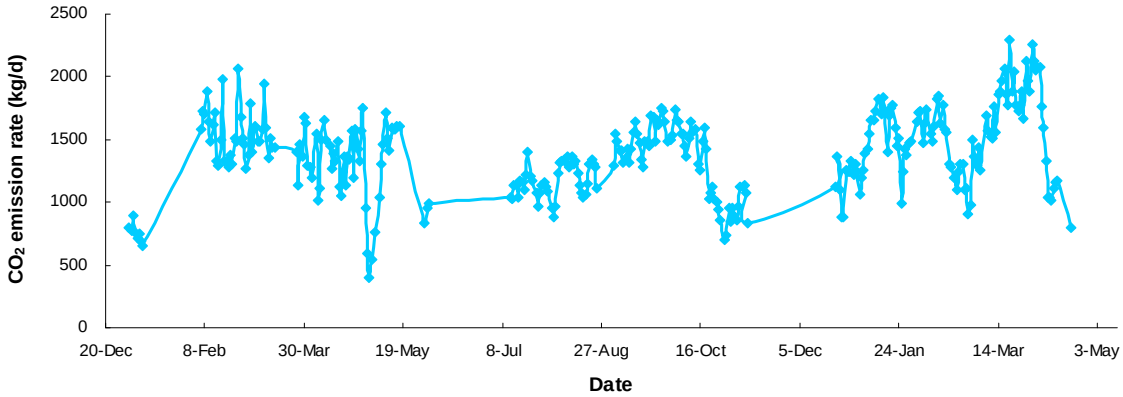

Figure B.10. Daily CO_2 emission rate from Jan, 2003 to April, 2004.

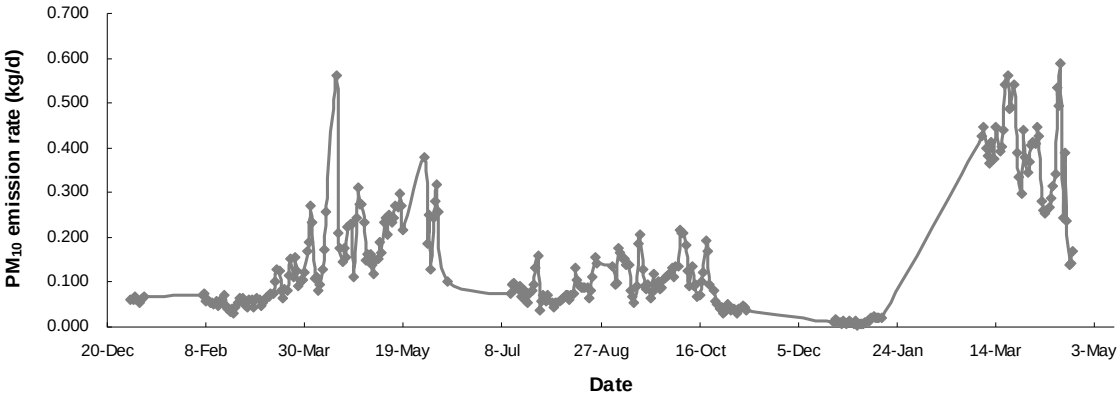

Figure B.11. Daily PM_{10} emission rate from Jan, 2003 to April, 2004.

APPENDIX C. TMY3 DAILY DATA

The TMY3 data is from International airport, Des Moines, Iowa (Class I site).

Date	Outside T (^{o}C)	Outside RH (%)	Wind speed (m/s)	GHI (w/m^2)
1-Jan	-2.2	49	5.2	76
2-Jan	-3.8	61	3.8	75
3-Jan	-4.5	64	3.1	103
4-Jan	1.6	76	4.3	60
5-Jan	-0.1	76	5.7	43
6-Jan	-1.7	69	4.0	81
7-Jan	4.4	61	5.0	107
8-Jan	7.9	42	5.6	105
9-Jan	1.0	43	9.3	95
10-Jan	-7.3	43	7.8	105
11-Jan	-10.3	51	2.6	106
12-Jan	-4.1	50	5.2	111
13-Jan	-7.9	37	2.9	71
14-Jan	-9.0	50	5.5	114
15-Jan	-10.6	51	3.0	93
16-Jan	-9.1	67	5.8	64
17-Jan	-14.8	59	4.1	71
18-Jan	-9.8	69	6.1	91
19-Jan	-5.6	75	4.0	63
20-Jan	-7.7	49	3.9	73
21-Jan	-10.9	51	3.8	92
22-Jan	-13.5	55	5.5	52
23-Jan	-18.0	52	4.3	95
24-Jan	-11.5	58	4.8	56
25-Jan	-9.0	72	3.6	98
26-Jan	-15.6	63	4.2	102
27-Jan	-7.2	64	5.5	67
28-Jan	-2.1	82	3.2	23
29-Jan	-6.2	65	2.8	77
30-Jan	-0.7	68	5.7	116
31-Jan	0.8	85	5.5	54
1-Feb	-16.5	51	2.6	139
2-Feb	-15.0	56	3.3	139
3-Feb	-11.6	56	2.1	117
4-Feb	-11.9	71	5.2	68
5-Feb	-14.1	71	2.1	107
6-Feb	-16.4	60	5.1	146
7-Feb	-16.3	56	3.1	147
8-Feb	-11.3	58	4.9	121
9-Feb	-5.7	73	4.9	60
10-Feb	-5.4	83	5.5	91
11-Feb	-9.2	70	7.1	153
12-Feb	-11.0	63	5.4	161
13-Feb	-7.7	66	6.9	90
14-Feb	-9.7	56	7.1	167
15-Feb	-10.4	63	4.2	111
16-Feb	0.3	66	6.5	146
17-Feb	1.4	59	3.3	150
18-Feb	1.4	62	5.8	168
19-Feb	0.1	73	4.8	135
20-Feb	2.0	90	6.2	71
21-Feb	7.2	95	4.0	59
22-Feb	3.2	91	2.5	88
23-Feb	2.3	93	5.7	57
24-Feb	1.0	83	5.4	89
25-Feb	2.7	85	5.8	106
26-Feb	0.4	72	6.7	96
27-Feb	-0.4	68	3.3	168
28-Feb	5.7	61	5.6	183

T: temperature; RH: Relative humidity; GHI: Global horizontal irradiance

Date	Outside T (^{o}C)	Outside RH (%)	Wind speed (m/s)	GHI (w/m^2)
1-Mar	0.6	86	5.4	53
2-Mar	1.2	87	5.1	81
3-Mar	-2.3	69	6.2	94
4-Mar	-1.1	81	5.2	68
5-Mar	-7.8	68	7.2	194
6-Mar	-3.4	68	5.2	213
7-Mar	-1.1	66	4.4	205
8-Mar	-1.4	62	2.9	111
9-Mar	2.3	74	3.2	156
10-Mar	1.8	74	3.3	96
11-Mar	4.5	76	6.3	123
12-Mar	2.5	75	9.9	76
13-Mar	-2.4	53	6.0	212
14-Mar	2.3	56	5.3	160
15-Mar	-0.5	57	3.7	131
16-Mar	-1.6	56	5.5	207
17-Mar	3.1	59	4.6	201
18-Mar	12.3	50	5.5	165
19-Mar	16.1	57	7.6	188
20-Mar	11.2	47	9.2	221
21-Mar	1.2	46	6.6	232
22-Mar	3.8	49	4.4	194
23-Mar	12.2	44	9.4	206
24-Mar	13.0	34	8.2	216
25-Mar	12.9	55	6.8	163
26-Mar	10.6	68	7.2	89
27-Mar	6.8	50	4.5	246
28-Mar	11.3	52	7.8	173
29-Mar	9.6	84	4.1	91
30-Mar	6.4	61	9.0	188
31-Mar	5.5	55	5.0	177
1-Apr	11.1	42	2.3	252
2-Apr	5.9	52	4.7	221
3-Apr	4.4	45	3.4	269
4-Apr	10.7	52	6.2	159
5-Apr	-0.5	51	6.3	107
6-Apr	1.8	41	2.8	249
7-Apr	6.3	39	4.5	216
8-Apr	12.1	45	5.7	229
9-Apr	10.4	39	2.9	139
10-Apr	10.7	40	4.8	256
11-Apr	8.0	57	6.9	79
12-Apr	6.3	97	4.0	69
13-Apr	10.9	67	4.6	262
14-Apr	16.5	62	3.7	260
15-Apr	9.8	56	8.8	207
16-Apr	12.9	41	4.9	289
17-Apr	15.8	46	3.9	270
18-Apr	22.6	39	5.3	281
19-Apr	14.7	32	3.9	254
20-Apr	11.4	49	3.5	132
21-Apr	10.8	73	3.2	226
22-Apr	11.7	55	2.9	302
23-Apr	16.1	52	5.3	294
24-Apr	21.7	70	5.4	225
25-Apr	22.0	71	6.0	199
26-Apr	17.7	55	9.0	284
27-Apr	6.5	68	6.0	149
28-Apr	5.4	89	6.5	74
29-Apr	5.1	68	4.3	222
30-Apr	3.7	89	2.7	78

T: temperature; RH: Relative humidity; GHI: Global horizontal irradiance

Date	Outside T (^{o}C)	Outside RH (%)	Wind speed (m/s)	GHI (w/m^{2})
1-May	14.9	65	2.4	233
2-May	20.0	46	3.4	279
3-May	20.0	42	2.5	286
4-May	21.6	39	2.9	300
5-May	22.2	33	5.5	247
6-May	17.1	28	5.8	266
7-May	10.0	35	5.1	317
8-May	9.4	37	3.3	317
9-May	14.3	36	4.2	303
10-May	16.9	55	6.4	204
11-May	11.0	47	4.1	243
12-May	14.9	54	4.4	186
13-May	12.7	52	5.2	240
14-May	14.7	47	3.6	228
15-May	17.0	47	5.4	311
16-May	12.5	66	6.6	110
17-May	13.4	81	4.0	131
18-May	13.2	85	3.4	113
19-May	15.5	74	1.9	151
20-May	18.1	66	1.9	268
21-May	19.7	56	1.1	323
22-May	21.5	45	3.0	344
23-May	19.4	57	2.7	182
24-May	21.5	58	3.2	258
25-May	23.5	55	4.1	337
26-May	22.8	60	4.5	195
27-May	24.6	57	3.9	273
28-May	23.2	60	4.0	260
29-May	26.0	59	6.0	282
30-May	19.6	67	7.0	210
31-May	19.2	65	3.7	210
1-Jun	17.5	69	4.9	282
2-Jun	16.6	57	2.9	311
3-Jun	19.7	57	3.8	260
4-Jun	21.3	50	4.4	325
5-Jun	21.7	49	2.2	299
6-Jun	22.3	63	3.1	274
7-Jun	20.1	68	6.0	245
8-Jun	16.2	51	3.6	352
9-Jun	22.1	48	4.2	346
10-Jun	25.2	53	8.8	343
11-Jun	26.1	56	6.4	221
12-Jun	22.0	48	5.2	329
13-Jun	21.9	46	3.5	342
14-Jun	21.4	60	6.7	170
15-Jun	24.1	69	7.2	297
16-Jun	28.9	62	6.9	294
17-Jun	26.6	65	6.1	285
18-Jun	21.9	51	3.4	349
19-Jun	23.8	55	6.4	316
20-Jun	19.3	75	4.3	240
21-Jun	20.0	59	2.3	341
22-Jun	20.3	63	4.8	164
23-Jun	21.6	83	3.2	183
24-Jun	26.2	79	3.0	241
25-Jun	28.4	75	3.4	257
26-Jun	26.8	69	4.5	295
27-Jun	25.3	64	2.7	273
28-Jun	25.1	74	3.0	215
29-Jun	26.7	74	3.2	217
30-Jun	29.0	70	4.2	319

T: temperature; RH: Relative humidity; GHI: Global horizontal irradiance

Date	Outside T (^{o}C)	Outside RH (%)	Wind speed (m/s)	GHI (w/m^2)
1-Jul	25.4	70	3.4	283
2-Jul	26.3	70	4.2	325
3-Jul	29.5	68	3.8	333
4-Jul	28.3	69	4.2	274
5-Jul	25.2	77	3.1	304
6-Jul	26.6	71	5.3	282
7-Jul	26.9	76	4.0	239
8-Jul	22.8	86	4.3	140
9-Jul	23.7	84	3.8	189
10-Jul	22.0	72	6.6	257
11-Jul	23.1	64	5.1	305
12-Jul	22.6	68	2.1	321
13-Jul	23.8	68	2.8	315
14-Jul	26.6	70	5.8	302
15-Jul	26.3	62	3.8	327
16-Jul	24.6	71	3.0	269
17-Jul	28.4	69	3.8	314
18-Jul	24.8	80	4.5	261
19-Jul	23.3	83	2.8	170
20-Jul	26.7	78	3.5	197
21-Jul	23.7	66	5.0	291
22-Jul	21.0	64	4.2	277
23-Jul	20.8	61	2.1	293
24-Jul	22.5	62	4.4	305
25-Jul	26.8	60	6.3	308
26-Jul	30.0	60	5.5	306
27-Jul	24.7	86	3.2	81
28-Jul	24.6	69	3.2	280
29-Jul	24.1	71	1.7	293
30-Jul	23.8	74	2.7	239
31-Jul	24.6	71	3.3	217
1-Aug	21.4	74	4.1	273
2-Aug	22.9	81	4.0	222
3-Aug	23.1	88	2.2	122
4-Aug	22.6	73	3.9	278
5-Aug	19.3	64	4.2	286
6-Aug	18.9	60	2.2	296
7-Aug	19.5	64	1.7	271
8-Aug	19.8	68	3.1	305
9-Aug	21.8	70	3.6	301
10-Aug	22.5	78	2.4	245
11-Aug	22.8	80	2.1	236
12-Aug	20.1	84	3.3	160
13-Aug	19.9	78	2.4	272
14-Aug	21.6	79	4.2	252
15-Aug	22.6	82	2.6	241
16-Aug	22.8	88	3.7	153
17-Aug	27.0	76	4.5	291
18-Aug	27.8	72	5.0	291
19-Aug	24.7	84	3.6	204
20-Aug	23.0	88	3.3	133
21-Aug	20.9	85	2.7	136
22-Aug	21.1	85	2.9	126
23-Aug	24.1	83	5.0	274
24-Aug	25.3	80	4.2	227
25-Aug	27.3	79	4.4	259
26-Aug	28.5	74	4.9	253
27-Aug	29.2	68	4.4	249
28-Aug	27.1	75	3.5	232
29-Aug	23.6	77	2.5	237
30-Aug	22.6	76	3.0	276
31-Aug	25.4	68	4.8	272

T: temperature; RH: Relative humidity; GHI: Global horizontal irradiance

Date	Outside T (^{o}C)	Outside RH (%)	Wind speed (m/s)	GHI (w/m^{2})
1-Sep	22.6	71	3.8	230
2-Sep	20.7	64	2.7	277
3-Sep	25.4	68	6.3	262
4-Sep	21.6	65	3.0	216
5-Sep	22.9	69	2.7	253
6-Sep	24.5	75	4.2	232
7-Sep	27.0	68	4.2	244
8-Sep	27.3	66	3.7	246
9-Sep	18.7	60	5.9	151
10-Sep	16.6	57	2.1	237
11-Sep	20.2	63	5.0	180
12-Sep	25.6	67	5.2	204
13-Sep	20.1	74	4.0	129
14-Sep	17.1	72	3.6	108
15-Sep	17.6	76	4.2	189
16-Sep	13.0	71	4.9	94
17-Sep	11.5	62	3.4	202
18-Sep	18.0	60	3.8	242
19-Sep	23.0	69	6.3	200
20-Sep	24.8	62	6.4	201
21-Sep	20.8	66	3.7	217
22-Sep	17.5	61	5.4	180
23-Sep	12.9	55	2.4	227
24-Sep	13.3	70	3.5	99
25-Sep	12.4	63	5.2	193
26-Sep	12.1	57	3.0	208
27-Sep	18.2	51	4.5	172
28-Sep	16.8	52	3.6	204
29-Sep	16.4	70	4.6	128
30-Sep	19.9	65	3.6	200
1-Oct	16.6	48	4.2	149
2-Oct	11.5	46	6.3	115
3-Oct	6.6	58	3.1	91
4-Oct	7.8	63	1.9	157
5-Oct	10.8	56	4.0	199
6-Oct	15.5	50	3.0	204
7-Oct	17.6	48	3.5	192
8-Oct	18.8	44	3.3	184
9-Oct	17.2	52	2.6	188
10-Oct	16.4	34	7.3	199
11-Oct	10.3	45	6.4	175
12-Oct	6.9	55	1.9	196
13-Oct	13.6	47	5.2	103
14-Oct	15.8	55	5.2	182
15-Oct	9.1	88	5.2	51
16-Oct	16.6	84	6.7	94
17-Oct	10.3	60	6.4	131
18-Oct	6.0	64	5.6	94
19-Oct	8.8	60	3.7	159
20-Oct	13.0	59	3.9	166
21-Oct	10.4	52	3.7	134
22-Oct	12.6	52	5.3	145
23-Oct	10.5	75	5.0	71
24-Oct	3.9	69	6.2	87
25-Oct	3.0	61	5.8	71
26-Oct	0.7	65	2.6	95
27-Oct	1.4	76	6.3	64
28-Oct	0.0	69	4.9	163
29-Oct	-1.2	71	2.6	138
30-Oct	4.4	66	4.2	144
31-Oct	8.3	62	3.2	127

T: temperature; RH: Relative humidity; GHI: Global horizontal irradiance

Date	Outside T (^{o}C)	Outside RH (%)	Wind speed (m/s)	GHI (w/m^{2})
1-Nov	6.9	51	3.7	132
2-Nov	7.1	58	5.8	115
3-Nov	11.4	67	2.9	117
4-Nov	10.4	88	5.0	78
5-Nov	2.4	82	9.6	59
6-Nov	3.2	56	8.6	129
7-Nov	4.1	63	4.0	94
8-Nov	6.9	64	3.0	93
9-Nov	7.1	74	3.7	47
10-Nov	2.1	67	6.1	118
11-Nov	1.0	72	4.7	81
12-Nov	4.1	87	5.6	43
13-Nov	7.3	74	4.4	118
14-Nov	7.8	73	4.9	99
15-Nov	13.8	87	5.8	55
16-Nov	-0.2	74	10.4	65
17-Nov	3.9	65	4.0	115
18-Nov	8.4	59	5.4	102
19-Nov	2.1	84	5.5	54
20-Nov	-3.7	71	6.3	113
21-Nov	-2.9	73	3.7	117
22-Nov	2.8	69	5.9	105
23-Nov	7.2	62	6.2	107
24-Nov	9.6	55	6.4	107
25-Nov	5.0	76	5.8	53
26-Nov	3.4	92	5.4	40
27-Nov	-1.5	77	10.8	59
28-Nov	-4.0	67	5.5	102
29-Nov	1.2	78	5.6	49
30-Nov	-0.7	72	5.7	92
1-Dec	1.0	84	7.0	54
2-Dec	-1.5	73	2.1	92
3-Dec	0.7	81	6.7	46
4-Dec	0.6	77	4.4	71
5-Dec	0.2	78	3.8	88
6-Dec	4.8	71	4.8	75
7-Dec	4.1	74	6.4	101
8-Dec	1.5	58	4.6	68
9-Dec	-3.1	75	4.1	61
10-Dec	-3.2	66	4.2	52
11-Dec	0.8	55	4.3	55
12-Dec	1.0	79	2.5	47
13-Dec	1.7	82	2.2	50
14-Dec	-4.5	70	5.0	100
15-Dec	-8.6	75	3.7	41
16-Dec	-10.7	74	5.6	51
17-Dec	-16.5	62	6.3	102
18-Dec	-17.6	61	4.0	102
19-Dec	-17.0	59	3.0	97
20-Dec	-6.8	68	7.5	45
21-Dec	1.4	85	4.7	55
22-Dec	-1.8	72	5.5	61
23-Dec	-3.2	64	5.9	89
24-Dec	-2.9	63	4.8	100
25-Dec	-1.6	69	4.1	86
26-Dec	-0.7	69	4.9	59
27-Dec	-3.1	76	3.3	49
28-Dec	-10.5	72	4.8	98
29-Dec	-10.9	71	4.0	86
30-Dec	-3.2	64	5.9	68
31-Dec	-5.9	68	7.6	52

T: temperature; RH: Relative humidity; GHI: Global horizontal irradiance

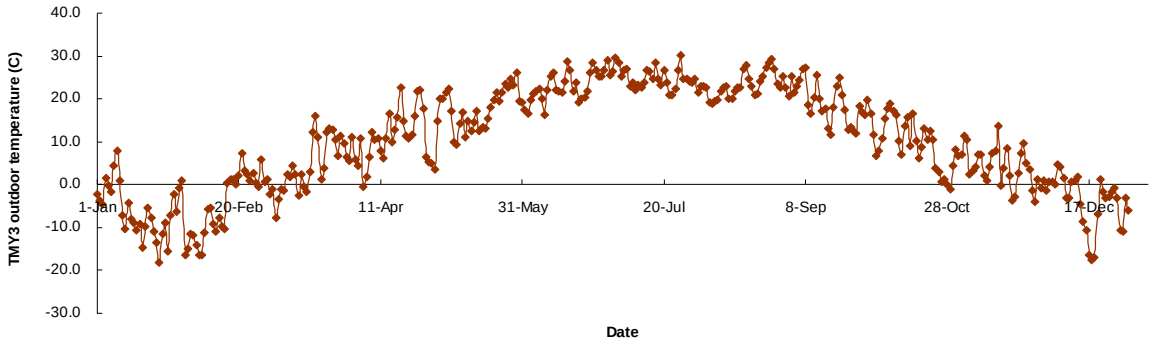

Figure C.1. Daily TMY3 outdoor temperature throughout the year.

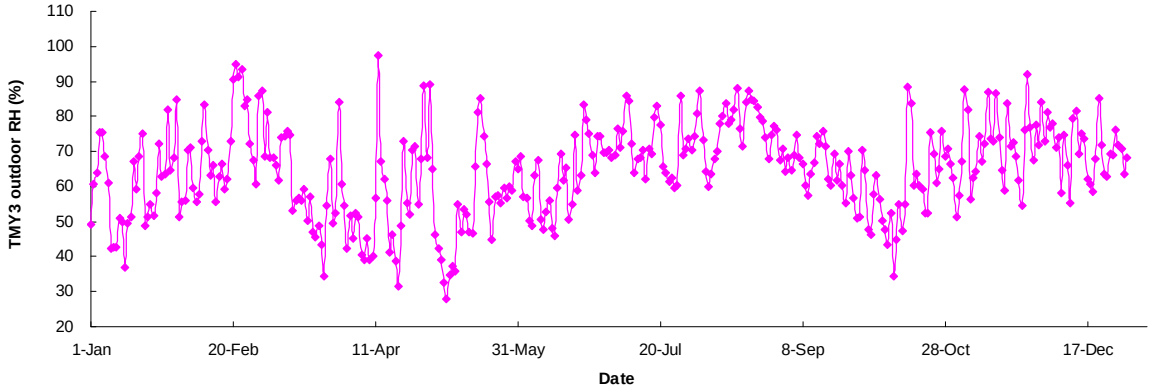

Figure C.2. Daily TMY3 outdoor RH throughout the year.

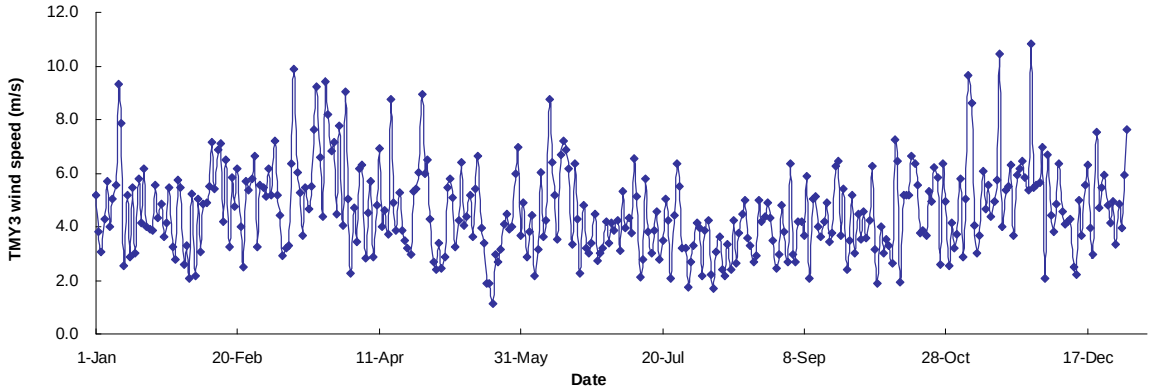

Figure C.3. Daily TMY3 wind speed throughout the year.

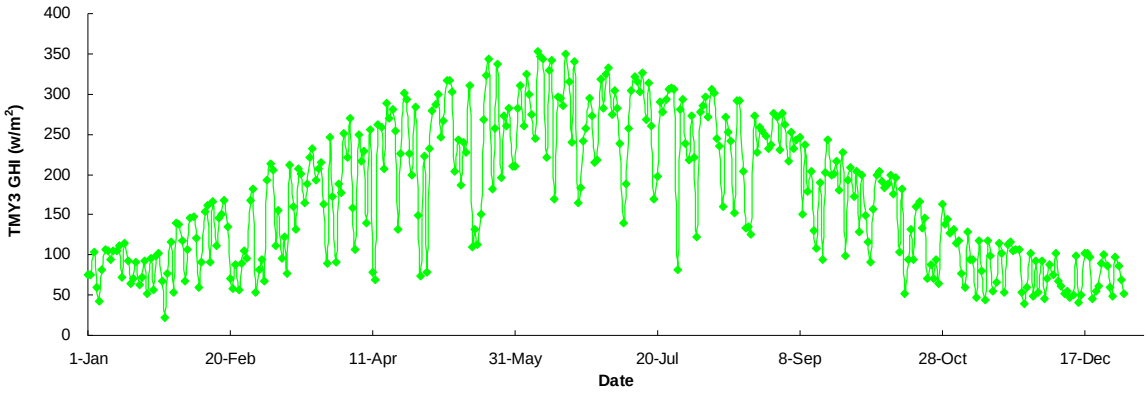

Figure C.4. Daily TMY3 GHI throughout the year.

ACKNOWLEDGMENTS

I would first like to express my sincere gratitude and appreciate to my major professor, Dr. Steven Hoff, for his guidance, support, and wisdom throughout my PhD study. He has undoubtedly provided me every opportunity possible to peruse my dreams. I am glad to pronounce that I have had a wonderful time working under his supervision and cherished each and every moment with him. I wish every graduate student could have such an excellent mentor, teacher and friend.

To my committee members Dr. Dianne Cook (statistics PhD minor professor), Dr. Jay Harmon, Dr. D. Raj Raman, and Dr. Ron Nelson, I extend thanks for their generous contribution of time and valuable comments on my research project. I also want to thank Iowa State University for the dedication towards providing students such a great graduate education.

A special thanks to the research group members and faculty members who provided support and encouragement during my graduate studies: Mr. Brian Zelle, Dr. Lide Chen, Dr. Lingshuang Cai; and Dr. Joseph Chen, Dr. Kenneth Stalder, and Dr. Lie Tang. I also wish to give thanks to all the brothers and sisters in the Church in Ames and all of my fellow graduate students and officemates in the Department of Agricultural and Biosystems Engineering.

Finally, I would like to dedicate this dissertation and express special gratitude to my family. I definitely would have not succeeded without their loving support and continuous encouragement.